RESPONSES OF HETEROTROPHIC AND AUTOTROPHIC PICO- AND NANO-PLANKTON TO NUTRIENT AVAILABILITY AND ENRICHMENT ACROSS MARINE SYSTEMS IN THE NORTHERN GULF OF MEXICO

A Dissertation

by

ALICIA KAIL SHEPARD

Submitted to the Office of Graduate and Professional Studies of
Texas A&M University
in partial fulfillment of the requirements for the degree of

DOCTOR OF PHILOSOPHY

Chair of Committee,	Antonietta Quigg
Committee Members,	Daniel Thornton
	Jay Rooker
	Gilbert Rowe
Head of Department,	Debbie Thomas

August 2015

Major Subject: Biological Oceanography

Copyright 2015 Alicia Kail Shepard

ABSTRACT

It is predicted that ubiquitous marine microbial communities adapt to shifts in their immediate environment that are reflected in changing community abundance, structure, production, interactions and functions. This study describes spatiotemporal microbial dynamics in two unique marine settings with naturally occurring variations in surface water inorganic nutrient concentration, including an estuarine and an open ocean system. Mesocosm experiments were conducted using combinations of inorganic nutrients expected to influence microbial communities in order to support *in situ* interpretations. A statistical examination of flow cytometric derived microbial groupings, based on physiological rather than taxonomic characteristics revealed important relationships between inorganic nutrients and marine microbial communities. Correlations specifically indicated the importance of temperature, salinity and inorganic nutrients to changes in microbial physiological community structure. Heterotrophic microbes in the Trinity River Basin of Galveston Bay appear to undergo episodic nitrogen limitation that occurs when high temperature stimulates increased cellular metabolic activity and carbon is saturated beyond heterotrophic requirements. A step-wise spatiotemporal co-limitation of autotrophic and heterotrophic fractions of microbial plankton in Galveston Bay exists such that temperature ultimately limits abundance, followed by inorganic phosphorous at a station where nutrient pulses stimulated by freshwater inflows are infrequent. If inorganic phosphorous is available, as occurs in the Trinity River Basin then dissolved inorganic nitrogen becomes the limiting factor. Finally, nutrient limitation processes influence microbial plankton abundance and physiological community structure similarly in the northern Gulf of Mexico, where nutrients are made available by mesoscale circulation and coastal entrainments. Continued exploration into the complex environmental connections to marine microbial ecology is required to better understand and predict microbial impacts on biogeochemical cycles.

ACKNOWLEDGEMENTS

I would like to thank my committee chair, Dr. Antonietta Quigg, and my committee members, Dr. Rooker, Dr. Thornton, and Dr. Rowe, for their guidance and support throughout the course of this research.

Thanks also go to the several friends and colleagues who have supported my progress toward this degree, and the Departments of Oceanography and Marine Biology faculty and staff for making my time at Texas A&M University and Texas A&M University Galveston a successful experience. I also want to extend my gratitude to the National Science Foundation, the Texas A&M University Office of Graduate and Professional Studies, Texas Sea Grant, and the Integrated Ocean Drilling Program, which provided research and scholarly funding during my graduate experience.

Finally I would like to thank my wonderful family Harry, Clair-ann, Katelyn and Breanana-may Shepard and my future husband, Josh Williams, for their extraordinary support and devotion as I have navigated the journey of completing this degree.

NOMENCLATURE

NGOM	Northern Gulf of Mexico
HNAB	High nucleic acid containing bacteria
MNAB	Mid nucleic acid containing bacteria
LNAB	Low nucleic acid containing bacteria
DOC	Dissolved Organic Carbon
TOC	Total Organic Carbon
TN	Total Nitrogen
DIN	Dissolved Inorganic Nitrogen
TP	Total Phosphorous
P_i	Inorganic Phosphorous
TSS	Total suspended solids
FWI	Freshwater inflow
GP	Gross primary productivity
AIC_c	Akaikes Information Criterion Corrected
BIC	Bayesian Information Criterion

TABLE OF CONTENTS

Page

LIST OF FIGURES

Page

LIST OF TABLES

Page

CHAPTER I
INTRODUCTION AND LITERATURE REVIEW

1.1 Introduction

Microbial populations are ubiquitous and abundant in the sea with approximately a billion cells in every liter of water (1,2). These organisms are characterized across all three domains of life and their immense diversity is reflected in their significant contribution to many different cycles in the ocean (1). Historically marine microorganisms have been difficult to study; however, the advent of molecular and bio-optical technologies has allowed major forward progress into the overall understanding of these groups. One important finding is the substantial contribution of the smallest size fraction of plankton to many marine processes (3). For example, the fixation of CO_2 by autotrophic picoplankton like cyanobacteria (e.g. *Synechococcus sp.* and *Prochlorococcus sp.*) contributes >50% of available carbon to open ocean systems (4). It has been proposed that under projected increases in sea surface temperature, smaller organisms may increase in abundance, and therefore their importance in biogeochemical cycling and food webs (3).

Potentially the most important contribution of microbial plankton to marine systems is their role in carbon fixation and cycling. Field et al. (5) estimated that approximately half of Earth's total primary productivity could be attributed to autotrophic marine plankton. The conversion of inorganic carbon to biologically available organic carbon by autotrophic plankton directly or indirectly fuels abundant heterotrophic organisms within the sea (1). Recent attention has also been paid to the potential for microbial impacts on carbon sequestration (6). The planktonic microbial system can cycle carbon in the upper water column on time scales of days to months but also contributes to long-term (millennia) storage of carbon in the deep-ocean or marine sediments through the microbial carbon pump (6). Therefore, understanding the microbial component within oceanic mitigation of currently increasing atmospheric carbon concentrations remains a salient directive.

Microbial carbon cycling is extremely important in marine ecosystems, and thus it is important to determine and understand controls of carbon associated microbial processes. Both autotrophic and heterotrophic marine microbial plankton processes can be limited by the availability of inorganic nutrients, influencing microbial impacts on the carbon cycle (7–9). Liebig defined limitations to crop growth as the nutrient that is the least available for growth (10). Similarly, Blackman (11) examined limitations in photosynthesis within leaves. Since these pivotal publications, Liebig's Law of the minimum has been applied to microbial populations e.g. (12). Autotrophic phytoplankton carbon assimilation is limited by availability of inorganic nutrients leading to changes in production, growth, and increased cellular activity (9). It has also been shown that heterotrophic bacteria require inorganic nutrients in order to take up dissolved organic carbon, which is essential to their growth, activity and function (7). Since heterotrophic organisms cannot generate their own organic carbon source, it is believed that they will only be limited by inorganic nutrients in the presence of abundant organic carbon (13–15). Competition for inorganic nutrients has been shown to exist between heterotrophic and autotrophic plankton in marine systems e.g. (7,14,16,17). Heterotrophic bacteria should be able to assimilate inorganic nutrients more efficiently than phytoplankton since they have a larger surface area to volume ratio (16,18). Therefore, if not limited by organic carbon, heterotrophic bacteria are expected to outcompete phytoplankton for nutrients (13,14). Recent studies suggest that in heterogeneous natural planktonic communities, nutrient co-limitation is predicted (19). This can occur when multiple nutrients limit microbial planktonic growth simultaneously (19). It has also been shown that microbial plankton can be co-limited by a combination of different nutrients dependent upon aquatic conditions and locality (18,19).

The most extensively studied limiting inorganic nutrients for marine microbial plankton growth include the different forms of nitrogen, phosphorus, and silica (7,8,16). Nitrogen (as nitrate) and phosphorus are the prevailing limiting nutrients in most marine systems. However, which nutrient(s) are limiting depends on chemical, biological and

physical factors (8,9,12). It has traditionally been accepted that nitrogen is the limiting nutrient to productivity and phytoplankton growth in the open ocean (9,20). It has more recently been suggested that open ocean nutrient limitation can be due to either nitrogen or phosphorus (8,9,12,21,22). Tyrell (21) also explained that nutrient limitation in the ocean is dependent on the time and spatial scales to which the question is applied. He described the 'proximate limiting nutrient' as the local, short-scale limitation to productivity along side the 'ultimate limiting nutrient' which is the limitation to the total system over geological time-scales (thousands of years and longer) based on the ultimate fate of nutrient cycling. This paradigm is intimately linked with organisms that are capable of nitrogen fixation (8,9,21). When nitrogen is limiting, organisms capable of fixing nitrogen will gain the competitive advantage when sufficient energy is available in the form of light or excess carbon, and contribute biologically available nitrate to surface waters. The energetic cost of nitrogen fixation is then no longer favored and other plankton will grow, eventually depleting the system of nitrate again. Since there is no biological mechanism to replenish surface phosphate concentrations, phosphate will ultimately limit productivity (21). However, typically trace amounts of phosphate are detected in the open-ocean, where nitrate is undetectable, and evidence indicates that nutrient enrichment with nitrate stimulates growth and productivity from these systems while often phosphate does not (21). Accordingly on local, short time-scales nitrate is the limiting nutrient to productivity while prolonged nutrient cycling of phosphate limits productivity on system-wide scales and over long time periods based on geochemical evidence. Biologically, the plasticity of phosphorous- containing macromolecules is greater than nitrogen-containing macromolecules. Therefore, nitrogen has the potential to be more limiting than phosphorous overall (23).

In estuarine and coastal environments, the dominant limiting nutrient reflects unique chemical and physical parameters to each location. Howarth and Marino (8) suggested that high salinity estuaries limit nitrogen fixing cyanobacterial growth rates, preventing them from overcoming grazing pressures, driving an overall nitrogen limitation. Turbidity also plays a significant role in driving nutrient limitation because in

shallow, clear estuaries benthic cyanobacterial mats and seagrasses contribute to the pool of available nitrate through substantial nitrogen fixation leading to phosphate limitation. However, in deeper, turbid estuaries nitrogen fixation contributes much less nitrate (8,24) favoring a nitrogen limited system. In addition to nitrogen and phosphorous limiting systems, some autotrophic organisms construct tests composed of silica, making dissolved silicate a limiting nutrient for diatom population growth in some regions (25,26). Interestingly, the marine autotrophic cyanobacteria *Synechococcus sp*. has also been shown to contain high levels of silica under certain conditions. Although the reasons and mechanisms for uptake are not yet described, it has been hypothesized that uptake of silica by *Synechococcus* may alter diatom production and subsequently the silica cycle in the open ocean (27,28). Therefore, abundant evidence exists supporting the importance of nutrient availability for marine microbial plankton. Nutrient stimulated relationships among microbial plankton have the potential to be important given that heterotrophic bacteria and many autotrophic cyanobacteria are within the same size range (pico- to nano- plankton) and both require inorganic nutrients to thrive. However, the integration of how heterotrophic and autotrophic microbial plankton simultaneously respond to nutrients has not been extensively studied in marine systems (7,14,17,18,23)**.**

Nutrient availability has also been shown to determine the dominant size of organisms within microbial populations (16,26,29,30). Smaller phytoplankton (<20 μm) have been shown to dominate under low nutrient concentrations, making it common to observe high abundances of small size phytoplankton and cyanobacteria in oligotrophic open ocean systems (29). The observation of a shift in community composition toward smaller phytoplankton and bacteria in oligotrophic systems may be because they can outcompete larger organisms for limited inorganic nutrients (16). Alternatively, in high nutrient environments it is expected that large taxa outcompete the small taxa regardless of their uptake capacity, driving the smaller organisms into a realized niche within oligotrophic systems. Correspondingly, it has been observed that coastal marine systems associated with increased nutrient availability host higher concentrations of larger marine plankton cells, biomass, and primary productivity (31). Interestingly, shifts from

larger eukaryotes to smaller prokaryotes have been observed simultaneously to increasing primary productivity and increased biomass at the Hawaii Ocean Time-series location (32,33). Studies have also shown heterotrophic responses to nutrient addition in coastal zones (15,17) indicating that small microorganisms remain important throughout varied marine nutrient regimes.

Microbes are intimately linked with marine food webs as the foundation of multiple energy transfer pathways to higher trophic levels e.g. (1,26,34). Nutrient limitation can have significant impacts on microbial community structure, function, and interactions driving potentially important shifts in overall ecosystem stability (7). Specifically, the limitation of microbial growth could decrease the carbon assimilated into food webs and subsequently transferred to higher trophic levels (7,32,33). Alternatively, competition for limited inorganic nutrients may drive shifts in heterotrophic versus autotrophic dominated microbial communities, impacting interactions with grazers of each group (14). Nutrient driven shifts in marine microbial plankton community structure and subsequent changes in their predators could ultimately impact the carbon export to the deep sea and marine sediments (6,30). Nevertheless, the intricate workings of interactions within the marine microbial community and among microbial plankton and their predators remain unconstrained (29,34). Since nutrient driven shifts in microbial communities are linked to changes in productivity and energy, the resolution of how these populations are changed is important in order to better understand the potential impacts on the greater ecosystem.

Only a few previous studies have examined microbial autotrophic and heterotrophic abundance simultaneously in order to evaluate the potential competition for inorganic nutrients within this size fraction of the community (14,17,18). For example, in a coastal environment, Joint (17), conducted a single mesocosm experiment over the course of 6 days. The heterotrophic bacterial population was not observed to have significant change in abundance when exposed only to inorganic nutrients, but dominated the community in the presence of inorganic nutrients plus organic carbon. The microbial autotrophic community declined in abundance associated with the same

treatment and little alteration of pigment concentration. This indicated that autotrophic and heterotrophic microbial communities likely compete for inorganic nutrients when abundant organic matter is available. Similarly, in the Arctic Ocean, Thingstad (14), examined a diatom-dominated autotrophic response in relationship to heterotrophic responses in a 13-day mesocosm experiment. Microbial responses to additions of silicate and inorganic carbon indicated competition as bacterial abundance and productivity increased but the organic carbon pool decreased (14). Both autotrophic and heterotrophic microbial populations were found to respond to nutrients from five locations ranging across a latitudinal transect from 26°N to 29°S in the central Atlantic Ocean (18). However, there was no consistent pattern to these responses at all sites, indicating that the relative importance of these nutrients on marine microbial dynamics varied spatially (18). Considering the potential importance of how microbial communities respond to nutrient additions, there are still major gaps in our understanding of responses to naturally occurring nutrient pulses under ambient carbon concentrations in a variety of systems.

1.2 Trait-Based Microbial Ecology

Trait-based ecology is a framework designed to address ecological questions using the measurable physiological properties of an individual (35,36). Key traits confer specific levels of fitness to an organism and can affect that individual's performance and impact on the environment (37). A classic example is size, which often provides more valuable information about an individual's ecological footprint than phylogenetic assignment (30,35,36). A trait focus is also being applied at higher organizational levels in order to examine connections between community and ecosystem structures and functions (37).

The advent of molecular techniques has dramatically changed the scientific understanding of marine microbiology (38,39). However, with the great wealth of information provided by examining the microbial genome, transcriptome and proteome in varying marine contexts, comes challenges that remain to be overcome. In order to

bring ecological context to genomic data, operational taxonomic units identified in marine microbial communities have invariably been related to “species”, often (somewhat arbitrarily) being defined as having 97% similarity in nucleic acid structure (40). This definition presumes similar structure corresponds to function which may not be accurate because of widely observed intra-specific variation, or “ecotypes” within a given microbial taxon (41) compounded by functional redundancy within individual genomes and community level metagenomes (42). Although there are apparent patterns in marine microbial diversity, how that diversity translates into their relationships with co-existing biology and chemistry is poorly understood (41,43–45). Finally, as “Big Data” repositories of molecular information continue to grow, utilizing these data to derive meaningful information will require careful management strategies and statistical evaluations (46,47).

Addressing ecological questions using a trait-based approach has been successful for marine phytoplankton (48) and if combined with molecular tools, could derive valuable insight into the outstanding questions in marine microbial ecology (41,45,49,50). Flow cytometric methodology conveniently targets microorganisms within the nano- and pico-plankton size fraction, and can provide information related to physiological cell characteristics at a single cell level (47,49,51,52). Further, the automated enumeration of microbial populations using flow cytometry greatly increases counting capacity which ultimately reduces statistical and microscopy biases (51,52). Organizing microbial communities based on observable traits rather than taxonomy has been termed the “physiological community structure” (53) and comparisons herein utilize this type of microbial community classification. Within this study examinations of heterotrophic groupings based on nucleic acid content characteristics, of heterotrophic and autotrophic groups based on photo-pigment presence/absence, and of a combination of heterotrophic groups based on nucleic acid content and autotrophic groups based on different photo-pigment concentrations were conducted. The application of trait-based ecology to marine microbes using flow cytometry will continue to develop new and interesting insights.

1.3 Objectives and Hypotheses

The overarching objective of this study was to evaluate the abundance of marine microorganisms within the nano- (0.2-2 μm) and pico- (2-20 μm) plankton size fractions (herein termed microbial plankton) to determine potential spatiotemporal relationships with inorganic nutrient availability. Although taxonomic and functional microbial responses to nutrient availability have been evaluated in some marine systems, very few have focused on relationships among physiologically derived subsets of these communities. Specifically, these relationships have not yet been examined in the Northern Gulf of Mexico, Galveston Bay Estuary or when using the same technique across naturally occurring nutrient gradients. Flow cytometric evaluation of *in situ* variability in microbial plankton combined with complementary bioassay experiments evaluating responses to nutrient enrichment were examined to confirm potential nutrient limitation of abundance or nutrient driven shifts in physiological community structure. Three specific experiments were conducted to address different questions targeting (1) relationships among estuarine heterotrophic groups, (2) relationships between estuarine heterotrophic and autotrophic groups, and (3) relationships between open ocean heterotrophic and autotrophic groups.

In the first analysis (Chapter 2), findings are described for inorganic nutrient influences on groups of estuarine heterotrophic microbial plankton. Groupings of heterotrophic pico- and nano-plankton have been detected using flow cytometry based on relatively different nucleic acid contents across varying marine systems and conditions globally. The ecological context of why these groupings are consistently observed remains under investigation. This study evaluated the variability in relative abundance of heterotrophic groups defined by nucleic acid content in the Trinity River Basin of Galveston Bay, an estuarine location temporally impacted by high or low river inflows. Significant variability was observed *in situ* and was correlated to a combination of temperature and dissolved inorganic nitrogen (DIN) concentration using a distance based linear model. *In vitro* experimentation confirmed corresponding episodic nitrogen limitation of heterotrophic organisms. When the lowest *in situ* DIN concentrations were

observed (<0.006 μMol L^{-1}), heterotrophs containing relatively lower nucleic acids dominated *in situ* assemblages and responded to enrichment rapidly (within 24-48 hours), while heterotrophs containing relatively higher nucleic acids responded more slowly (after 72 hours). These findings support that cellular nucleic acid content can be used to detect shifts in heterotrophic communities associated with inorganic nutrient use, which provides insight into potential microbial ecological strategies.

In the second analysis (Chapter 3), the influence of inorganic nutrients on the relationships between estuarine heterotrophic and autotrophic microbial plankton are evaluated. Limitation of autotrophic and heterotrophic marine microbes by inorganic nutrients has been observed in several marine environments and is predicted to be more likely in coastal systems where heterotrophic carbon requirements may be surpassed by *in situ* availability. This study evaluated the spatiotemporal dynamics in heterotrophic and autotrophic pico- and nano-plankton abundance simultaneously to target potential nutrient limitation and nutrient driven shifts between these fractions at two stations in Galveston Bay, Texas. Significant spatiotemporal variability in microbial plankton was correlated to temperature, dissolved inorganic nitrogen, dissolved inorganic phosphorous and total organic carbon such that temporal nitrogen limitation was expected at a station frequently exposed to freshwater inflow events compared to phosphorous limitation at a station primarily exposed to Gulf of Mexico tidal influences. Corresponding nutrient enrichment experiments suggest that nitrogen, phosphorous or a combination of both temporally limits microbial plankton carrying capacity at both stations in Galveston Bay. The occurrence of phytoplankton blooms may influence competition for inorganic nutrients among autotrophic and heterotrophic fractions of estuarine marine microbes, potentially influencing ecosystem dynamics.

Finally, in the third analysis (Chapter 4), coastal and mesoscale driven influences on inorganic nutrient availability to both heterotrophic and autotrophic microbial plankton are investigated. Mesoscale circulation generated by the Loop Current in the Northern Gulf of Mexico (NGOM) delivers growth-limiting nutrients to the microbial plankton of the euphotic zone. Consequences of physicochemically driven community

shifts on higher order consumers and subsequent impacts on the biological carbon pump remain poorly understood. This study evaluates microbial plankton (0.2 to 20 μm) abundance and community structure across both cyclonic and anti-cyclonic circulation features in the NGOM using flow cytometry (SYBR Green I and autofluorescence parameters). Non-parametric multivariate hierarchical cluster analyses indicated that significant spatial variability in community structure exists such that stations that clustered together were defined as having a specific 'microbial signature' (i.e. statistically homogeneous community structure profiles based on relative abundance of microbial groups). Salinity and a combination of sea surface height anomaly and sea surface temperature were determined by distance based linear modeling to be abiotic predictor variables significantly correlated to changes in microbial signatures. Correlations between increased microbial abundance and availability of nitrogen suggest nitrogen-limitation of microbial plankton. Regions of combined coastal water entrainment and mesoscale convergence corresponded to increased heterotrophic prokaryote abundance. The results provide the first evidence of how mesoscale circulation influences on microbial plankton in the NGOM.

CHAPTER II
CYTOMETRIC ANALYSIS OF HETEROTROPHIC ESTUARINE PLANKTON RESPONSES TO INORGANIC NUTRIENT AVAILABILITY

2.1 Introduction

Heterotrophic marine pico- and nano-plankton ranging in size from 0.2 to 20 μm (herein microbial heterotrophs) have been studied extensively throughout the global oceans (54). As molecular methodology becomes increasingly robust, the immense phylogenetic diversity of marine microbial heterotrophs continues to be elucidated (39) and refs. therein). The application of traditional ecological concepts to these diverse organisms is complicated by their ability to rapidly grow, horizontally transfer genetic information and interact with both their environment and biology. Therefore, in addition to taxonomic categorization it has been suggested that marine heterotrophic assemblages also be organized based on physiological traits, termed physiological community structure by Del Giorgio and Gasol (53), to examine potential heterotrophic microbial ecological strategies (55).

Flow cytometry has detected globally ubiquitous groupings of marine heterotrophic microbes based on nucleic acid content (52,56). Typically these groups have been defined as either low or high nucleic acid containing bacterial fractions e.g. (57–59) (herein HNAB and LNAB) but additional groups have also been observed (60,61) (herein 'medium nucleic acid containing' MNAB). Several analyses have suggested that organisms with higher nucleic acid content represent a more active fraction of the community, which is supported by strong positive correlations to bacterial production, growth rates and bulk activity (59,62–64). Based on these studies it has been hypothesized that LNAB are inactive and act as a reservoir for genetic information and/or species that can eventually become active under optimal environmental conditions (56,65,66). However, highly active members of the community have been detected within the LNAB fraction (55,60,67). Recent molecular evidence suggests that certain species are distinct to specific physiological fractions while others are not (66,68)

indicating that nucleic acid content based groupings are not defined simply by taxonomic differences (56,66). These findings have prompted ongoing efforts to understand the ecological context of this potentially important physiological distinction in marine microbial heterotrophic assemblages.

The increased fluorescent signal defining HNAB cells is conceivably related to increased genome length (66,69). These longer genomes may include additional functional regions conveying the ability to conduct a broader range of processes to these organisms. Therefore, it is predicted that heterotrophs with relatively higher nucleic acid content may be able to occupy more diverse niches and better adapt to changing environments; i.e. exhibiting generalist survival strategies (66,69). This possibility is supported by evidence that the HNAB fraction has been found to be more abundant and maintain higher nucleic acid content in highly productive coastal marine regions compared to oligotrophic systems (56). Conversely, lower nucleic acid containing heterotrophic microbes would be expected to exhibit specialist survival strategies. Supporting this hypothesis is the observation of significantly lower taxonomic diversity in LNAB compared to HNAB fractions suggesting that fewer niches are available to organisms with this particular physiological constraint (66).

Although heterotrophic marine microorganisms require external carbon resources, previous analyses have shown that inorganic nutrients can be among factors that contribute to limitations on their growth rate, abundance and production (7,15,70,71). Specifically in estuaries, allochthonous carbon sources are predicted to augment autochthonous carbon, potentially alleviating carbon limitation of heterotrophic microbes (15). Additionally, other regulating environmental factors, such as temperature and salinity, have been highly correlated to heterotrophic community dynamics in estuaries (55). Estuarine systems are therefore ideal to evaluate the potential impacts of inorganic nutrients on heterotrophic groups defined by varying nucleic acid physiology in order to potentially provide important insight into their ecology.

The purpose of this study was to characterize temporal variability of abundance and relative nucleic acid content among three heterotrophic groups, LNAB, MNAB and

HNAB, in the Trinity River Basin of Galveston Bay where episodic freshwater discharge influences nutrient availability (72). We hypothesize that heterotrophic temporal dynamics will be related to *in situ* nitrogen or phosphorous concentrations and that physiologically distinct heterotrophic groups will have different responses to nutrient enrichment based on potential differences in ecological strategy.

2.2 Study Location

Galveston Bay (Texas) is 1554 km^2 in area (Figure 2.1) making it the 7^{th} largest estuary in the United States and the second largest in the western Gulf of Mexico (73–75). Its watershed includes two major metropolitan areas Dallas/Ft. Worth and Houston, as well as large industrial and agricultural areas (73,74). Galveston Bay is considered a shallow estuary, with an average depth of 2-3 m and physical wave dynamics are primarily wind driven (76,77). Previous research has estimated the whole system residence time at an average of 0.035 d^{-1} for 30 days (75). Exchange with the Gulf of Mexico is limited to a narrow channel (Figure 2.1) and the bay experiences tidal ranges between 0.1 and 0.5 m (75). Two rivers, the San Jacinto and the Trinity contribute freshwater inputs that are influenced by seasonal rainfall (74). Significant negative correlations between salinity and either nitrate and phosphorous have been observed close to the Trinity River mouth, suggesting river driven nutrient inputs to the Bay (72). Prolonged elevated nutrient inputs have contributed to Galveston Bay becoming one of the most eutrified systems in the Gulf of Mexico (78). Dominant nitrogen sources include agriculture and sewage waste constituting 87.6% of the total nitrogen input to Galveston Bay (73).

Nutrient flux and hydraulic displacement associated with freshwater inflow dynamics have been documented to influence phytoplankton populations in Galveston Bay (75). The spatiotemporal availability of nitrogen (N), phosphorous (P) and a combination of both has been observed to limit overall primary productivity (74,75,79). Additionally, of five significant fish kills in Galveston Bay since 1971, four can be attributed to low dissolved oxygen or toxic algal blooms linked to bay-wide nutrient

dynamics (80). Despite several research initiatives examining the total phytoplankton community in Galveston Bay, to the authors' best knowledge resident marine heterotrophic and autotrophic pico- and nano-plankton have not been extensively studied.

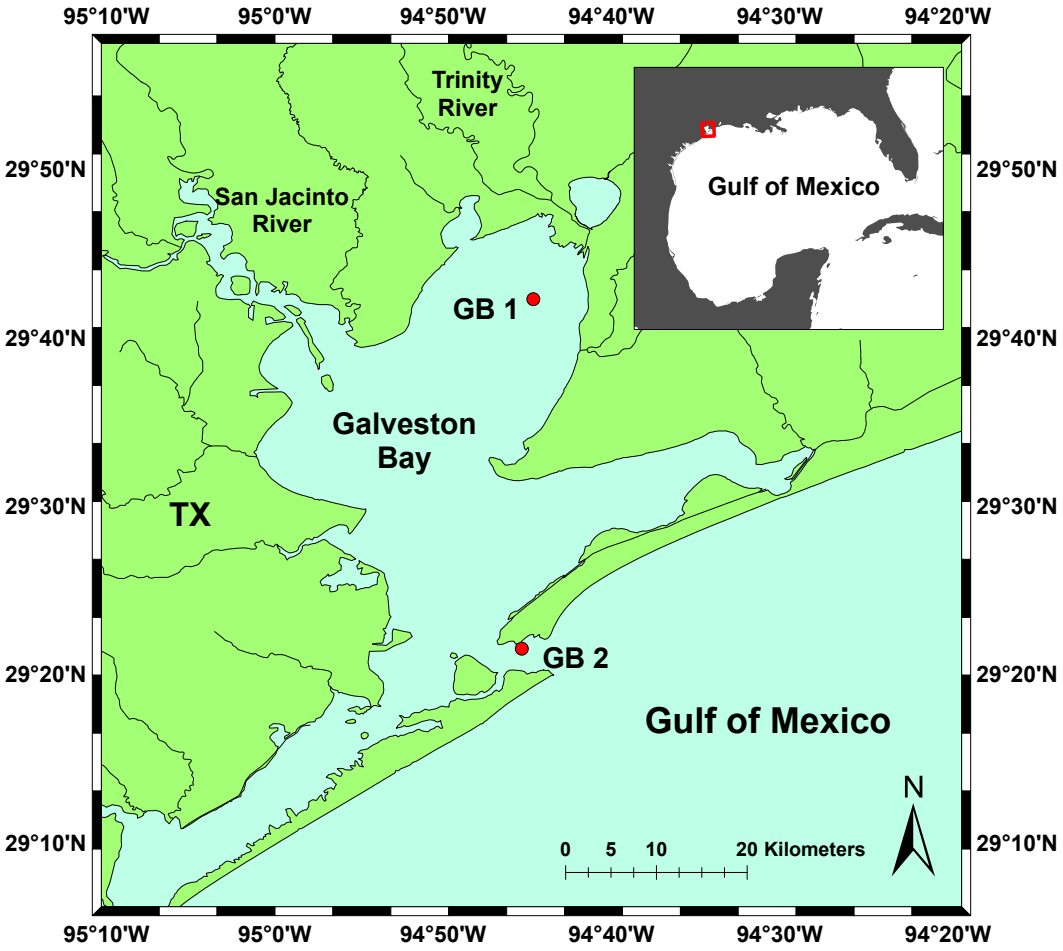

Figure 2.1 Map of Galveston Bay. Station GB1 is located at the mouth of the Trinity River where large freshwater inflow events contribute to temporal variability in environmental conditions. Station GB2 is located at the mouth of the bay, in the tidal exchange channel. Temporal variability in environmental conditions at this station are predominantly influenced by the Gulf of Mexico.

2.3 Methods

2.3.1 Sampling Procedures

Surface water samples (top 1 m) were obtained onboard the RV Phyto I at monthly intervals for 9 months beginning in March of 2013 and ending in January of 2014 at station GB1 (29.70°N, 94.74°W). Poor weather conditions prevented sampling in July and September. *In situ* abiotic data were collected simultaneously to biological sampling each month. Temperature (°C), salinity (unit-less practical salinity scale), pH and conductivity (mS cm^{-1}) were obtained using a *Dataflow* apparatus calibrated and geo-referenced with a GPS, to rapidly quantify physicochemical variables from ~10 cm below the surface (81). Water transparency (m) was determined by deployment of a 20 cm diameter Secchi Disk Code 1062 (LaMotte Company, Maryland, USA).

Freshwater inflows (FWI) from the Trinity River were obtained from a USGS monitoring station (Trinity River at Romayer; USGS gauge 08066500). Antecedent flow (volume discharged, $m^3 s^{-1}$) was determined by taking an average of the volume discharged on the sampling date and the five previous days. This time frame was validated by preliminary tests showing microbial responses to nutrient enrichment within <5 days (data not shown).

The concentration of the total suspended solids (TSS) (mg L^{-1}) was obtained by filtering water (150 mL) through a pre-combusted (400°C, 5 hrs), pre-weighed 0.7 μm glass fiber filter (GF/F, Whatman, Kent, UK) and rinsed with double deionized water before drying at 60°C for a week and re-weighing. Determination of dissolved nitrate (NO_3^-), nitrite (NO_2^-), ammonium (NH_4^+), phosphate (P_i) and silicate ($HisO_3$) concentrations (μmol L^{-1}) was achieved by filtering water (50 mL) through a GF/F to remove particulates; filtrate was then stored in sterile centrifuge tubes at -20°C until processing. Total nitrogen and phosphorus concentrations were determined on the same unfiltered sample. All nutrients were determined using an auto-analyzer (Astoria-Pacific, Clackamas, OR) at Texas A&M University Geochemical and Environmental Research Group. Resulting data were quality checked against replicated standards and were

significantly correlated ($r \geq 0.99$). The ratio of inorganic nitrogen (DIN) to P_i was calculated after summing the dissolved nitrogen inputs ($DIN = NO_3^- + NO_2 + NH_4^+$).

Concentrations of dissolved and total organic carbon (DOC, TOC; mg L^{-1}) were determined on a Shimadzu TOC-L (Shimadzu, Columbia, MD) for three replicates of each sample against a standard calibration curve. Standards of potassium hydrogen phthalate at 0, 1, 2 and 5 mg L^{-1} comprised the calibration curve. Inorganic carbon was removed from each sample with 1N HCL. Ultrapure air was used as the carrying and purging gas, and calibration was validated after every 10 samples (82,83).

Gross primary productivity (g C m^3 d^{-1}) was calculated based on dissolved oxygen concentration pre- and post incubation of water under light or dark conditions. Water was collected into 300 mL glass Wheaton Biological Oxygen Demand (BOD) bottles with glass stoppers in triplicate for each treatment. Light bottles were incubated under shade cloth providing a 50% reduction of sunlight. BOD was determined after a minimum of 2-hour incubation using a portable Luminescent/Optical Dissolved Oxygen Probe HQ-40D (HACH, Loveland, CO).

2.3.2 Bioassay Incubations

Bioassays were conducted for every *in situ* sampling event. Water samples were collected from the surface (top 1 m) and distributed to triplicate pre-acid washed carboys (4 L) for control and two nutrient enrichment treatments (total of 9 carboys). All sampling equipment was cleaned with distilled water between stations and rinsed with sample water three times. Nitrogen ($NaNO_3$) and a combination of nitrogen and phosphate (NaH_2 PO_4 H_2O) were added to their respective enrichment category (+N) or (+N+P), corresponding to f/2 medium (https://ncma.bigelow.org/algal-recipes). Carboys were deployed into mesocosm corrals within the Texas A&M University at Galveston boat basin, which experiences similar environmental conditions to the adjacent Galveston Bay including natural wave and tidal motions as well as ambient diel cycles of light and dark (shade cloth provided a 50% reduction of surface sunlight) (79,84).

Initial (*in situ)* and incubated water were sampled from each replicate carboy (i.e. in triplicate) at 0, 24, 48, 72, 96, 120, 144 and 168 hours. For the purposes of this study, we compared enriched treatments individually to the control using all data from the 168-hour incubation and also at each 24-hour interval to examine overall and higher resolution dynamics patterns. Plankton were isolated for flow cytometric analysis by passing 1mL of sample water through a 20 μm mesh-size sieve into sterile 1.5 mL microcentrifuge tubes containing 0.2 μm filtered paraformaldehyde and molecular biology grade gluteraldehyde at final concentrations of 1% and 0.01% respectively (85). All samples were stored at -20°C and maintained frozen until processing for flow cytometry. The preservation method employed herein considered previous reports that storage temperature (4°C or flash freezing to -80°C) had little effect on cell loss or histogram visualization (85) and that these biases were reduced when combining both paraformaldehyde and gluteraldehyde as fixatives (62). A 20 μm sieve was chosen with recognized constraints associated with flow cytometry in mind but primarily because it allowed us to focus on the nano (<2 μm) and pico (2-20 μm) plankton size fractions.

2.3.3 Flow Cytometry

Plankton were stained with SYBR Green I following procedures modified from Marie et al. (86) and enumerated on a Gallios^{TM} 3-laser flow cytometer (Beckman Coulter, Brea, CA). Aliquots of preserved sample were stained with 1/1000 diluted 10000X concentrated SYBR Green I (Invitrogen, Carlsbad, CA). SYBR Green staining and persistent fluorescence was enhanced by the addition of potassium citrate (30 m mol L^{-1} final concentration) to each sample (86). Preliminary experimentation indicated that increased temperature during incubation resulted in significantly greater (students paired two-tailed t-test, $p \leq 0.05$) SYBR Green I binding efficiency in both naturally pigmented and non-pigmented cells with this cytometer (data not shown). Therefore, incubation was carried out at ~60°C for 15 min. Internal size (10 μm) and enumeration (973 beads μL^{-1}) standard flow count fluorophores were added to each sample tube post incubation (Beckman Coulter, Brea, CA.). Fluorescence was evaluated on particles isolated within

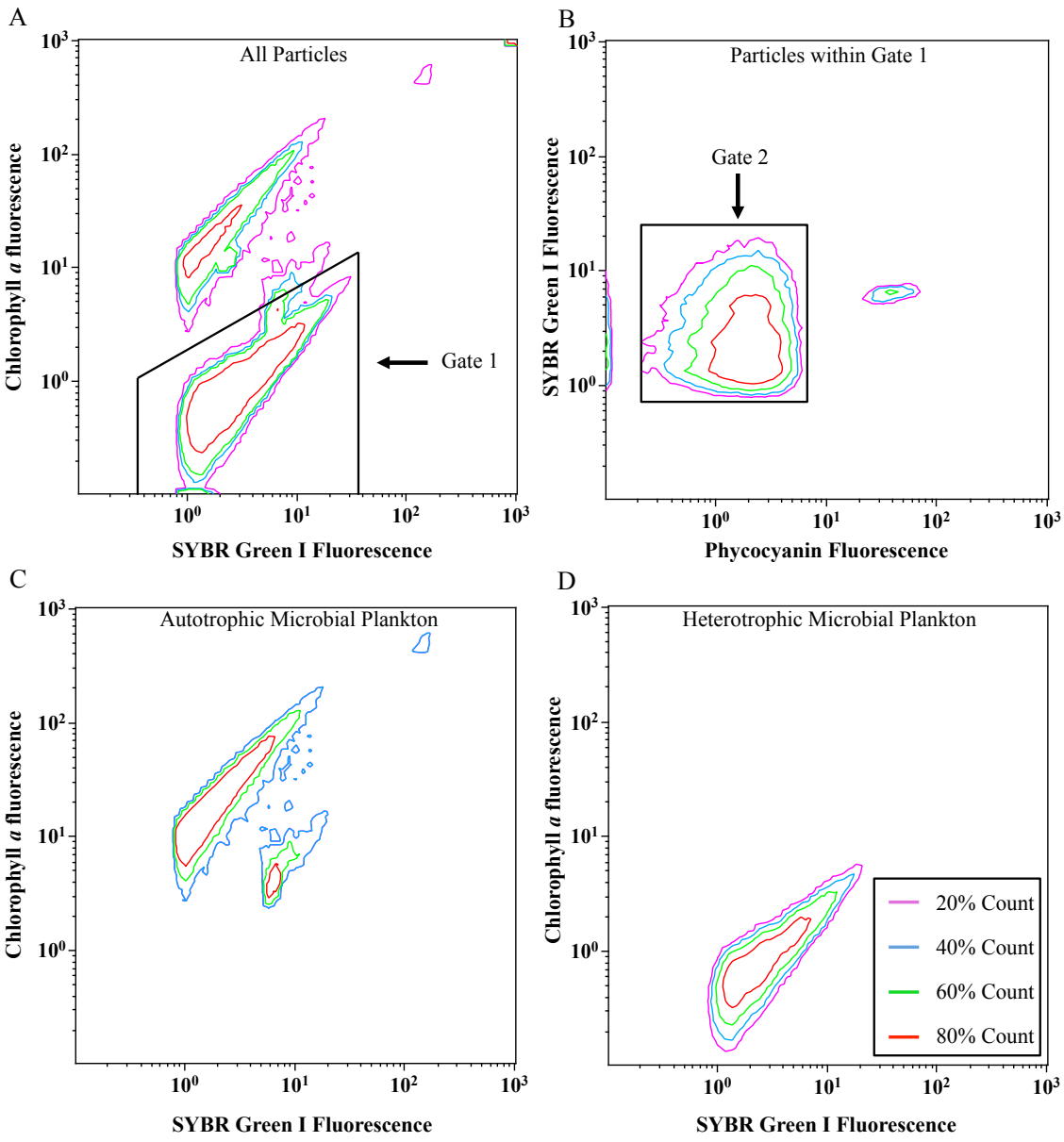

Figure 2.2 Cytograms visualizing microbial plankton groups of similar physiological characteristics. Magnitude of fluorescence is plotted on a logarithmic scale (x and y axes) and colored lines represent percentage of total count. (A) Gate targeting heterotrophic microbial plankton with Chlorophyll a fluorescence ≤10, SYBR Green I fluorescence ≥1. (B) Gate isolating heterotrophic microbial plankton with phycocyanin and SYBR Green I fluorescence (≤10, ≥0) respectively. (C) Cytogram plotting Boolean gate of particles within gate 2 subtracted from all particles resolving the autotrophic plankton. (D) Cytogram plotting a Boolean gate of all particles within gate 2, resolving the heterotrophic plankton.

IsoFlow sheath fluid (Beckman Coulter, Brea, CA) and exposed to 488 nm and 638 nm excitation by lasers. Light scatter generated from particle disruption of the laser was collected from a low-angle, referred to as forward angle light scatter (52). SYBR Green I emission maximum of 522 nm was targeted by collection through a 525 nm band-pass filter ± 15 nm. Chlorophyll *a* emission maximum of 667 nm was targeted by collection through a 695 nm band-pass filter ± 15 nm. Phycoerythrin emission maximum of 576 nm was targeted by collection through a 575 band-pass filter ± 15 nm. Phycocyanin emission maximum of 642 nm was targeted by collection through a 660 nm band- pass filter ± 15 nm. Samples were analyzed for 5 min. at a flow rate of 4-8 μL $min.^{-1}$ discriminating on SYBR Green I fluorescence.

Data analysis was conducted using Kaluza Cytometry Analysis software (Version 1.2 Beckman-Coulter, Brea, CA). For this study, only the heterotrophic fraction of microbial plankton was targeted. Heterotrophic cells were discriminated from other particles by applying Boolean gating to a combination of bivariate logarithmic scale scatter plots (cytograms) of SYBR Green I, orange, and red fluorescence (Figure 2.2). Particles defined as heterotrophs using this method are likely to be bacteria (86), but the authors acknowledge that eukaryotic nano- and pico-heterotrophs may be contributing to counts within this size range. Cells were grouped by similarity in nucleic acid content resolved with SYBR Green I Fluorescence on the basis of previously reported thresholds observed in the environment and culture verification (60,61,86). Three groups were resolved including low nucleic acid containing bacteria (LNAB), medium nucleic acid containing bacteria (MNAB) and high nucleic acid containing bacteria (HNAB) (60,61) (Figure 2.3). The relative abundance of the three heterotrophic groups is herein defined as heterotrophic community structure.

To quantify abundance (cells mL^{-1}), the volume of sample measured during flow cytometry was calculated by dividing the number of beads counted by the number of internal beads uL^{-1} in the sample. To quantify noise, an aliquot of each sample was filtered through a 0.2 μm sterile syringe filter (VWR, Radnor, PA) and processed immediately following each sample. Percent noise was eliminated by subtraction.

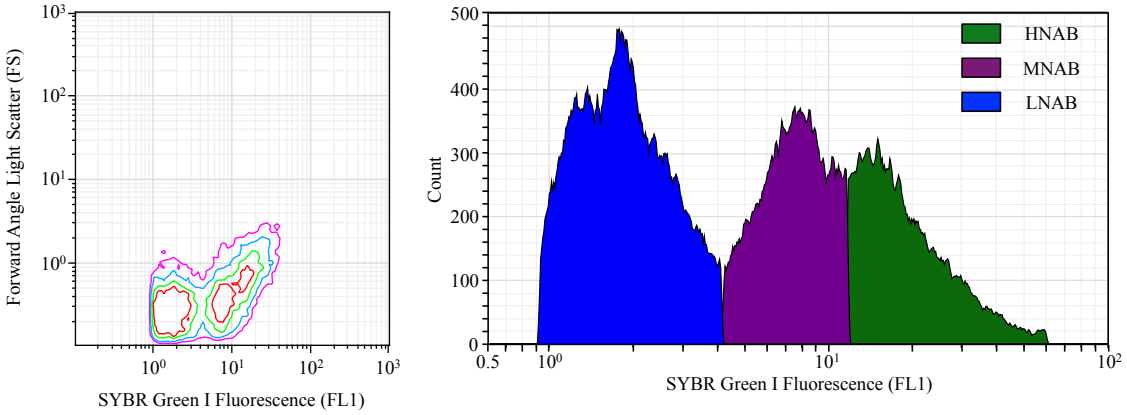

Figure 2.3 Cytogram and histogram visualizing thresholds for heterotrophic group identification. Thresholds were identified based on SYBR Green I fluorescence representing relative nucleic acid content. Approximate ranges for LNAB (0-4), MNAB (4-11) and HNAB (≥11) are shown.

2.3.4 Statistical Evaluation

Analyses were performed using PRIMER V6.1.15 and PERMANOVA V1.0.5 (87,88). A second-stage comparison of dissimilarity matrices for untransformed, square-root, fourth-root and log (X+1) transformation options (Figure 2.4) was conducted for both abiotic and biotic data. This process was conducted in order to select appropriate transformation procedures to reduce skewedness, increase linearity. The least severe transformation that correlated most strongly to all other transformation possibilities and maximized linearity in draftsman plots was selected (Figure 2.4F). In addition draftsman plots were generated and evaluated in order to eliminate collinear variables from further analysis (Figure 2.5). Non-collinear variables included in the analysis had correlations $|r| \leq 0.90$ which is a more stringent threshold than suggested by Anderson et al. (87) in order to further reduce model bias. Ultimately, abiotic data were square-root transformed and then normalized to account for differences in units of measurement and analyzed using Euclidean distance dissimilarity resemblance matrices. Heterotrophic abundance data were fourth-root transformed. Although this is biological data, because no zeros

were present, these data were also analyzed using Euclidean distance dissimilarity resemblance matrices (87,88).

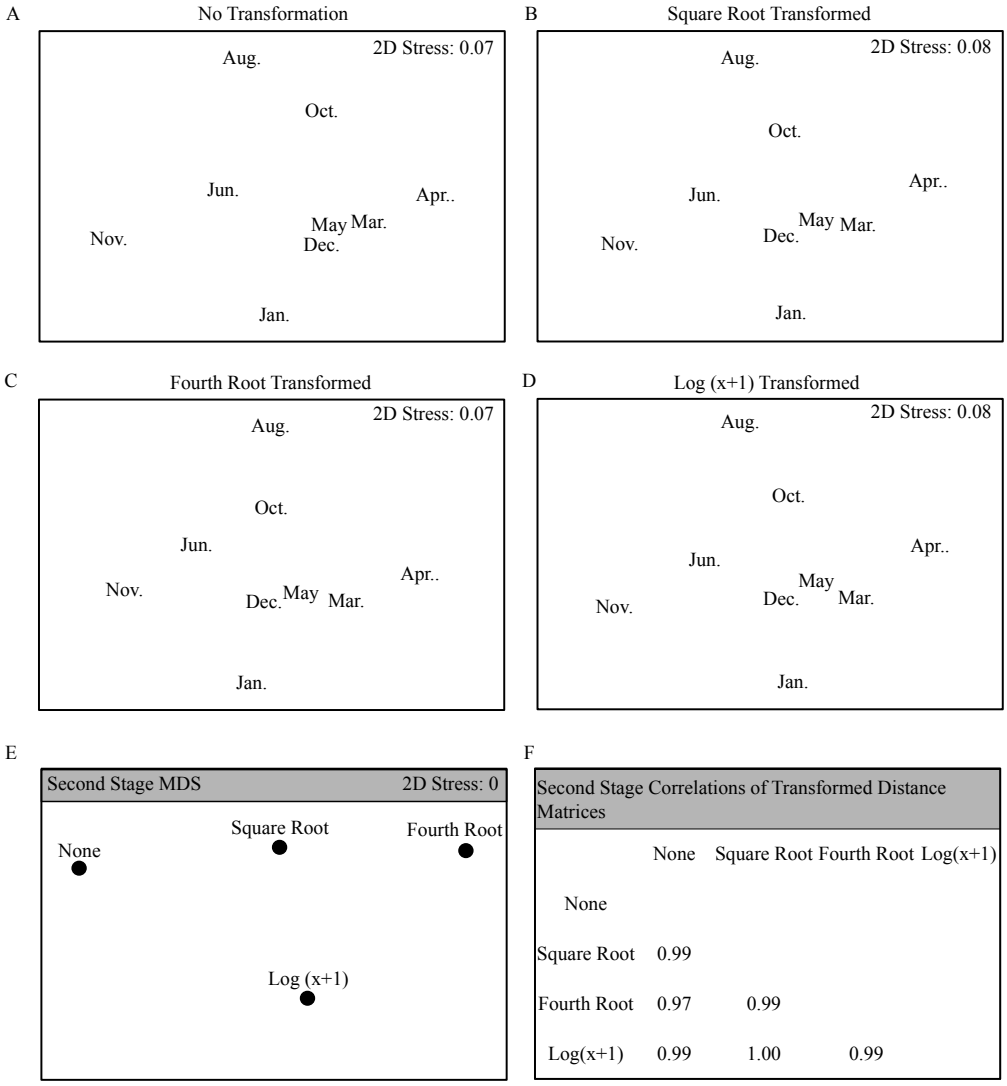

Figure 2.4 Abiotic parameters exposed to different transformations. Non-parametric multi-dimensional scaling ordinations (nMDS) of temporal variability in abiotic parameters (A) No transformation. (B) Square-root transformation. (C) Fourth-root transformation. (D) Log(x+1) transformation. (E) nMDS visualizing a second-stage correlation between the individual transformation patterns. (F) Spearman ρ values for correlations between different transformation options.

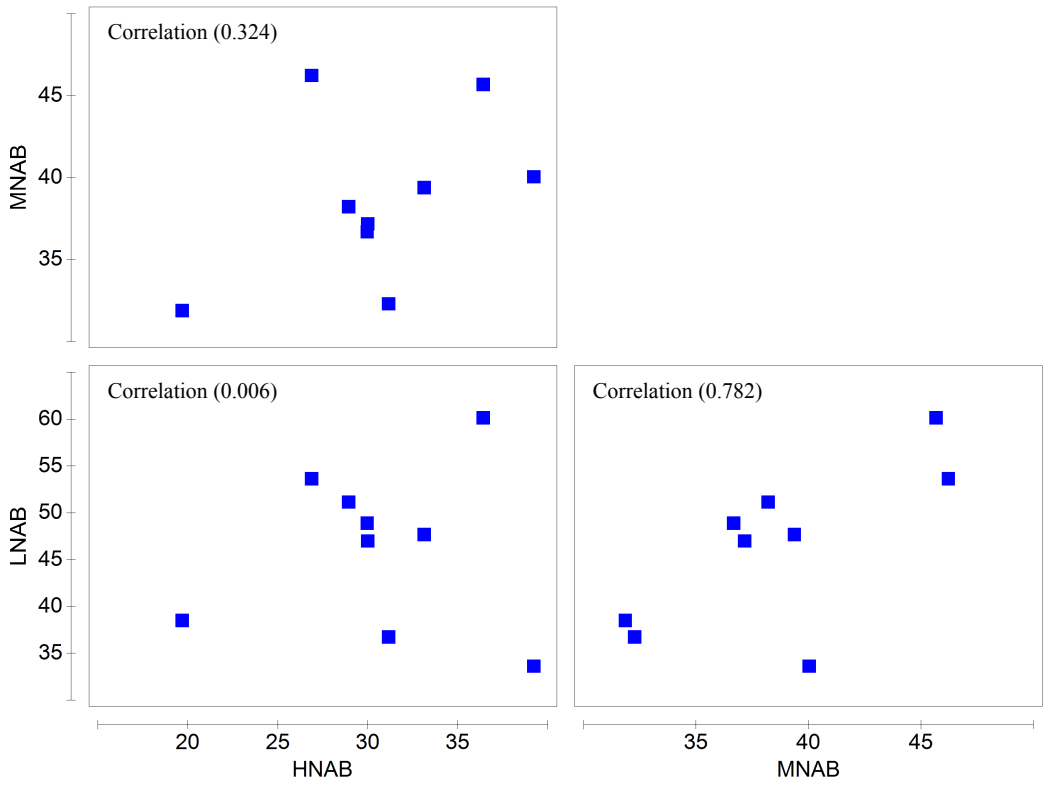

Figure 2.5 Draftsman plots of microbial groups (LNAB, MNAB and HNAB). Visualizes correlations to verify linearity. Spearman ρ values are ≤0.90 indicating that these variables are not beyond the colinearity threshold for statistical evaluation.

Significant *in situ* variability of individual heterotrophic groups (LNAB, MNAB or HNAB) through time was determined using type III partial sums of squares PERMANOVA main-test with unrestricted permutation for the fixed factor month (n=9). Hierarchical cluster (CLUSTER) and similarity profile (SIMPROF, 97% similarity, 9999 permutations) analyses were performed on combined *in situ* data (abiotic: 13 non-collinear parameters) and (biotic: 3 non-collinear groups) to evaluate temporal variability in overall environmental conditions and heterotrophic community structure. Significant differences identified by clusters in SIMPROF were verified by subsequent type III (partial) sums of squares PERMANOVA pairwise tests where permutation of data was unrestricted using a single factor assigned according to the clustered groups (87). Non-parametric multi-dimensional scaling (nMDS) ordinations were used to

visualize dissimilarities in environmental conditions through time. The nMDS two-dimensional representation is considered acceptable for interpretations when the stress is less than 0.1 (88). Relationships among individual abiotic parameters and their variability through time were visualized using spearman derived correlated vectors (88). Dendrograms were used to visualize statistical variability in heterotrophic community structure through time (88).

Environmental predictor variables significantly correlated to temporal changes in heterotrophic community structure were identified using distance-based linear modeling (DISTLM). Models were generated using all possible combinations of predictor variable inputs with the "BEST" selection technique and the Akaike information criterion corrected (AICc) which, as in this study, is optimally applied to situations where the number of abiotic predictor variables is greater than biological variables (87,88). The amount of variability in biotic data explained by the environmental predictor variables identified by the model was quantified within DISTLM. Secondary clustering of biotic data was conducted based on significantly correlated environmental predictor variables using the LINKTREE and SIMPROF analyses (97% similarity, 9999 permutations) (89). Environmental thresholds were determined by successive binary division of predictor variable data and utilized to re-cluster biotic data (89).

Responses of heterotrophic community structure to enrichment with +N or +N+P were evaluated each month by comparison to control treatments. The overall impact of nutrient enrichment was determined using data from all samples obtained over the 168-hour incubation period and was analyzed using a one-way Analysis of Similarities (ANOSIM) test for the fixed factor of treatment (control, +N, +N+P). Response to nutrient enrichment was considered significant if random permutations of the data achieving an R statistic greater than the actual (non-permuted real data) R statistic were <5 out of 9999 permutations ($\alpha \leq 0.05$).

A type-III partial sums of squares PERMANOVA design with unrestricted permutations of raw data was used to evaluate pair-wise comparisons between treatments at each twenty-four hour interval over the 168-hour incubation. The two fixed

factors incubation time (24, 48, 72, 96, 120, 144 and 168 hours) and treatment (control, +N, +N+P) were crossed to evaluate potential interactions among these factors based on the PERMANOVA main test. Shifts in heterotrophic community structure in response to nutrient enrichment were considered significant if the P(Perm) ≤0.05 under >9900 permutations. In cases where >9900 permutations were not possible, an approximate *p*-value (considered significant if α ≤0.05) was determined using Monte Carlo random sampling of the asymptotic permutation distribution (87). Although this experimental design is considered a repeated measures test, the potential for correlation structure through time to confound significant treatment test results was minimized by the underlying randomization of samples in ANOSIM or PERMANOVA analyses (87).

Table 2.1 Collinearity of abiotic parameters at GB1. Spearman correlation ρ values among individual abiotic parameters. Salinity was correlated to conductivity and freshwater inflow (FWI) beyond the threshold of collinearity (ρ ≤ 0.90). Total phosphorous (Total P) and dissolved inorganic phosphorous (Pi) were also collinear. Therefore, salinity and Pi were included in statistical analyses as representatives of their collinear parameters.

	Temperature	Salinity	pH	Conductivity	Secchi	GP	Pi	HSiO3	Total N	Total P	TSS	DOC	TOC	FWI	DIN	DIN:Pi
Temperature																
Salinity	-0.16															
pH	-0.33	-0.06														
Conductivity	-0.09	**0.99**	-0.07													
Secchi	-0.04	-0.09	-0.72	-0.10												
GP	-0.12	-0.48	-0.21	-0.48	0.59											
Pi	0.53	-0.27	0.07	-0.17	0.07	0.38										
HSiO3	0.50	-0.61	0.13	-0.54	0.03	0.60	0.77									
Total N	0.09	-0.62	0.45	-0.65	-0.07	0.08	0.08	0.39								
Total P	0.54	-0.37	0.23	-0.28	-0.12	0.20	**0.95**	0.72	0.27							
TSS	0.49	-0.04	0.55	-0.02	-0.65	-0.38	0.36	0.31	0.42	0.56						
DOC	0.56	-0.40	0.45	-0.31	-0.45	-0.06	0.70	0.73	0.44	0.79	0.62					
TOC	-0.24	0.78	-0.33	0.71	0.14	-0.45	-0.58	-0.86	-0.50	-0.60	-0.17	-0.78				
FWI	0.07	**-0.90**	-0.18	-0.87	0.27	0.59	0.25	0.51	0.27	0.24	-0.32	0.23	-0.70			
DIN	-0.41	-0.55	0.01	-0.52	0.29	0.60	0.25	0.25	0.07	0.23	-0.38	-0.03	-0.43	0.63		
DIN:Pi	-0.63	-0.44	0.24	-0.44	-0.08	0.22	-0.23	-0.08	0.13	-0.15	-0.31	-0.16	-0.26	0.45	0.82	

Visualization of heterotrophic plankton responses to nutrient enrichment was achieved using histograms for the total 168-hour incubation and using nMDS ordinations

for pairwise comparisons at each 24-hour interval. Concentrations of heterotrophic groups as defined by nucleic acid content were represented on the ordinations by Spearman correlated vectors.

2.4 Results

2.4.1 In situ *Abiotic Conditions*

Collinearity based on a threshold of $|r| \geq 0.90$ was detected among abiotic parameters measured throughout the sampling term in the Trinity River Basin. Salinity was correlated to conductivity (r=0.99) and also negatively correlated to FWI (r=-0.90) (Table 2.1). Similarly, P_i and Total P were strongly correlated (r=0.95) (Table 2.1). Salinity and P_i were chosen to represent their collinear parameters in subsequent statistical analyses. Significant temporal variability was observed in environmental conditions based on the relationships between co-occurring individual parameters (SIMPROF, $p \leq 0.01$, PERMANOVA, p=0.0005).

Table 2.2 Environmental conditions at station GB1. Non-collinear physical and chemical parameters in surface water (~1m depth) at station GB1 measured at approximately monthly intervals from March 2013 through January 2014.

Time-point	Temperature (°C)	Salinity	pH	Secchi (m)	TSS (mg L^{-1})	Gross Prod. (g C m^{-2} d^{-1})	Pi (µmol L^{-1})	HSiO3 (µmol L^{-1})	DIN (µmol L^{-1})	DIN:Pi (µmol L^{-1})	Total N (µmol L^{-1})	DOC (mg L^{-1})	TOC (mg L^{-1})
March	14.61	18.68	8.29	0.79	0.02	0.46	1.03	16.84	0.23	0.22	68.36	8.48	17.74
April	19.83	20.71	8.05	0.65	0.03	0.52	1.10	12.11	0.21	0.19	41.97	5.53	21.14
May	19.63	16.21	8.18	0.69	0.03	0.99	0.76	49.57	0.62	0.82	64.72	8.15	16.00
June	28.12	10.55	8.09	0.69	0.02	1.02	1.71	71.46	0.44	0.26	66.02	12.52	12.24
August	29.56	14.00	8.56	0.47	0.11	0.73	4.43	92.40	0.01	0.01	77.60	17.31	13.07
October	27.51	17.64	8.22	0.60	0.03	0.71	4.95	74.37	1.44	0.29	49.41	16.07	13.01
November	14.72	10.10	8.22	0.88	0.02	2.14	3.59	75.61	11.08	3.09	66.92	9.66	12.49
December	10.33	17.69	8.49	0.60	0.02	1.48	1.71	53.54	1.14	0.67	53.84	9.28	14.24
January	12.25	13.89	8.62	0.35	0.04	0.28	0.69	25.34	2.40	3.48	65.84	11.87	14.07

Temperature ranged more than 19 °C during the nine month sampling period with its maximum (29.6 °C) and minimum (10.3 °C) observed in August and December, respectively (Table 2.2). Two months of reduced salinity were observed in June (10.6)

and November (10.1) (Table 2.2). Several important relationships between salinity and other abiotic parameters existed, supporting the importance of temporal FWI dynamics to this location (Figure 2.6). The relationships between salinity and P_i, $HSiO_3$, DIN,

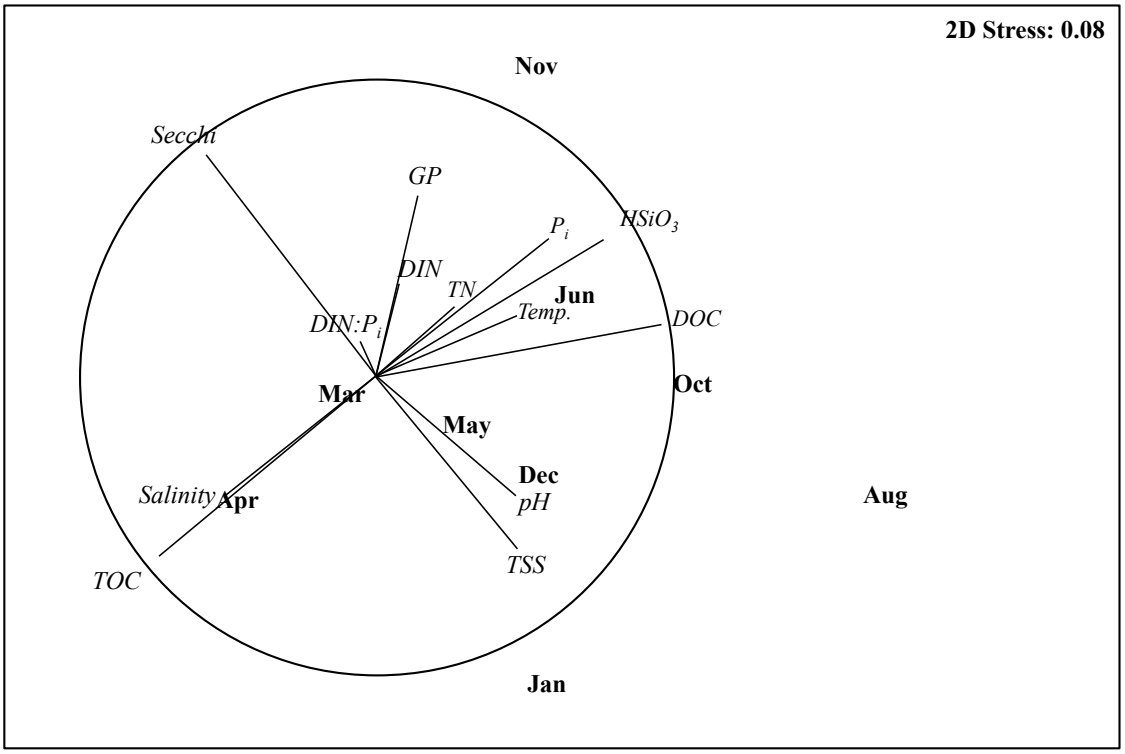

Figure 2.6 nMDS ordination of temporal variability in measured abiotic parameters at GB1. Spearman correlations for each individual abiotic parameter to the overall variability in environmental conditions (combined abiotic parameters) during each month are identified. Line length within the frame of reference circle represents the relative strength of the correlation and direction corresponds to a positive relationship.

$DIN:P_i$, and TN were all negative (Figure 2.6), suggesting freshwater inputs of dissolved and total inorganic nutrients to the Trinity River Basin. While the relationship of salinity with DOC concentration was also negative, a positive correlation was observed with TOC concentration (Figure 2.6). Gross primary production was also negatively

correlated with salinity (Figure 2.6) connecting freshwater driven nutrient availability to phytoplankton production. A negative relationship was observed between TSS concentration and turbidity (Figure 2.6). Water transparency was high during November (0.9 m) corresponding to low TSS (0.02 mg L^{-1}) and low during August (0.5 m) corresponding to high TSS (0.11 mg L^{-1}) (Table 2.2).

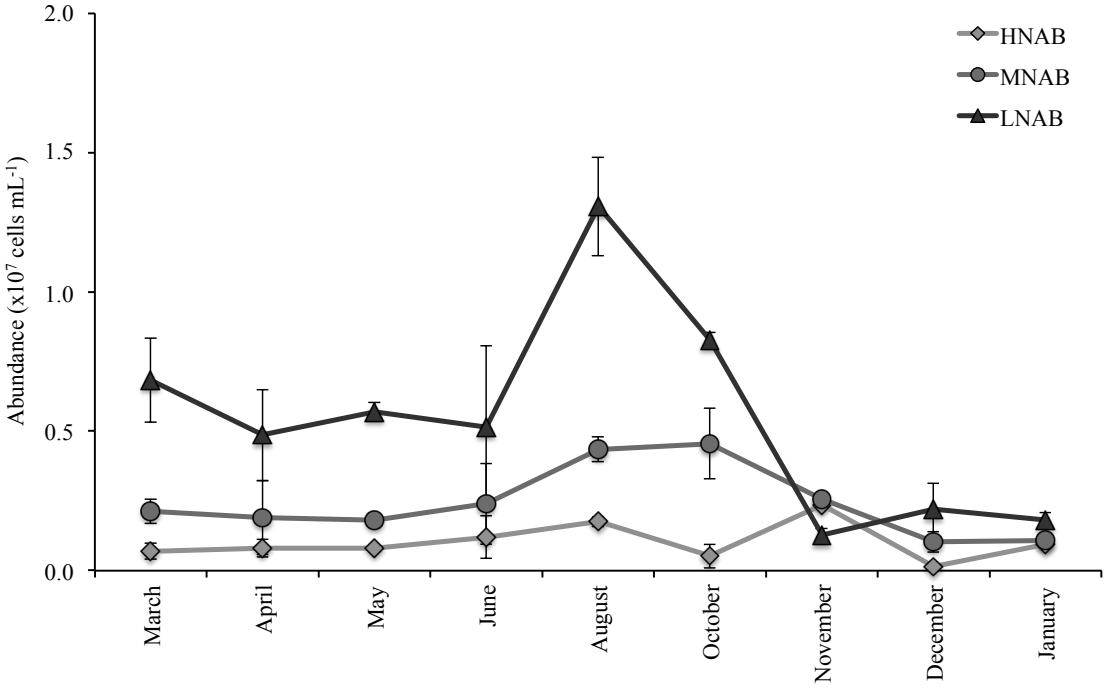

Figure 2.7 Abundance (cells mL^{-1}) of the three heterotrophic groups identified at station GB1 from March 2013 through January 2014. These values were derived from an average of three replicates for each sample.

2.4.2 In situ *Heterotrophic Group Abundance*

The abundance of LNAB varied significantly through the nine month sampling term (PERMANOVA p=0.0001). The maximum concentration of LNAB (1.3 $x10^7 \pm 1.8$ $x10^6$) was observed in August and the minimum concentration (1.3 $x10^6 \pm 2.4$ $x10^5$) was

observed in November (Figure 2.7). The abundance of MNAB varied significantly through the nine month sampling term (PERMANOVA p=0.0014). The maximum concentration of MNAB (4.6 x10^6±1.3 x10^6) was observed in October and the minimum concentration (1.0 x10^6±3.7 x10^5) was observed in December (Figure 2.7).

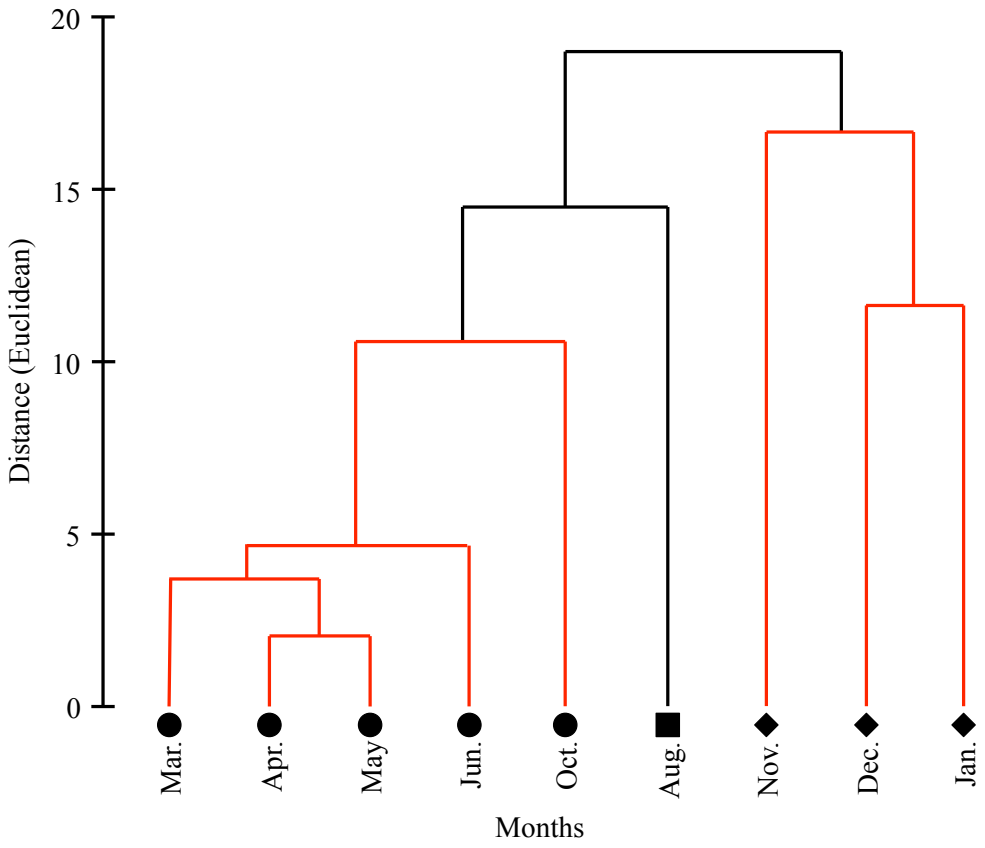

Figure 2.8 Dendogram of group average hierarchical cluster analysis based on heterotrophic physiological community structure. Black lines indicate that there is internal multivariate structure in the data at 97% similarity threshold significant ($p \leq 0.01$) based on the SIMPROF test. Red lines indicate a non-significant test result; samples below these intersections are considered homogeneous in physiological community structure. Three significantly different clusters were identified and are visualized by symbols with unique shapes; circles represent samples within cluster 1, squares represent samples within cluster 2 and diamonds represent samples within cluster 3.

The maximum concentration of MNAB ($4.6 \times 10^6 \pm 1.3 \times 10^6$) was observed in October and the minimum concentration ($1.0 \times 10^6 \pm 3.7 \times 10^5$) was observed in December (Figure 2.7). The abundance of HNAB also varied significantly through the nine month sampling term (PERMANOVA p=0.0002). The maximum concentration of HNAB ($2.4 \times 10^6 \pm 7.1 \times 10^4$) was observed in November and the minimum concentration ($1.5 \times 10^5 \pm 5.4 \times 10^4$) was observed in December (Figure 2.7). The relative abundance of LNAB:MNAB:HNAB (herein defined as heterotrophic community structure) varied significantly through time (SIMPROF $p \leq 0.01$). The heterotrophic community structure was homogeneous (SIMPROF, $p \geq 0.01$) during March, April, May, June and October (Figure 2.8).

Table 2.3 Results of distance based linear model. Significant correlations ($p \leq 0.05$) between individual abiotic parameters and variability in heterotrophic physiological community structure are identified using a Marginal Test. The combination(s) of abiotic parameters that are most strongly correlated are identified based on the Akaike information criterion corrected (AICc) and the BEST test.

DISTLM RESULTS		
	Marginal Test	
Variable	p-value	Proportion Variability Explained
Temperature	**0.0045**	50.60%
Salinity	0.2433	17.30%
pH	0.9464	0.00%
Secchi	0.9399	0.00%
Gross Productivity	0.5145	0.01%
P_i	0.1729	21.2%
$HSiO_3$	0.4763	10.49%
Total N	0.5352	0.01%
TSS	0.1167	27.40%
DOC	0.2151	18.93%
TOC	0.7465	0.00%
DIN	**0.0330**	35.09%
DIN:P_i	**0.0065**	47.92%
	Overall BEST Solutions	
Variable	AIC_c	Proportion Variability Explained
Temperature and DIN	42.044	72.27%
Temperature and Salinity	42.281	71.53%

The community structure was significantly different from all other months during August (Figure 2.8) and was homogeneous during November, December and January (Figure 2.8).

2.4.3 Statistical Correlation of in situ *Data*

Three individual parameters, temperature, DIN, and DIN:P_i were significantly correlated with temporal variability in heterotrophic community structure (Table 2.3). A combination of temperature and DIN were the most influential parameters explaining 72.3% of variability (Table 2.3). A second combination of parameters, temperature and salinity, was also strongly correlated explaining 71.5% of variability (Table 2.3).

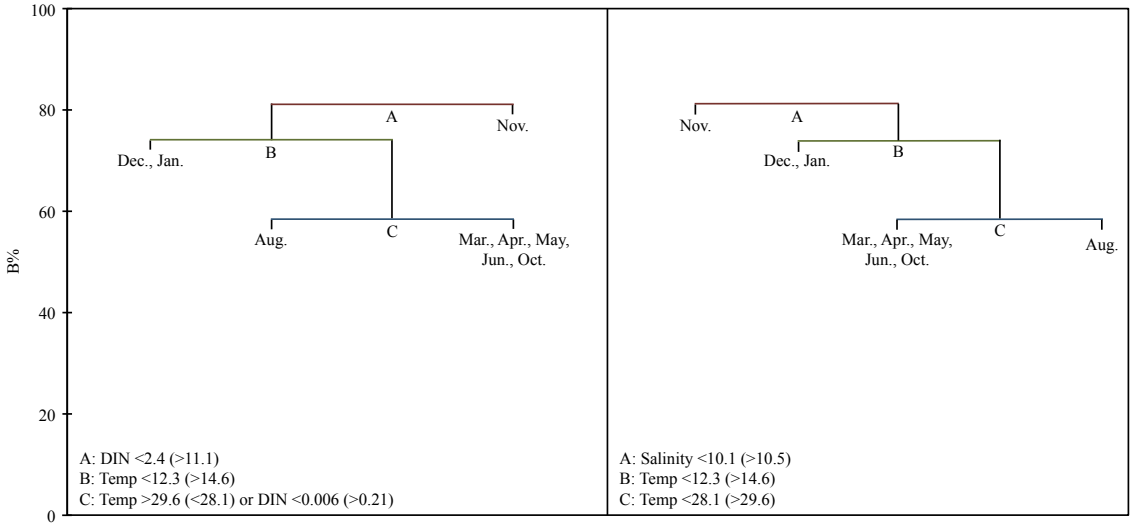

Figure 2.9 Dendogram visualizing clustering inferred from abiotic thresholds. Temporal variability in heterotrophic physiological community structure is segregated based on thresholds derived from binary division of significant abiotic predictor variables identified by DISTLM using LINKTREE. Each binary division A (red line), B (green line), or C (blue line) is significant ($p \leq 0.05$) based on the SIMPROF test. The abiotic factor(s) accounting for clustering to the left are listed first, followed by the factor(s) accounting for the clustering to the right (in parenthesis). The B% indicates dissimilarity between grouping: the higher the B%, the greater the dissimilarity between the cluster.

Thresholds among the abiotic parameters identified by DISTLM were used to statistically organize temporal variability in heterotrophic community structure (Figure 2.9). Using the combination of temperature and DIN (Figure 2.9A), November was segregated (A) based on an *in situ* concentration of DIN (11.1 μmol L^{-1}), higher than other months (all <2.4 μmol L^{-1}). December and January were separated from March, April, May, June, August and October (B) based on having temperatures <14.6 °C. August was separated from March, April, May, June and October (C) because of a warmer temperature (29.6°C), and extremely low DIN concentration of 0.006 μmol L^{-1}. Using the combination of temperature and salinity (Figure 2.9B), November was again segregated from all other months (A) based on salinity <10.5. Remaining temporal variability in relative heterotrophic abundance was associated with temperature as described above. Based on these results, August and November represented 'extreme' environmental conditions during the sampling period and these specific conditions were significantly related to shifts in microbial community structure. Therefore, although all sampling events included corresponding bioassays to access the heterotrophic response to nutrient enrichment, further analysis focused on August and November.

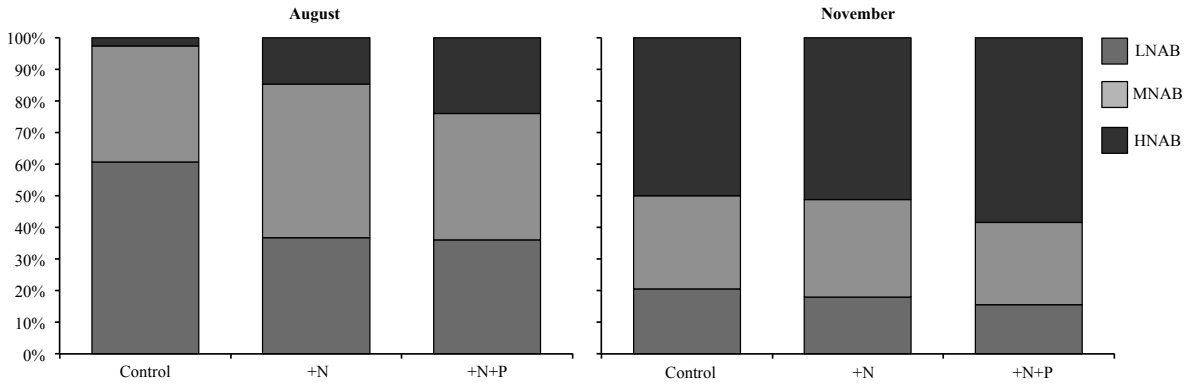

Figure 2.10 Heterotrophic nutrient enrichment response (168-hours). % LNAB, MNAB, and HNAB in the total heterotrophic microbial community (average of all samples in 168 hour incubation period in control, nitrogen (+N) and a combination of nitrogen and phosphorous (+N+P) enrichment treatments. (A) August 2013. (B) November 2013.

2.4.4 Heterotrophic responses to nutrient enrichment

Heterotrophic responses to nutrient enrichment were compared using an average of all samples taken over the 168-hour incubation (i.e. 21 samples, 3 replicates for each 24-hour interval) for the control, and enrichment treatments (N and a combination of N and P additions) in August and November (Figures 2.10 and 2.11). This initial analysis was conducted to examine the overall impact of nutrient enrichment on heterotrophic community structure throughout the 168-hour experiment. In August, the control

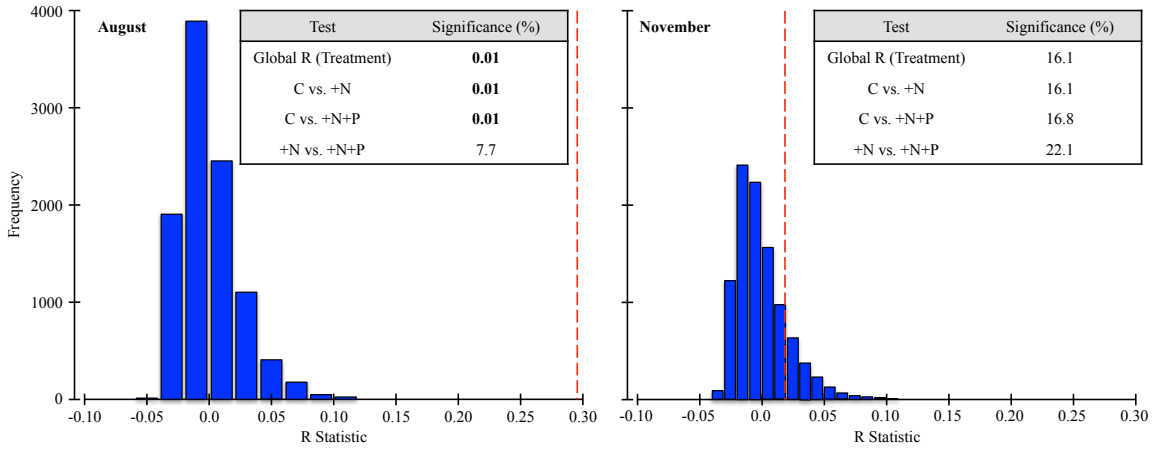

Figure 2.11 ANOSIM of 168-hour nutrient enrichment responses. Histogram of the distribution of the ANOSIM R statistic when data are under permutation and test statistics for a one-way crossed test between the levels of factor: treatment (3 Levels, Control, +N, +N+P) in August and November. Analysis was conduced on all samples taken through the 168-hour incubation. Differences between levels were considered significant if the random permutations of the data achieving an R statistic greater than the actual (non-permuted real data) were <5 out of 9999 permutations (significance level 0.05).

heterotrophic community was composed of 60% LNAB, 37% MNAB and 3% HNAB (Figure 2.10A). When enriched with N, LNAB, MNAB and HNAB comprised 36%, 49% and 15% of the heterotrophic community respectively (Figure 2.10A). When

Table 2.4 Results of main and pair-wise PERMANOVA tests between two factors in August. Three levels of treatment (control, +N, +N+P) and seven levels incubation (24, 48, 72, 96, 120, 144, and 168 hours) were examined. Significant results P(Perm) ≤ 0.05 under >9999 permutations in the main tests indicate an interaction between the two factors (treatment and incubation). Shifts in heterotrophic community structure in response to nutrient enrichment were considered significant if p ≤ 0.05 under >9999 permutations between the control and either +N or +N+P treatments. In cases where >9900 permutations were not possible a Monte Carlo value generated by random sampling of the asymptotic permutation distribution, was utilized. Differences were considered significant if p(MC) ≤ 0.05.

PERMANOVA RESULTS August

Main Test (>9900 Unique Permutations)			
Factor	Degrees of Freedom	Pseudo-F	P(Permutation)
Incubation	6	21.6	**0.0001**
Treatment	2	29.5	**0.0001**
Incubation x Treatment	12	6.8	**0.0001**

Pairwise Test (Incubation x Treatment for levels of Treatment)			
Incubation (Hours)	Treatment	P(MC)	Unique Permutations
24	C vs. +N	**0.0218**	10
	C vs. +N+P	**0.0250**	10
	+N vs. +N+P	**0.0142**	10
48	C vs. +N	0.1274	10
	C vs. +N+P	**0.0001**	10
	+N vs. +N+P	0.1371	10
72	C vs. +N	**0.0047**	10
	C vs. +N+P	**0.0001**	10
	+N vs. +N+P	**0.0020**	10
96	C vs. +N	0.0591	10
	C vs. +N+P	**0.0074**	10
	+N vs. +N+P	0.2729	10
120	C vs. +N	**0.0009**	10
	C vs. +N+P	**0.0003**	10
	+N vs. +N+P	0.5014	10
144	C vs. +N	**0.0358**	10
	C vs. +N+P	**0.0045**	10
	+N vs. +N+P	**0.0476**	10
168	C vs. +N	**0.0038**	10
	C vs. +N+P	0.1232	10
	+N vs. +N+P	**0.0207**	10

enriched with a combination of N and P, LNAB, MNAB and HNAB comprised 36%, 40% and 24% of the heterotrophic community respectively. In November the control heterotrophic community was composed of 21% LNAB, 29% MNAB and 50% HNAB. When enriched with N, LNAB, MNAB and HNAB comprised 18%, 31% and 51% of the heterotrophic community respectively (Figure 2.10B). When enriched with N and P, LNAB, MNAB and HNAB comprised 16%, 26% and 58% of the heterotrophic community respectively (Figure 2.10B). The heterotrophic community structure shifted significantly when enriched by N and a combination of N and P in August (ANOSIM, Global R=0.295, Sig.= 0.01%) (Figure 2.11A) but did not in November (ANOSIM, Global R=0.019, Sig.= 16.1%) (Figure 2.11B). In both months, the difference between enrichment with N or a combination of N and P was not significant (Figure 2.11).

The pattern of heterotrophic response to nutrients at 24-hour intervals within the 168-hour experiment was further analyzed by pairwise Monte Carlo PERMANOVA tests. A significant interaction effect was observed between the treatment (C, N, NP) and incubation length (24, 48, 72, 96, 120, 144, and 168 hours) factors in August (Table 2.4). Significant differences between treatments were observed at all incubation lengths (Table 2.4). In November, significant differences between control and enriched treatments were observed after 96, 120 and 144 hours (Table 2.5). Variability was large between replicates of the N treatment at 48 and 96 hours in August, potentially compromising the detection of significant differences between treatments at those incubation lengths (Figure 2.12A). Significant differences between the enrichment treatments (N or a combination of N and P) were observed at 24, 72, 144 and 168 hours (Table 2.4). Individual heterotrophic groups responded to treatment differently through time. LNAB responded initially (24-48 hours), followed by MNAB and finally HNAB increased abundance after 72 hours (Figure 2.12A). In November, After 96 and 120 hours enrichment with a combination of N and P caused increased HNAB abundance (Figure 2.12). Enrichment with N alone was not significantly different from the control at these time points supporting that phosphorous was the

Table 2.5 Results of main and pair-wise PERMANOVA tests between two factors in November. Three levels of treatment (control, +N, +N+P) and seven levels incubation (24, 48, 72, 96, 120, 144, and 168 hours) were examined. Significant results P(Perm) ≤ 0.05 under >9999 permutations in the main tests indicate an interaction between the two factors (treatment and incubation). Shifts in heterotrophic community structure in response to nutrient enrichment were considered significant if p ≤ 0.05 under >9999 permutations between the control and either +N or +N+P treatments. In cases where >9900 permutations were not possible a Monte Carlo value generated by random sampling of the asymptotic permutation distribution, was utilized. Differences were considered significant if p(MC) ≤ 0.05.

PERMANOVA RESULTS November			
Main Test (>9900 Unique Permutations)			
Factor	Degrees of Freedom	Pseudo-F	P(Permutation)
Incubation	6	152.1	**0.0001**
Treatment	2	4.5	**0.0127**
Incubation x Treatment	12	3.0	**0.0049**
Pairwise Test (Incubation x Treatment for levels of Treatment)			
Incubation (Hours)	Treatment	P(MC)	Unique Permutations
24	C vs. +N	0.5647	10
	C vs. +N+P	0.1944	10
	+N vs. +N+P	0.4960	10
48	C vs. +N	0.2716	10
	C vs. +N+P	0.4121	10
	+N vs. +N+P	0.3007	10
72	C vs. +N	0.7063	10
	C vs. +N+P	0.1457	10
	+N vs. +N+P	0.5948	10
96	C vs. +N	0.2547	10
	C vs. +N+P	**0.0055**	10
	+N vs. +N+P	**0.0454**	10
120	C vs. +N	0.1104	10
	C vs. +N+P	**0.0007**	10
	+N vs. +N+P	**0.0135**	10
144	C vs. +N	**0.0433**	10
	C vs. +N+P	0.1918	10
	+N vs. +N+P	0.2518	10
168	C vs. +N	0.3671	10
	C vs. +N+P	0.6701	10
	+N vs. +N+P	0.1856	10

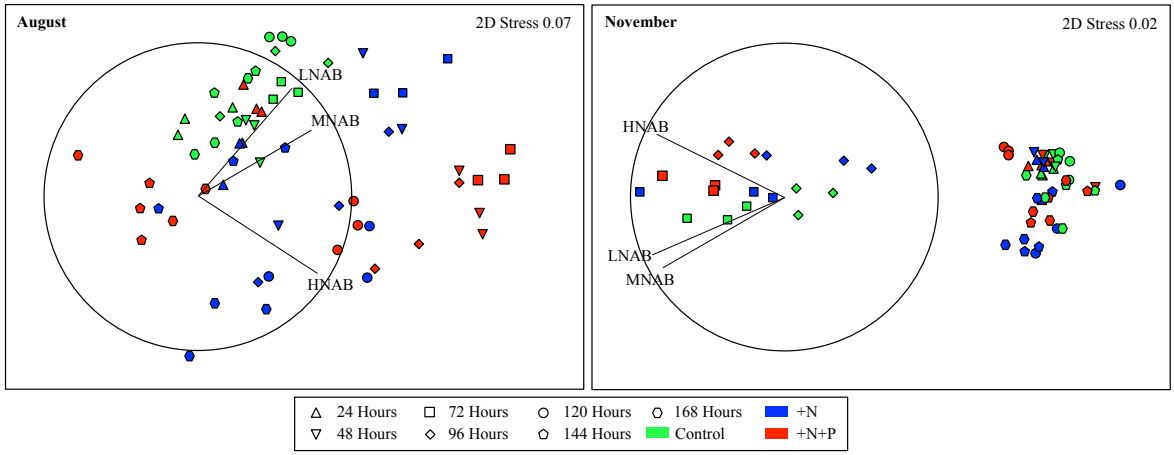

Figure 2.12 nMDS ordinations of variability in heterotrophic physiological community structure in response to two factors, enrichment and incubation. Three nutrient enrichment levels (Control, +N, and +N+P) and seven incubation length levels (24, 48, 72, 96, 120, 144, and 168 hours) were evaluated. Spearman correlations for each individual heterotrophic group to the overall variability in community structure are identified. Line length within the frame of reference circle represents the strength of the correlation and direction corresponds to a positive relationship. (A) Response patterns at 24-hour intervals in August. (B) Response patterns at 24-hour interval in November.

limiting factor (Table 2.5). After 144 hours significant enrichment with N was observed; however, because significance was not detected in the combined N and P treatment this may not be a reflection of nitrogen limitation (Table 2.5). Additionally, an incubation affect was clearly observed based on changes in the control and nutrient enriched replicates after 72 and 96 hours (Figure 2.12B). The impact of incubation was also observed in August, but differences were not as large as the responses stimulated by nutrient enrichment.

2.5 Discussion

Temporal dynamics in physiologically defined heterotrophic groups were significantly correlated to *in situ* nitrogen concentrations, temperature and salinity. Because salinity was included in the statistical analysis as a proxy for FWI, these results

suggest that episodic riverine input of nitrogen impacts estuarine heterotrophic microbes. Concurrent bioassays support that availability of inorganic nutrients can limit heterotrophic abundance and therefore influence the temporal carrying capacity of microbial heterotrophs in estuarine systems. *In situ* variability combined with the timing of significant responses to nutrient enrichment of different physiological groups within the heterotrophic assemblage is consistent with the hypothesis that fractions of the community utilize nutrients with strategies similar to specialists or generalists.

Total abundance of heterotrophic cells followed expected temporal trends that were similar to a previous study reporting heterotrophic dynamics in an estuary with cytometric methods (55). In general total abundance was substantially higher at this station in Galveston Bay compared to a northern temperate estuary, Waquoit Bay, Massachusetts, which is most likely related to the temperature being consistently ≥2°C warmer in Galveston Bay. As examples, August and December had the temperature maximum and minimum in Galveston Bay and in both cases temperature and consequently abundances were higher than Waquoit Bay (1.19×10^7 and 1.95×10^6 cells mL^{-1} higher respectively).

Temporal shifts in microbial heterotrophic physiological community structure (LNAB:MNAB:HNAB relative abundance) were significantly correlated to a combination of temperature and DIN concentration and/or a combination of temperature and salinity. Because heterotrophic variability was not significantly correlated to either TOC or DOC concentrations, it is predicted that carbon concentrations in the Trinity River Basin exceed heterotrophic requirements, potentially due to allochthonous carbon subsidies from the Trinity River. Without carbon control, heterotrophic requirements for inorganic nutrients could ultimately become limiting (15).

In August, temperatures were at a maximum while DIN concentration was at a minimum, corresponding to a physiological community structure where LNAB dominated the microbial heterotrophs. Based on these results it is predicted that the warmer temperatures resulted in increased abundance of LNAB due to faster enzymatic reactions during heterotrophic processes, ultimately leading to the depletion of DIN in

the system and its consequent limitation of microbial heterotrophic abundance. The dominance of LNAB suggests that this fraction was able to outcompete higher nucleic acid containing fractions for DIN, which possibly indicating that they are more specialized to utilize this resource. In November, temperature was considerably lower and salinity was at a minimum but DIN concentration was at a maximum, resulting in a physiological community structure where MNAB and HNAB dominated. Based on these results it is predicted that a high FWI event supplied DIN to the system, alleviating nitrogen limitation and allowing the MNAB and HNAB fractions to be competitive in newly available alternative niches.

August and November represented the maximum and minimum intensity of potential nitrogen limitation in the Trinity River Basin, which is reflected by the most extreme responses in the heterotrophic community. However, heterotrophic group response to 168-hours of enrichment (average of all samples per treatment) indicates that nitrogen limitation may occur consistently at this location. Significant (ANOSIM $p \leq 0.05$) overall enrichment responses to nitrogen were observed in March, April, May, June, August, October, and January. In all of these cases, the shift in heterotrophic community structure was related to an increase in abundance of the relatively higher nucleic acid containing groups. The only exceptions are November (as described above) and December, when the coldest water temperatures were observed, suggesting that temperature is the primary factor controlling heterotrophic abundance at this location. Importantly, these relationships indicate that there are environmental thresholds of DIN concentration (At least >2.4 $\mu mol\ L^{-1}$) that can potentially alter the heterotrophic processing of this substrate, which should likely be considered in future nutrient budgets for monitoring and management strategies.

Direct comparisons to previous studies examining relative abundances of heterotrophic groups defined by nucleic acid content is difficult because in this study three distinct groupings were resolved, which has not typically been observed elsewhere. In two studies conducted in the coastal Gulf of Mexico continental shelf region, four heterotrophic groups were enumerated using cytometry (60,61). In both cases, higher

nucleic acid containing groups were positively correlated to surface Chl *a* concentration, suggesting a link between primary productivity and heterotrophic cells with increased nucleic acid content (60,61). These findings are supported by literature considering only two (LNAB and HNAB) fractions (56,90). Although a direct relationship to inorganic nutrient concentration was not targeted and consequently not observed, Bouvier et al. (56) suggests that while productivity is strongly correlated to the distribution of cells into different nucleic acid containing fractions, other abiotic and biotic factors are also expected to contribute.

An evaluation of HNAB and LNAB dynamics has been conducted in the Waquoit Bay Estuary, a more comparable system to Galveston Bay (55). HNAB concentrations were greater than LNAB during May, June, July and December and were similarly abundant to LNAB in August and October. Contrastingly, in Galveston Bay, the LNAB contribution to total heterotrophic abundance was greater than HNAB and MNAB in all months except November. Moran et al. (55) specifically chose Waquoit Bay because they expected neither carbon nor inorganic nutrient concentrations to strongly impact heterotrophs under the eutrophic conditions there, allowing a focus on temperature controls. Therefore, it is possible that in the Waquoit Bay system nutrient replete conditions allow higher nucleic acid containing generalists to outcompete the specialists for the majority of the year, while in Galveston Bay the opposite is occurring. This is consistent with data from November in Galveston Bay when DIN concentrations were highest and both MNAB and HNAB abundance increased beyond the LNAB concentration. The comparison of these two studies highlights the importance for future analyses evaluating heterotrophic communities in estuaries to consider the environmental dynamics of the specific estuary of interest.

The heterotrophic physiological community structure shifted significantly when examining all samples taken during 168-hours of incubation with inorganic nitrogen and a combination of nitrogen and phosphorous in August but not in November. Because there was no significant difference between enrichment treatments, it was interpreted that nitrogen was the primary limiting factor of heterotrophic microbes in August

supporting *in situ* observations. Average relative contributions of LNAB, MNAB and HNAB to the physiological community structure during the bioassay in August indicate that the addition of nitrogen stimulated the growth of MNAB and HNAB. The LNAB fraction constituted ~60% of the community in the control and between 30% and 40% in nutrient enriched treatments. These results agree with the hypothesis that having a smaller genome conveys a competitive advantage under nitrogen stress, but having a larger genome conveys a competitive advantage when nitrogen is no longer limiting (91). In addition, a comparison between control treatments where initial communities were dominated by LNAB in August (~60%) and HNAB in November (~50%) supports the interpretation of nutrient control on the *in situ* heterotrophic community.

Heterotrophic physiological community structure responses to nutrient enrichment were also resolved at 24-hour intervals over the total 168-hour incubation. It is important to note that variability among three replicates within a nutrient enrichment treatment at certain time-points forced PERMANOVA results to not consistently support the overall visual patterns in nMDS ordinations. Although August was the only month shown to represent responses when *in situ* nitrogen limitation is expected, similar trends in heterotrophic group responses were observed in April and October, also months with relatively low *in situ* DIN concentrations (data not shown). In addition, the low stress of the nMDS suggests that the following interpretations are reasonable. Two important patterns in heterotrophic enrichment responses were observed in August. First, at certain time-points, significant differences existed between nutrient enrichment treatments (+N versus +N+P) when each individual treatment was also significantly different from the control. These findings indicate that inorganic nitrogen and phosphorous may actually co-limit heterotrophic abundance in August. Second, the different physiological fractions responded with different timing. Initially (24-48 hours) the LNAB abundance increased, followed by an increase in MNAB (42-72 hours) followed by an increase in HNAB after 120 hours of incubation. These results support the possibility that the smaller genomes of LNAB are adapted to rapidly utilize nutrient resources while the relatively larger

genomes in MNAB and HNAB are less competitive under nutrient stress but can utilize a broader range of niches once nutrient limitations are alleviated.

Two important patterns were also observed in November. First, a significant shift was observed in all treatments (control, +N, and +N+P) between 72 and 96 hours. This change is attributable to some effect on the assemblage from being incubated in a bottle termed "bottle enclosure effect" (92,93). The second important observation is a significant increase in the contribution of HNAB to the physiological community structure in +N+P enrichments after 96 and 120 hours. Because +N was not significantly different from the control but was significantly different from +N+P at these time points, it is predicted that phosphorous can limit HNAB abundance during high flow events, as observed in November in Galveston Bay. This finding also suggests that microbial heterotrophs with higher nucleic acid content may have a stronger relationship with inorganic nutrient limitation. This may be related to increased nutrient requirements of HNAB in order to support replication of a longer genome although the spatiotemporal variability in marine heterotrophic bacterial stoichiometry remains unresolved (71).

Previous studies have evaluated inorganic nutrient limitation of total heterotrophic microbial communities using bioassay experimentation (15,17,70) and studies have examined the relationship of HNAB to LNAB in several marine systems (55,56,90). However, very few analyses have targeted relationships among inorganic nutrients and physiologically derived heterotrophic groups using flow cytometry, and most have focused on size (94). Joint et al. (17) concluded that nitrogen limitation of bacterial activity could exist in Isefjorden, Denmark, which supports the results presented herein. Increased bacterial activity and abundance were observed when glucose was combined with nutrient enrichment indicating that heterotrophic microbes were primarily carbon limited in the Fjord (17). Although a lack of correlation among heterotrophic microbes and *in situ* carbon availability was observed in Galveston Bay, the surface water concentration of DOC was highest in August (Table 2.2), which could have potentially shifted the limiting factor to DIN. Bioassays confirming carbon saturation for heterotrophs would be an interesting future expansion of the work

contained herein. Pinhassi et al. (70) observed temporal variability in phosphorous limitation of bacterial activity and growth rates in the coastal Mediterranean Sea. They also observed significant shifts in bacterial community composition with nitrogen and phosphorous enrichment using denaturing gradient gel electrophoresis fingerprinting. These results support temporal variability in heterotrophic nutrient limitation, and that nutrient enrichment can stimulate growth of certain members of the heterotrophic community in accordance with the observations made in Galveston Bay. Hitchcock and Mitrovic (15) performed bioassay experiments examining total bacterial community growth rates and activity in the Bega and Clyde River estuaries in NSW, Australia. Different factors were found to control heterotrophic bacteria between two estuaries and also during high versus low freshwater inflow periods. Carbon was the primary limiting factor regardless of freshwater inputs in the Bega River Estuary, while a shift between carbon limitation during low-flow events and phosphorous limitation during high-flow events was observed in the Clyde River Estuary (15). These findings support that freshwater inflow can alter carbon and nutrient availability impacting estuarine heterotrophic microbes.

The results herein strongly support that groups of heterotrophic microorganisms that contain different levels of nucleic acid are limited differently by the availability of required inorganic nutrient substrates. Consequently, it is likely that these groups may be operating with fundamentally different ecological strategies where cells with higher nucleic acid content are more ecologically flexible than cells with lower nucleic acid content, similar to predictions made by Vila-Costa et al. (66). In addition, "streamlining theory" has recently been proposed hypothesizing that bacterial cells with small "streamlined" genomes that confer efficient nutrient use are selected for under nutrient limitation (91). It is important to note, that an ecological trade-off between heterotrophic size, which is positively correlated to nucleic acid content and susceptibility to predation has been reported, such that larger organisms are preferentially consumed (95). This study did not evaluate heterotrophic consumption but this process could have impacted the relative success of these heterotrophic groups. This important heterotrophic

connection to higher trophic levels emphasizes the need for further investigation on this topic in Galveston Bay, an estuary with large and developed fisheries (96,97). Future research efforts should continue to evaluate the potential of using heterotrophic microbial physiological traits to examine their ecology. The logical next step would be to combine molecular and cytometric approaches in order to potentially relate the genome, transcriptome and proteome to physiological characteristics of estuarine heterotrophic microbes. Eventually these data could be used to create a framework that could predict the temporal variability in the relationship between inorganic nutrients (and other controlling factors) and heterotrophic microbes, providing valuable information to estuarine policy and management strategy in order to maintain overall ecosystem health.

CHAPTER III
NUTRIENT LIMITATION OF MARINE PICO- AND NANO- PLANKTON IN GALVESTON BAY, TEXAS

3.1 Introduction

A fundamental connection between nutrient cycles and marine microbial ecology is nutrient limitation of biological growth and activity associated with the rate of specific cellular processes (7,23,54). The stoichiometric ratios of microbial cellular materials vary among taxa due to evolutionary pressures and environmental conditions consequently shifting nutrient requirements (23,71,98,99). While the heterotrophic fraction of marine microbes is reliant on bio-available carbon to respire (13,16,54,100) both autotrophic and heterotrophic microorganisms are limited by the availability of inorganic nutrients (7,13). Several studies have shown that marine bacteria can compete with phytoplankton for inorganic nutrients (17,18,101). Particularly in estuarine systems, riverine inputs of allochthonous carbon can contribute to heterotrophic carbon requirements, possibly shifting these organisms into competition with phytoplankton for nutrients (15,102). Relationships between autotrophic and heterotrophic microbial plankton, and their impacts on nutrient utilization may dramatically effect pelagic nutrient cycling in estuaries. But little is known.

The importance of size in nutrient uptake efficiency has previously been described (16,30,103). Smaller organisms with large surface area to volume ratios are capable of out-competing larger organisms for limiting resources, potentially giving heterotrophs a nutrient uptake advantage against larger autotrophic competitors (16). This study chose to focus on relationships between autotrophic and heterotrophic nano- and pico-plankton groups within the 0.2-20μm size fraction because physical constraints to nutrient uptake should be similar among these organisms, potentially influencing the competition dynamics for limited nutrients between them. Additionally these organisms are also typically within the same prey reservoir (104), and variability in top-down

control could impact competition for nutrients among pico and nano-plankton, ultimately playing a role in the outcome of estuarine microbial nutrient processing (34).

Among potential carbon and nutrient limitations of microbial abundance, temperature can also play a significant role in determining the carrying capacity of marine microorganisms (105–107). Seasonal increases in temperature can lead to increased rates of enzymatic reactions and subsequent faster microbial metabolic processing (100). Previous studies have observed increased autotrophic and heterotrophic microbial growth rates in relation to increased temperatures (105,108). Importantly, seasonal variability in nutrient limitation is predicted to influence bacterial metabolic dependence on temperature and both temperature and nutrients are often collinear in relation to variability in pico-phytoplankton growth (105,108). Therefore, furthering the understanding of relationships between how different physicochemical factors interact to potentially limit microbial groups in estuaries is important.

Despite several research initiatives examining the total phytoplankton community in Galveston Bay, to the authors' best knowledge resident marine heterotrophic and autotrophic pico- and nano-plankton have not been extensively studied. The purpose of this study was to quantify microbial plankton in Galveston Bay, Texas in order to determine how abiotic factors regulate spatiotemporal variability in their abundance and the relative abundance of autotrophic versus heterotrophic fractions of the microbial community. The study was designed to target potential limitation *in situ* by correlating abiotic parameters to changes in abundance and validate these findings using *in vitro* mesocosm nutrient enrichment experiments. We hypothesized that the varying environmental conditions at an estuarine station controlled by influences from the Trinity River (GB1) compared to a station controlled by influences from the Gulf of Mexico (GB2) will have consequent impacts on different fractions of the resident microbial plankton. Specifically, that the autotrophic and heterotrophic fractions may respond to variations in nutrient availability in different ways due to spatial differences in nutrient limitation. Additionally, it is expected that under nutrient limiting conditions these fractions potentially compete for nutrient substrates.

3.2 Study Location

The study location of Galveston Bay, Texas (Figure 2.1) is described in detail above (Section *2.2*). The selection of two stations GB1 (29.70°N, 94.74°W) and GB2 (29.35°N, 94.75°W) is based on previous research, which identified environmentally distinct regions in upper (GB1) and lower (GB2) Galveston Bay using hierarchical cluster analyses (75). Freshwater inflows (FWI) from the Trinity River were obtained from a USGS monitoring station (Trinity River at Romayer; USGS gauge 08066500). Antecedent flow (volume discharged, $m^3 s^{-1}$) was determined by taking an average of the volume discharged on the sampling date and the five previous days. This time frame was validated by preliminary tests showing microbial responses to nutrient enrichment within <5 days (data not shown).

3.3 Methods

3.3.1 Sampling Procedures

Surface water samples (top 1 m) were obtained onboard the *Phyto I* at monthly intervals for 12 months from January 2013 to January 2014 at station GB1 and GB2. Poor weather conditions prevented sampling in July and September. *In situ* abiotic data were collected simultaneously to biological sampling each month as described in section *2.3.1*. In addition, Chlorophyll *a* (Chl*a*) concentration was measured according to Arar and Collins (109).

3.3.2 Bioassay Incubations

Bioassays were conducted during March, April, May, June, August, October, November and December 2013 and January 2014 as described in section *2.3.2* except only control and +N+P enrichments were conducted (total of 6 carboys). Initial (*in situ)* and incubated water were sampled from each replicate carboy (i.e. in triplicate) at 0, 24, 48, 72, 96, 120, 144 and 168 hours. For the purposes of this analysis, we compared

enriched treatment to the control using all data from the 168-hour incubation. Plankton isolation and storage were conducted as described in section *2.3.2*.

3.3.3 Flow Cytometry

Flow cytometric methods were conducted as described above in section *2.3.3* with the following modifications: for this analysis, the total heterotrophic and autotrophic fractions of microbial plankton were targeted. Heterotrophic and autotrophic cells were discriminated from each other and noise particles by applying Boolean gating (Figure 2.2) to a combination of bivariate logarithmic scale scatter plots (cytograms) of SYBR Green I, orange, and red fluorescence with the same caveats as described above (Section *2.3.3*).

3.3.4 Statistical Evaluation

Analyses were performed using PRIMER V6.1.15 and PERMANOVA V1.0.5 (87,88) as described above (Section *2.3.4*) with the following modifications: strong initial linearity of microbial plankton abundance data was determined to require no transformation pre-statistical analysis (87,89). Significant *in situ* temporal variability in overall environmental conditions and total heterotrophic and autotrophic microbial plankton abundance were determined using type III partial sums of squares PERMANOVA main-test with unrestricted permutation for the fixed factor month (11 levels, January, February, March, April, May, June, August, October, November and December of 2013 and January 2014) crossed with the fixed factor station (2 levels GB1 and GB2). Hierarchical cluster (CLUSTER) and similarity profile (SIMPROF, 97% similarity, 9999 permutations) analyses were performed on combined biotic groups (both autotrophic and heterotrophic abundances) to evaluate temporal variability in the microbial community.

Responses of microbial communities to enrichment with +N+P were evaluated each month by comparison to control treatments. Variability between levels of treatment by pair-wise PERMANOVA for fixed factors time-point (9 Levels, March, April, May,

June, August, October, November, December 2013, January 2014) crossed with station (2 Levels, GB1 or GB2) and crossed with treatment (2 Levels, control or +N+P) using a type-III partial sums of squares PERMANOVA design. This design was applied to data

Table 3.1 Collinearity of abiotic parameters at GB1 and GB2. Spearman correlation ρ values between the temporal variability in individual abiotic parameters. None of the abiotic parameters included in this analysis had correlations ≥0.90, beyond the threshold of collinearity targeted herein, and therefore all parameters were included in subsequent statistical evaluations.

	Temperature	Salinity	P_i	Total N	Total P	TSS	DOC	TOC	FWI	DIN	DIN : P_i
Temperature											
Salinity	-0.04										
P_i	0.04	-0.58									
Total N	0.00	-0.87	0.51								
Total P	0.13	-0.74	0.86	0.76							
TSS	0.39	0.55	-0.17	-0.54	-0.30						
DOC	0.06	0.00	0.09	0.03	0.19	0.24					
TOC	-0.27	-0.37	0.29	0.40	0.33	-0.56	-0.26				
FWI	-0.30	-0.15	0.06	0.14	-0.03	-0.25	0.14	0.20			
DIN	-0.41	-0.01	0.24	-0.18	-0.01	0.08	-0.06	-0.03	0.40		
DIN : P_i	-0.01	0.42	-0.59	-0.50	-0.64	0.32	0.05	-0.38	0.34	0.44	

for all levels of factor incubation length to effectively target the response of microbial community structure across 168 hours during mesocosm experimentation (i.e. all samples taken during the 168 hour incubation at 24 hour intervals). Shifts in microbial plankton abundance in response to nutrient enrichment over the 168 hour incubation were considered significant if the P(Perm) ≤0.05 under >9900 permutations (87). Visualization of microbial responses was achieved by subtracting the concentration (average abundance across the seven incubation times) for each group of cells (autotrophs or heterotrophs) within the control treatment from the nutrient enriched treatment (I.E. visualization is the average Δ between three control and three nutrient enriched treatments).

3.4 Results

3.4.1 In situ *Abiotic Conditions*

Collinearity based on a threshold of $|r| \geq 0.90$ was not detected among individual abiotic parameters included in this analysis of water conditions at station GB1 and GB2 (Table 3.1). Combined abiotic parameters tested varied significantly between the two stations in Galveston Bay (Table 3.2). Yearlong data for each individual parameter were averaged and the values from GB2 were subtracted from values at GB1. These results indicated that lower temperature (-0.5 °C), salinity (-11.7), FWI (-374 $m^3 s^{-1}$), TSS (-0.04 mg L^{-1}), DOC (-2.3 mg L^{-1}), DIN (-0.3 µmol L^{-1}), and DIN:P_i (-3.0) were observed at station GB1 compared to GB2. Higher concentrations of P_i (1.4 µmol L^{-1}), Total N (26.8 µmol L^{-1}), Total P (2.1 µmol L^{-1}) and TOC (5.2 mg L^{-1}) were observed at station GB1 compared to station GB2.

Table 3.2 PERMANOVA Main Test of temporal variability in abiotic parameters. Non-parametric PERMANOVA results derived from Euclidean distances for combined individual abiotic parameters collected throughout a year at approximately monthly intervals (January, February, March, April, May, June, August, October, November, December 2013 and January 2014) from two stations GB1 and GB2 (Figure 2.1). Significant variability in environmental conditions was identified based on $p \leq 0.05$.

PERMANOVA Main Test				
Abiotic Parameters (n=22)				
Factor	df	pseudo-f	P(Perm)	# Permutations
Station	10	1.9	0.003	9852
Timepoint	1	11.6	0.0006	9940

Significant temporal variability in environmental conditions existed at station GB1 (Table 3.2). The lowest salinity (10.1) was observed in November and the highest (20.7) in April (Figure 3.1A). These salinities correspond to a large FWI event (3758 m^3

s^{-1}) in November and at the end of prolonged lower FWI (<1050 m^3 s^{-1}) during February, March and April (Figure 3.1A). Two additional large FWI events were observed in January 2013 (10840 m^3 s^{-1}) and in June (3858 m^3 s^{-1}) (Figure 3.1A). The maximum TSS (0.11 mg L^{-1}) was recorded in August and the minimum (0.02 mg L^{-1}) in November. The highest concentrations of total N and P were observed in August (77.6 and 6.2 µmol L^{-1} respectively) (Figure 3.1C). The lowest total N was recorded in February (38.8 µmol L^{-1}) and of total P in January 2013 (1.9 µmol L^{-1}) (Figure 3.1C). DIN ranged from (0.1 µmol L^{-1}) in August to (11.1 µmol L^{-1}) in November (Figure 3.1E). P_i ranged from (0.7 µmol L^{-1}) in January 2014 to (5.0 µmol L^{-1}) in October (Figure 3.1E). The ratio of DIN:P_i was highest (3.5) in January 2014 and lowest (0.01) in August (Figure 3.1E). Maximum TOC (32.3 mg L^{-1}) occurred in February and DOC (17.3 mg L^{-1}) occurred in August (Figure 3.1G). Minimum recorded TOC (12.2 mg L^{-1}) and DOC (5.5 mg L^{-1}) occurred in June and April respectively (Figure 3.1G). Temperature ranged from 9.9°C in January 2013 to 29.6°C in August (Figure 3.1G).

Temporal variability in environmental conditions was also significant at station GB2 (Table 3.2). The lowest salinity (19.9) was observed in June and the highest (36.0) in August (Figure 3.1B). These salinities correspond to a large FWI event (6486 m^3 s^{-1}) in June and lower FWI (1284 m^3 s^{-1}) during August (Figure 3.1B). Two additional large FWI events were observed in January 2013 (10112 m^3 s^{-1}) and in November (2837 m^3 s^{-1}) (Figure 3.1B). The maximum TSS (0.23 mg L^{-1}) was recorded in August and the minimum (0.02 mg L^{-1}) in June (Figure 3.1B). The highest and lowest concentrations of total N were observed in June and August (48.9 and 19.5 µmol L^{-1} respectively) (Figure 3.1D). The highest and lowest total P was recorded in November and August (2.3 and 0.6 µmol L^{-1} respectively) (Figure 3.1D). DIN ranged from (0.2 µmol L^{-1}) in May to (6.7 µmol L^{-1}) in January 2013 (Figure 3.1F). P_i ranged from (0.03 µmol L^{-1}) in June to (1.7 µmol L^{-1}) in January 2013 (Figure 3.1F). The ratio of DIN:P_i was highest (11.3) in June and lowest (1.3) in May (Figure 3.1F). Maximum recorded TOC (22.1 mg L^{-1}) occurred in January 2013 and DOC (39.7 mg L^{-1}) occurred in February (Figure 3.1H). Minimum

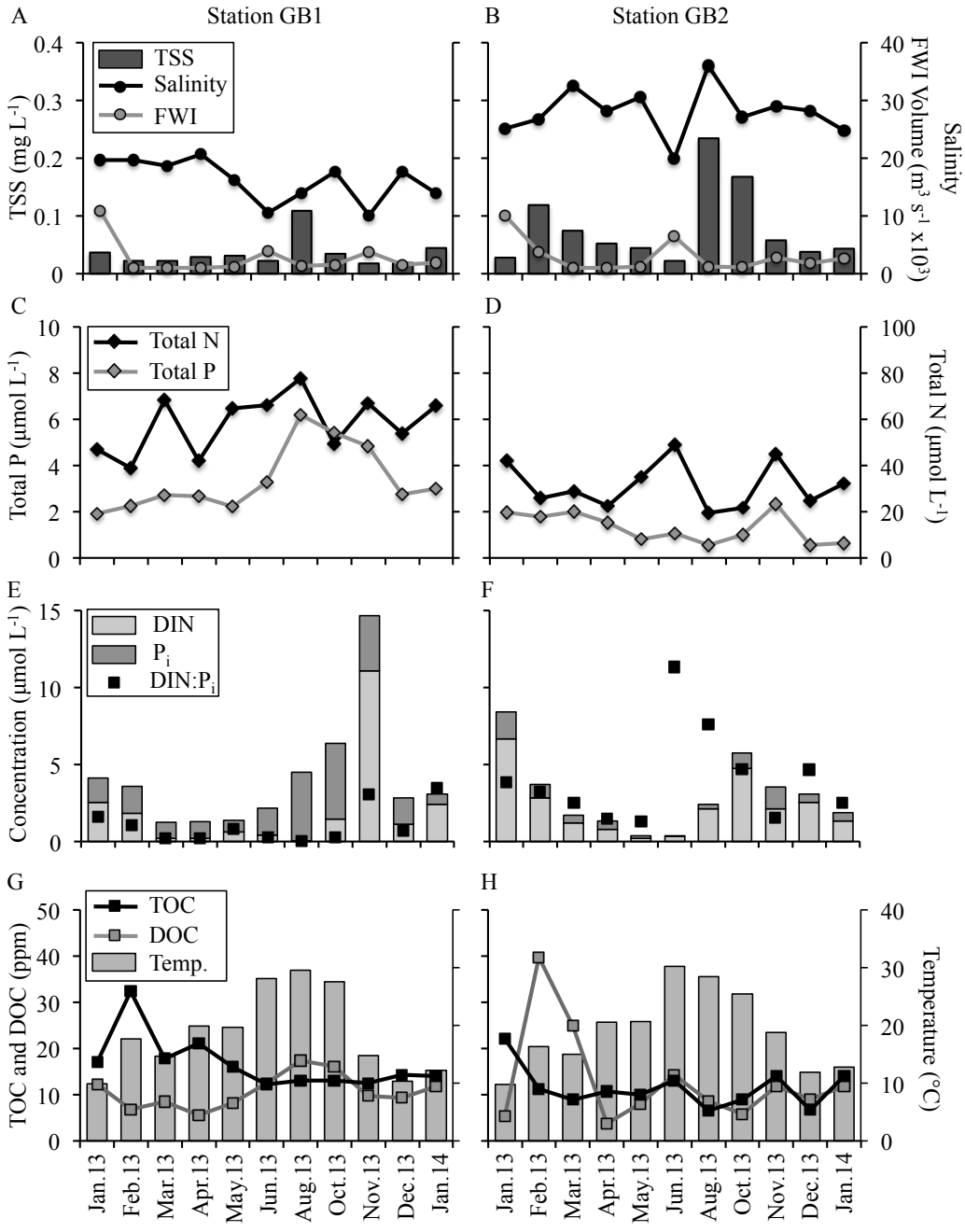

Figure 3.1 Concentrations of individual abiotic parameters at stations GB1 and GB2. (A, B) Total suspended solids (TSS) concentration (mg L-1), Salinity, and volume of freshwater inflow from the Trinity River (FWI, m3s-1). (C, D) Concentration of total nitrogen and phosphorous (µMol L-1). (E, F) Concentration of dissolved inorganic nitrogen (DIN), dissolved inorganic phosphorous (Pi) and the relationship of DIN:Pi (µMol L-1). (G, H) Temperature (°C), total organic carbon (TOC) and dissolved organic carbon (DOC) concentrations (mg L-1).

recorded TOC (6.5 mg L^{-1}) and DOC (3.8 mg L^{-1}) occurred in August and April respectively (Figure 3.1H). Temperature was similar to observations at GB1 and ranged from 9.7°C in January 2013 to 30.2°C in June (Figure 3.1H).

3.4.2 In situ *Chlorophyll and Productivity*

Significant temporal and spatial variability in chlorophyll *a* concentrations and gross primary productivity occurred in Galveston Bay during the study (PERMANOVA Main-test p≤ 0.01). At station GB1 the highest concentration of chlorophyll *a* (19.2 µg L^{-1})

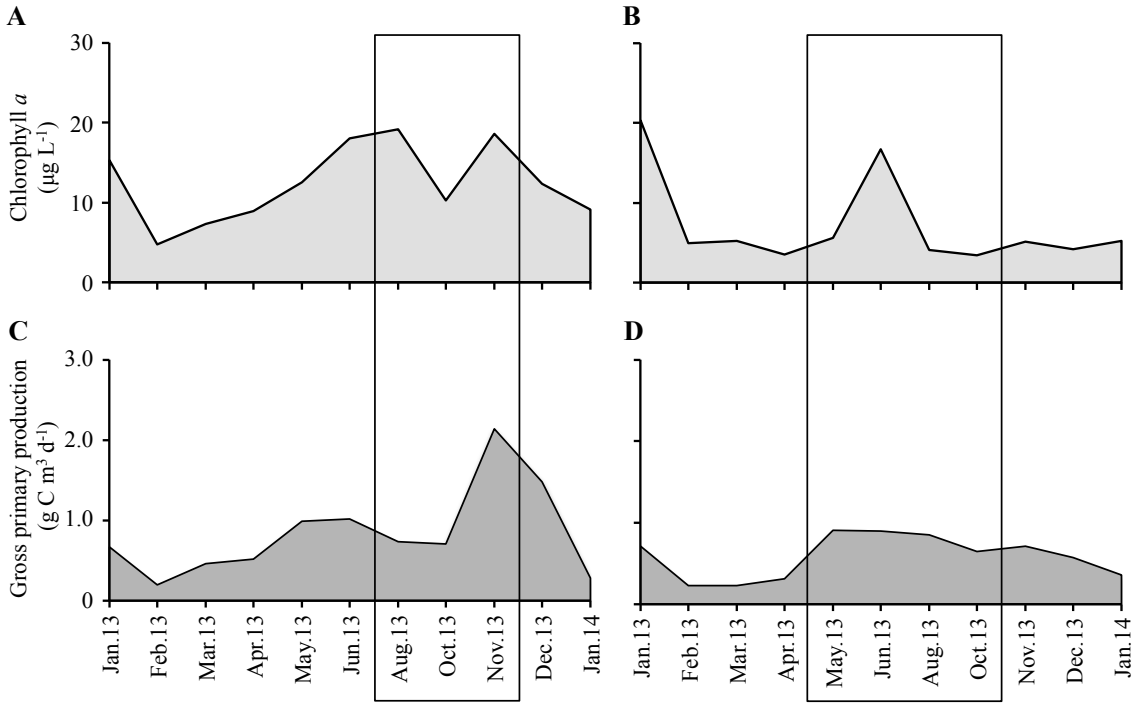

Figure 3.2 Total phytoplankton biomass and production parameters. Concentration of Chlorophyll a (µg L-1) is a proxy of phytoplankton biomass and rate of gross primary production (g C m3 d-1) indicates phytoplankton growth and activity. Measurements occurred at approximately monthly intervals from January 2013 through January 2014. Black boxes indicate months where significant shifts in heterotrophic and autotrophic microbial plankton were observed in response to enrichment with a combination of nitrogen and phosphorous. (A, C) Station GB1. (B, D) Station GB2.

was recorded in August (Figure 3.2A). Although this did not correspond to high rates of primary productivity, the second highest concentration of chlorophyll *a* (18.6 µg L^{-1}) and the highest gross primary production rate (2.1 g C m^3 d^{-1}) were recorded in November (Figure 3.2A, C). At station GB2 the highest concentrations of chlorophyll *a* (20.3 µg L^{-1}) occurring in June (Figure 3.2B). Highest rates of gross primary productivity occurred in May (0.90 g C m^3 d^{-1}) and June (0.89 g C m^3 d^{-1}) (Figure 3.2D). While the range in chlorophyll concentrations were similar at both stations, gross primary production was generally higher at GB1 than GB2 (Figure 3.2).

3.4.3 In situ *Microbial Plankton Abundance*

Significant spatial and temporal variability in autotrophic and heterotrophic abundance was observed (Table 3.3). At station GB1 autotrophic microbial abundance was highest during August (5.8 x10^6 cells mL^{-1}) and lowest during December (1.2 x10^5

Table 3.3 Variability in microbial abundance at GB1 and GB2. Non-parametric PERMANOVA results derived from Euclidean distances for individual microbial plankton groups (autotrophic or heterotrophic) collected throughout a year at approximately monthly intervals (January, February, March, April, May, June, August, October, November, December 2013 and January 2014) from two stations GB1 and GB2 (Figure 2.1). Significant variability in environmental conditions was identified based on $p \leq 0.05$.

PERMANOVA Main Test				
Autotrophic Microbial Plankton n=66				
Factor	df	pseudo-f	P(Perm)	# Permutations
Station	10	6.2	0.0001	9935
Timepoint	1	45.4	0.0001	9832
Station x Timepoint	10	4.8	0.0003	9945
Heterotrophic Microbial Plankton n=66				
Factor	df	pseudo-f	P(Perm)	# Permutations
Station	10	8.7	0.0001	9924
Timepoint	1	147.5	0.0001	9848
Station x Timepoint	10	5.8	0.0001	9934

cells mL^{-1}) (Figure 3.3A). Heterotrophic abundance was similarly highest during August and lowest during December, 1.7 $x10^7$ cells mL^{-1} and 2.8 $x10^6$ cells mL^{-1} respectively (Figure 3.3A). At station GB2 autotrophic abundance was highest during March (4.1 $x10^6$ cells mL^{-1}) and lowest during December (1.5 $x10^5$ cells mL^{-1}) (Figure 3.3B) while heterotrophic abundance was highest during November and lowest during February 3.4 $x10^6$ cells mL^{-1} and 1.1 $x10^6$ cells mL^{-1} respectively (Figure 3.3B). At station GB1 abundance of autotrophic and heterotrophic microbial plankton was 2.0 and 3.8 times higher respectively than at station GB2.

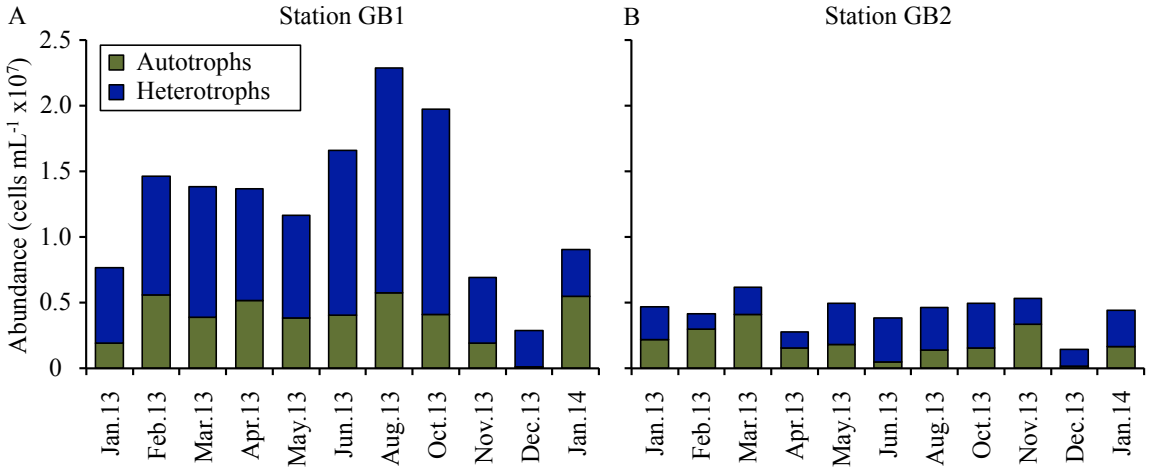

Figure 3.3 Heterotrophic (blue) and autotrophic (green) microbial abundance (cells mL^{-1}) based on an average of three replicates. (A) Temporal variability at station GB1. (B) Temporal variability at station GB2.

Significant variability in the combined heterotrophic and autotrophic abundance between the two stations in Galveston Bay can also be observed (Hierarchical cluster $p \leq 0.01$, PERMANOVA, $p=0.0001$) (Figure 3.4A). Cluster derived groupings (Cluster A) indicated that relative microbial plankton abundance at station GB2 was statistically similar throughout the year and also similar to station GB1 in January, November and

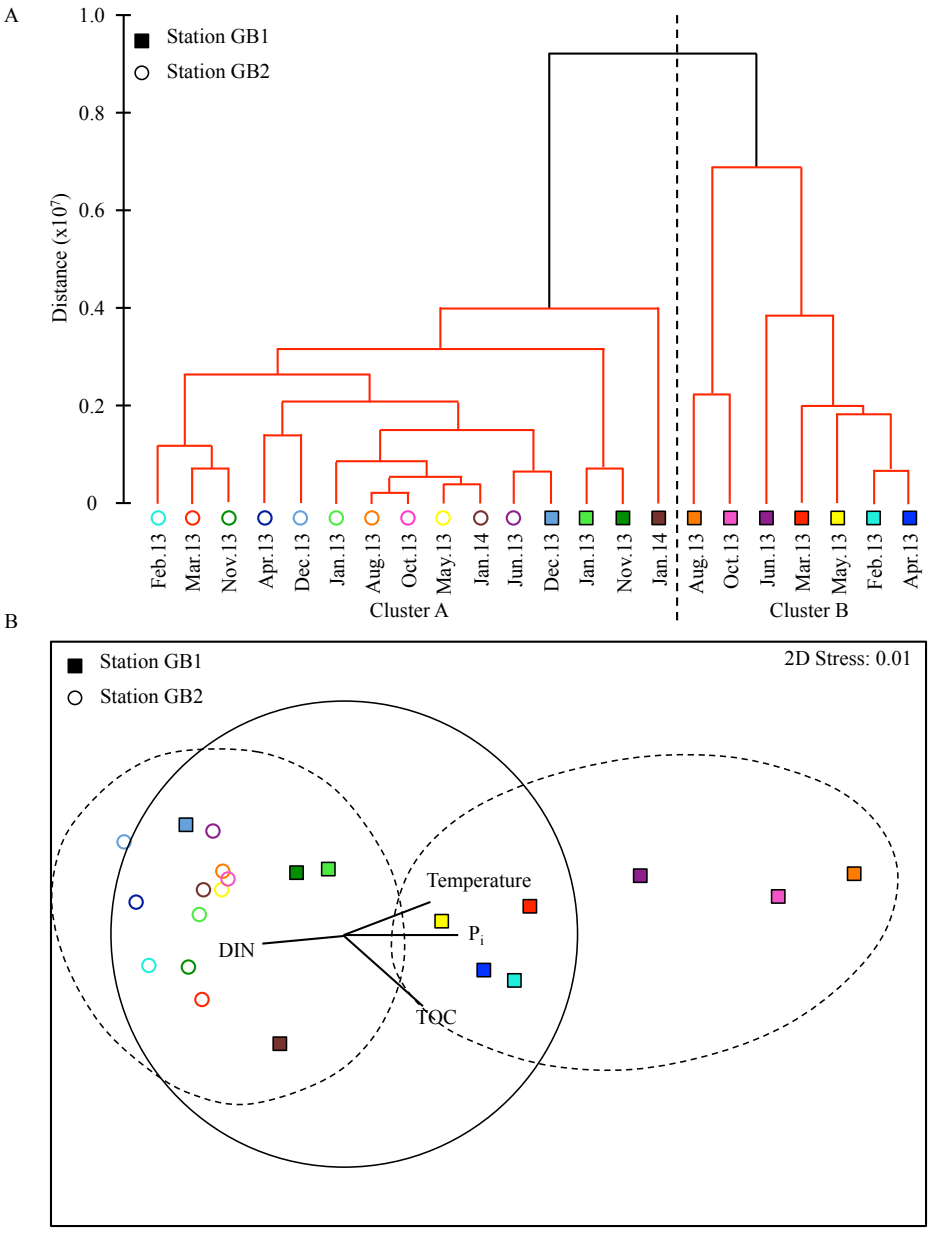

Figure 3.4 Variability in microbial abundance at GB1 and GB2. (A) Group average hierarchical cluster analysis. Black lines indicate internal multivariate structure in the data at a 97% similarity threshold (SIMPROF $p \leq 0.01$). Red lines indicate a non-significant result; i.e. samples are homogeneous. GB1 and GB2 are visualized by unique shapes; circles represent GB1, squares represent GB2. Time-points (months) are visualized by unique colors; bright green, bright blue, red, dark blue, yellow, purple, orange, pink, dark green, light blue and maroon represents January, February, March, April, May, June, August, October, November, December of 2013 and January of 2014 respectively. (B) nMDS ordination of the variability in heterotrophic and autotrophic abundance. Spearman correlations for abiotic parameters identified by DISTLM are related to the overall variability in community structure by vectors.

December of 2013 and January of 2014 (Figure 3.4A). At station GB1 relative microbial plankton abundance was similar during February, March, April, May, June, August and October of 2013 (Cluster B) (Figure 3.4A).

A combination of temperature, DIN, P_i and TOC were identified as influential predictor variables associated with the changes in the relative abundance of average autotrophic and heterotrophic microbial plankton (DISTLM, BEST, AICc=654.59) explaining 81.3% of the natural variation (Figure 3.4B). The primary environmental variables separating Clusters A and B are the concentration of DIN and P_i while temperature and TOC explained variability within clusters based on orientation of spearman correlated vectors (Figure 3.4B). Temperature, DIN, P_i and TOC each explained 19.8, 14.6, 42.5 and 11.2% of variability in microbial abundance (DISTLM, Marginal Tests). However, only temperature and P_i were significantly correlated (DISTLM, Marginal Test, $p \leq 0.05$). Of the remaining predictor variables tested, salinity, TN, TP, and DIN:P_i were individually significantly correlated to variability in microbial plankton abundance (DISTLM, Marginal Test, $p \leq 0.05$) while TSS, DOC and FWI were not.

3.4.4 In vitro *Microbial Response to Nutrient Enrichment*

Significant shifts in relative microbial plankton abundance were observed in response to enrichment with both N and P (Figure 3.5). Here we show the average of all samples taken through the 168-hour incubation. Temporal changes in the relative contributions of heterotrophic and autotrophic fractions to the total microbial abundance with nutrient enrichment were observed by subtracting the control abundance from nutrient enriched abundance for both autotrophs and heterotrophs (Figure 3.5). At station GB1 significant shifts were detected based on increases in total cellular abundance in August (3.7×10^6 cells mL^{-1}), October (5.4×10^6 cells mL^{-1}) and November (6.3×10^6 cells mL^{-1}) (Figure 3.5A). Microbial autotrophs dominated the responses in August and November representing 81.6%, and 60.7% of the total response respectively while microbial heterotrophs dominated the response in October, contributing 81.1% of the

total response. At station GB2, significant shifts in relative microbial plankton abundance were detected based on increases in total microbial abundance with nutrient enrichment observed in May (8.9 x10^6 cells mL^{-1}), June (8.3 x10^6 cells mL^{-1}), August (1.1 x10^7 cells mL^{-1}) and October (2.7 x10^6 cells mL^{-1}) (Figure 3.5B). Microbial heterotrophs dominated the significant responses to nutrient enrichment at station GB2 comprising 100.0, 63.1, 94.5, and 89.6% of the total responses respectively.

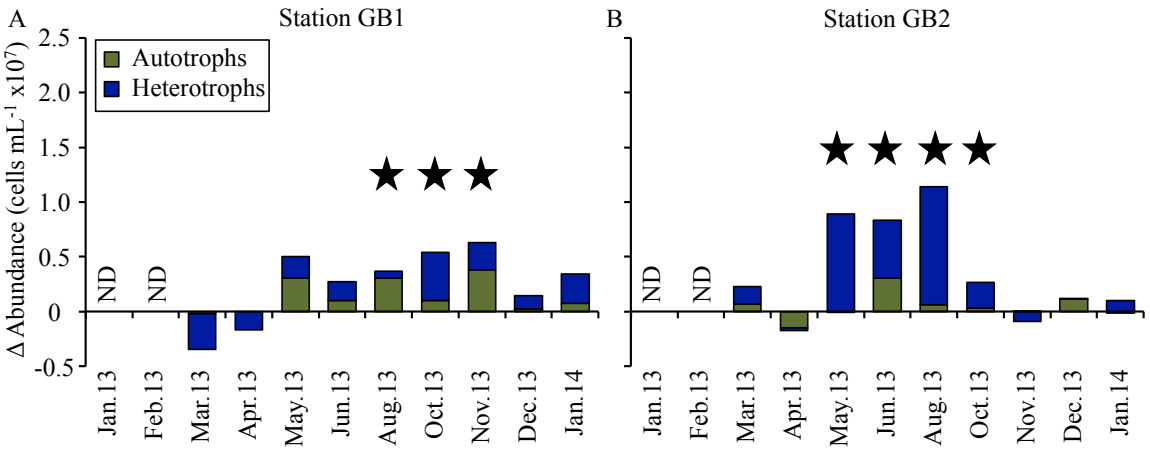

Figure 3.5 Autotrophic and heterotrophic nutrient enrichment response. Change in heterotrophic (blue) and autotrophic (green) microbial abundance (cells mL-1) based on an average of three replicates within a control treatment subtracted from replicates enriched with a combination of nitrogen and phosphorous. Black stars indicate months when significant shifts were detected between control and the nutrient enriched treatment. (A) Temporal variability at station GB1. (B) Temporal variability at station GB2.

3.5 Discussion

Combinations of abiotic factors limit pico- and nano- plankton abundance, potentially driving competitive relationships between autotrophic and heterotrophic fractions and also between organisms within this size fraction and larger primary producers. Data presented here suggest that trade-offs between temperature, nutrient

availability and potential biological competition co-limit fractions of the microbial community in different ways. Significant relationships between microbes and abiotic factors emphasize the potential importance of the microbial loop to nutrient cycling, which is still poorly understood.

My finding that pico- and nano-plankton were not consistently limited by nutrient availability at station GB1 was not entirely surprising given that the Trinity River introduces pulses nutrient loaded freshwater (72,74,79). Significant mesocosm responses at this station in August and October correspond with lowest freshwater inflows and longest periods with no flows. Supporting this was *in vivo* DIN concentrations near or below detection limits and concurrently highest *in situ* total concentrations of cells (Figure 3.1E). I found nitrogen was limiting microbial plankton abundance consistent with previous studies (74,79). Contrastingly, low temperatures, not DIN or P_i limited populations in November (Figure 3.1E, G).

At station GB2 significant positive shifts in pico- and nano-plankton after enrichment with nitrogen and phosphorous were observed *in situ* in May, August June and October (Figure 3.5B) suggesting that one or both of these nutrients limited abundances. Based on the environmental characteristics (Figure 3.1), I concluded that phosphorous was the limiting nutrient at this station. Additionally, only during warmer months when temperatures >20°C was a response to nutrient enrichment observed, suggesting again that temperature played a role in the capacity of microbes to utilize available nutrients at GB2 as was observed at GB1.

Overall, higher total concentrations of cells were observed consistently at GB1 compared to GB2. Previous research has shown that freshwater inflows from the Trinity River supplies nutrients to Trinity Bay, but that lower concentrations are often measured at GB2 consistent with a lack of freshwater influence at this station (74,75,79). These spatial differences appear to allow enhanced carrying capacity of pico- and nano-plankton at the stations in upper Galveston Bay compared to the lower part of the Bay.

I propose a step-wise spatiotemporal limitation, or co-limitation, of the microbial plankton in Galveston Bay beginning with temperature. Because temperature controls

enzymatic activities that regulate several microbial cellular processes, microbial plankton are expected to have temperature thresholds for activity and growth (100). Once the temperature threshold is reached, the availability of phosphorous limits microbial plankton populations, as evidenced by availability of DIN but lack of P_i at station GB2 where plankton abundance never exceeds (6.2×10^5 cells mL^{-1}). However, if P_i is available, as occurs at station GB1, then DIN becomes the limiting factor and microbial plankton abundance can increase up to 2.3×10^7 cells mL^{-1} eventually depleting that resource. Finally, even when nutrients are abundant and temperature is predicted to limit microbial abundance (e.g. in November), biological competition may cause microbial nutrient limitation.

The relative contribution of autotrophic or heterotrophic plankton to significant nutrient enrichment responses varied through space and time. The significant response to nutrient enrichment in August and November at GB1 and June at GB2 was predominantly increases in autotrophic microbial plankton abundance. Correspondingly, *in situ* chlorophyll *a* concentrations were highest at these times indicating increased concentrations of total phytoplankton. I propose that when phytoplankton bloom in Galveston Bay, competition for limiting nutrients intensifies among microbial plankton and therefore shifts between fractions in response to nutrient enrichment are observed. To determine if the total phytoplankton population was also nutrient limited during August and November at GB1 and June at GB2, mesocosm data for chlorophyll *a* concentrations were also evaluated (data not shown). Chlorophyll *a* concentration was significantly increased relative to a control (Monte Carlo PERMANOVA, $p \leq 0.01$), suggesting that the total phytoplankton community was limited by either nitrogen or phosphorous or both. These results support that competition for limiting nutrients between macro- (>20μm) and micro- (<20μm) autotrophic plankton likely exists in Galveston Bay.

During months when total phytoplankton abundance is low, heterotrophs contribute large proportions of the microbial plankton response to nutrient enrichment, indicating that the autotrophs were not nutrient limited. However, bloom induced stress

may intensify competition between heterotrophic and autotrophic fractions for nutrients. Therefore, the potential for autotrophic and heterotrophic pico- and nano-plankton competition for limiting nutrients is highest when autotrophic pico- and nano-plankton are also competing with larger phytoplankton during bloom events. Consequences of competition for nutrients during a bloom might subsequently influence the timing and potential efficiency of heterotrophic utilization of carbon impacting the microbial carbon pump (110). Additionally, how these relationships might impact nutrient cycling in Galveston Bay demonstrates the need for further detailed investigation.

CHAPTER IV
SPATIAL VARIABILITY IN PICO- AND NANO-PLANKTON ABUNDANCE IN THE NORTHERN GULF OF MEXICO

4.1 Introduction

Microbial populations are ubiquitous and abundant in the sea (1,2). These organisms are characterized across all three domains of life and their immense diversity is reflected in significant contributions to many different marine processes (1,16). Microbes that constitute the smallest size fractions of plankton, pico and nano-plankton (0.2-20 μm), herein are defined as microbial plankton. This group includes dominant open ocean species (e.g. *Synechococcus sp.*, *Prochlorococcus sp.*), which are believed to contribute >50% of biologically available carbon to oligotrophic systems (4). The conversion of inorganic carbon to biologically available organic carbon by autotrophic microbial plankton directly or indirectly fuels abundant heterotrophic organisms, contributing to multiple energy transfer pathways and food webs (1,14). Microbial cycling of fixed organic carbon in the euphotic zone is a major component of the biological pump and can ultimately alter the long-term sequestration of carbon in deep-ocean or marine sediments (6). Therefore, understanding complex microbial contributions to varied marine processes is important and remains a salient directive of current oceanographic research (23,54,111).

Marine microbial growth, production and activity are regulated by a variety of abiotic and biotic factors (54). Both autotrophic and heterotrophic marine microbial plankton have multiple cellular requirements for inorganic nutrients (23) and therefore limitations by single or multiple nutrients can contribute to overall microbial community dynamics (9,19). Although not exclusive, typical limiting nutrients of plankton in the ocean are nitrogen, phosphorous, iron and for some species silica (23). Identification of potential limiting nutrient(s) is important for understanding spatio-temporal controls on microbial communities (8,21,25). Microbial plankton dominance in oligotrophic regions is attributed to nutrient limitation prohibiting the growth of larger plankton or

alternatively as a recognized niche because autotrophic prokaryotic plankton cannot out-compete larger phytoplankton in higher nutrient environments (16,30). Physical mechanisms, such as mesoscale circulation, have been proposed to supply limiting nutrients to the euphotic zone in oligotrophic waters potentially initiating planktonic responses of increased productivity and changes in community structure (28,112).

Mesoscale (50-200 km in diameter) cyclonic, anti-cyclonic and mode-water circulation patterns have been observed throughout the global oceans (31) and can cause pycno-, thermo-, and nutri-clines to dome upward or downward, depending on the direction of circulation (31). In the Northern hemisphere, cyclonic and mode-water circulation are predicted to result in the upwelling of deeper water, supplying nutrients to the euphotic zone (31). Several research initiatives have been developed to evaluate mesoscale circulation impacts on biochemical processes (112). Diatom blooms were observed in the deep chlorophyll maximum in cyclone *Opal* formed leeward of the Hawaiian Islands in February 2005 (113) and in mode-water eddies in the North Atlantic Subtropical Gyre (NASG) (114). However, analysis of several cyclonic eddies in the NASG have shown a dominance of autotrophic prokaryotes at the deep chlorophyll maximum (28,114,115). Bibby *et al.* (28) propose that this discrepancy in the dominant plankton is caused by a difference in the availability of nitrate (NO_3^-) and silicate ($Si[OH]_4$) supplied to the euphotic zone by upwelling in the NASG. Small microbial plankton can dominate the plankton community in cyclonic features when silicate is depleted relative to nitrate because diatoms require a 1:1 ratio (28). The tracer Si*, which is the relative abundance of silicate [$Si(OH)_4$] – nitrate [NO_3^-], has been shown to accurately reflect the dominance of phytoplankton communities in different eddy types (28).

In the Gulf of Mexico, mesoscale circulation associated with the Loop Current forms as the Caribbean Current enters the Yucatan Channel (116–119). Cyclonic and anti-cyclonic eddies are often shed from the Loop Current (116), and these features can persist for at least 1.3 to 9.6 months (119). Due to the narrowing of the continental shelf in the northeastern regions of the NGOM, mesoscale circulation interacts frequently with

coastal shelf waters, including entrainment that can transport shelf water up to 300 km seaward (120–122). This is particularly important in the region of the Louisiana/Texas continental shelf slope where the Mississippi River and Atchafalaya River freshen and increase nutrient concentrations in continental shelf waters (121,123). Dorado et al. (124) examined phytoplankton, zooplankton and the N_2 fixing cyanobacterium *Trichodesmium spp*. isotopic ratios to evaluate the contribution of different nitrogen sources to primary productivity across a low salinity (<32) freshwater plume and anti-cyclonic circulation NGOM feature. Their findings reveal influences from the Mississippi River system and N_2 fixation impact pelagic food webs in the NGOM (124). It is predicted that upwelled nutrients from circulation combining with coastal water will increase nutrient availability and promote primary production (123,125). Hence, determining the impact of combined physicochemical coastal and open ocean influences on microbial plankton in the NGOM is important.

The study described herein uses flow cytometry derived quantification and characterization of microbial plankton across mesoscale circulation features of the NGOM. We hypothesize that variability in community composition is linked to the dynamic physicochemical conditions in the NGOM. Flow cytometry methods allow physiological (trait) based grouping of microorganisms and have recently been combined with multivariate statistical approaches to provide significant and important insights on changes in relative abundance of microbes and their potential ecological functions (36,52,126,127). These data establish a baseline to understand and predict the role of NGOM cyclonic circulation to influence microbial plankton abundance and drive microbial plankton dominance, which can be used to examine potentially significant impacts on higher order consumers and carbon dynamics.

4.2 Study Location

A survey of microbial plankton (0.2-20 μm) was conducted in the NGOM during a research cruise from 18 July to 22 July 2012 onboard the RV Blazing Seven. Thirteen

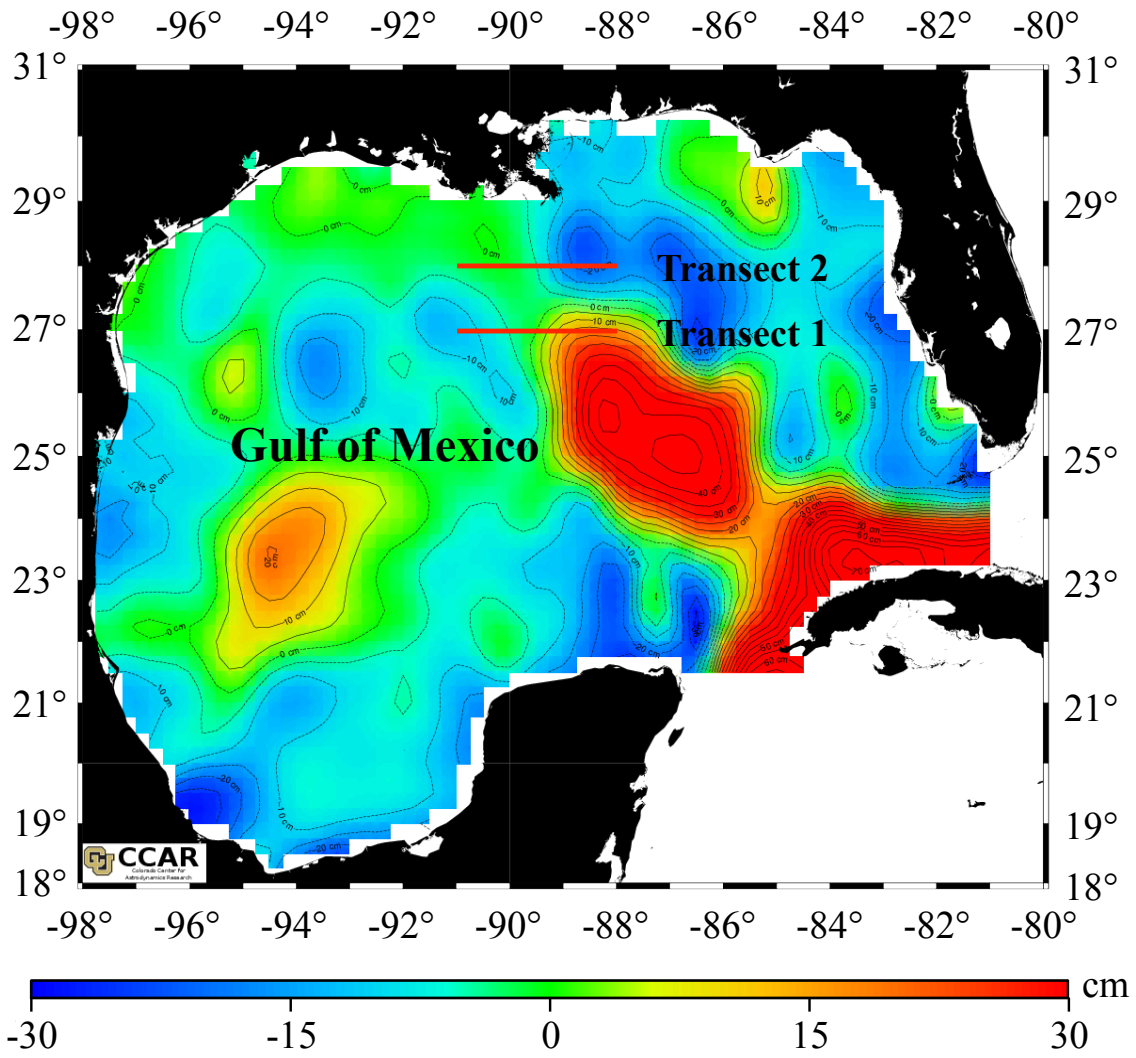

Figure 4.1 Map of the Gulf of Mexico. Sea surface height anomaly (SSH) (cm) is represented. Cyclonic features are represented by cooler colors indicating negative SSH while the anti-cyclonic loop current is represented by warmer colors indicating positive SSH. Black dashed lines delineate contours of similar SSH at intervals of 10 cm. Transect 1 and 2 are highlighted in red lines.

stations were sampled along 27°N and 28°N (Transect 1 and 2 respectively; 26 total) running west to east from 88°- 91°W (Figure 4.1). These transects intersected cyclonic eddies and the anti-cyclonic Loop Current (Figure 4.1). The sea surface height anomaly (SSH) map for 20 July 2012 represents approximate conditions throughout the cruise.

The map was generated from the Colorado Center for Astrodynamics Research (http://eddy.colorado.edu/ccar/data_viewer). We used satellite derived SSH data to predict the locations of mesoscale features with the understanding that there are inherent limitations to the resolution of circulation using this method. For example, satellite remote sensing of SSH does not provide information on vertical variability in eddy parameters through the water column, and cannot currently resolve rapid or small-scale (<100km) spatial changes (128). Sea surface temperature (°C) (SST) was measured with a calibrated Conductivity Temperature Depth (CTD) sensor and salinity (unitless practical salinity scale) was determined with a calibrated Sonde 6920 Environmental Monitoring System (YSI Inc.).

4.3 Methods

4.3.1 Sample Collection and Preservation

Seawater samples were collected from the surface (top 1 m) and depth (~30 m) into 20 L carboys and processed immediately. All sampling equipment was cleaned with distilled water between stations and rinsed with sample water three times. Seawater was passed through a 20 μm mesh-size sieve and stored in sterile 50 mL conical tubes containing 0.2 μm filtered paraformaldehyde and molecular biology grade gluteraldehyde at final concentrations of 1% and 0.01% respectively (85), and all samples were stored at -20°C and maintained frozen until processing for flow cytometry. The preservation method employed herein considered previous reports that storage temperature (4°C or flash freezing to -80°C) had little effect on cells loss or histogram visualization (85) and that these biases were reduced when combining both paraformaldehyde and gluteraldehyde as fixatives (62).

4.3.2 Nutrient Concentration Determination

Determination of dissolved nutrient concentrations was achieved by filtering seawater (50 mL) through a 0.7 μm glass fiber filter (Whatman, Kent, UK), and the

filtrate was stored in sterile centrifuge tubes at -20°C until processing. The Texas A&M University Geochemical and Environmental Research Group determined concentrations of nitrate (NO_3^-), nitrite (NO_2^-), ammonium (NH_4^+), phosphate (P_i –inorganic pool), silicate (Si), and urea from each water sample using an auto-analyzer (Astoria-Pacific, Clackamas OR) according to (Koroleff, 1999). Resulting concentrations were quality checked against replicated standards and were significantly correlated ($r \geq 0.99$). The tracer Si* was calculated by subtracting nitrate [NO_3^-] from silicate. The ratio of dissolved inorganic nitrogen (DIN) to phosphate (PO_4-P) was calculated after summing the dissolved nitrogen inputs ($DIN = NO_3^- + NO_2 + NH_4^+$).

4.3.3 Flow Cytometry

Heterotrophic and autotrophic microbial plankton groups were resolved using SYBR Green I staining procedures modified from (86) on a Gallios™ 3-laser flow cytometer (Beckman Coulter, Brea, CA). Aliquots of preserved sample were stained with 1/1000 diluted 10000X concentrated SYBR Green I (Invitrogen, Carlsbad, CA). SYBR Green staining and persistent fluorescence was enhanced by the addition of potassium citrate (30 mmol L^{-1} final concentration) to each sample (86). Samples were incubated in the dark at ~60°C for 15 min. based on preliminary experiments which indicated increased binding efficiency of SYBR Green I at that temperature for the Gallios cytometer (data not shown). Internal size (10 μm) and enumeration (973 beads μL^{-1}) standard flow count fluorophores were added to each sample tube post incubation (Beckman Coulter, Brea, CA.). Particles were isolated within IsoFlow sheath fluid (Beckman Coulter, Brea, CA) and were exposed to 488 nm and 638 nm excitation by lasers and fluorescence was evaluated. Chlorophyll *a* emission was collected through a 695 nm band-pass filter ± 15 nm targeting its emission maximum of 667 nm. SYBR Green I emission was collected through a 525 nm band-pass filter ± 15 nm targeting its emission maximum of 522 nm. Phycoerythrin emission was collected through a 575 band-pass filter ± 15 nm targeting its emission maximum of 576 nm. Phycocyanin emission was collected through a 660 nm band- pass filter ± 15 nm targeting its emission

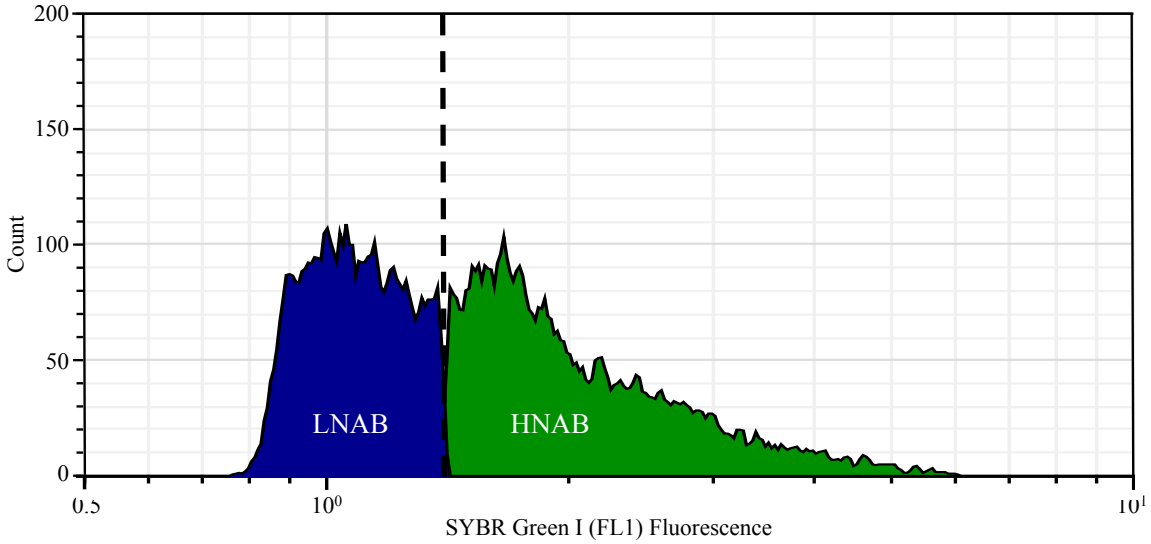

Figure 4.2 Histogram of heterotrophic particle count. The spectrum of SYBR Green I fluorescence (x-axis, plotted on a logarithmic scale) was used to classify heterotrophic cells in to physiological groups. The delineation between relatively lower nucleic acid containing bacteria (blue) and relatively higher nucleic acid containing bacteria (green) is marked by a black dashed line.

maximum of 642 nm. Samples were analyzed for 5 min. at a flow rate of 4-8 µL min^{-1} discriminating on SYBR Green I fluorescence. Data analysis was conducted using Kaluza Cytometry Analysis software (Version 1.2 Beckman-Coulter, Brea, CA).

Autotrophic and heterotrophic cells were discriminated using Boolean gating on a combination of bivariate scatter plots (cytograms) or histograms with parameters including SYBR Green I, orange, and red fluorescence. Cells were grouped by similarity in physiological characteristics on the basis of previously reported thresholds observed in the environment and culture verification (51,61,62,86,129,130). Heterotrophs were separated into high nucleic acid containing bacteria (HNAB) and low nucleic acid containing bacteria (LNAB) corresponding to their nucleic acid content resolved with SYBR fluorescence (Figure 4.2) (60,61). We used nomenclature of A1-A5 for the 5 physiologically unique autotrophic groups (Figure 4.3A, B and C). Based on earlier studies (61,86,130), we can say the microbial plankton in this study are most likely

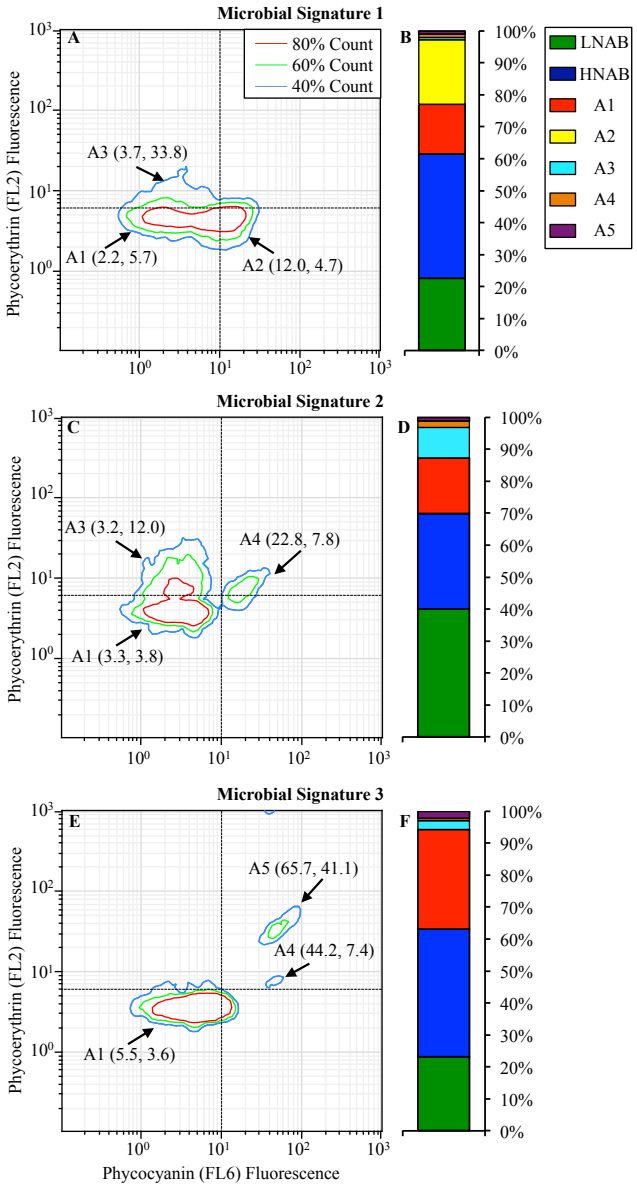

Figure 4.3 Identification and quantification of autotrophic groups. (A, C, E) Cytograms visualizing autotrophic groups of similar physiological characteristics. Colored lines represent percentage of total count. Mean relative phycocyanin (x-axis) and phycoerythrin (y-axis) fluorescence for groups is given in parentheses. Thresholds to segregate groups are visualized as black dashed lines. Group A1 was defined by mean values (<10, <6), group A2 (>10, <6), A3 (<10, >6), A4 (>10, >6) and A5 (>10, >10) of phycocyanin and phycoerythrin respectively. (B, D, F) Relative proportion of groups defined using cytograms or histograms (Fig. 2). A representative is shown for each of three significantly different microbial signatures.

Prochlorococcus (A1), *Synechococcus* groups lacking or containing different concentrations of phycourobilins and pico-eukaryotic algae (A2-A5). However, taxonomic verification with molecular methods was not possible for the current study. Hence, we do not provide specific taxonomic identifiers as suggested in the recent reviews by (49,52) which detail both cautions and caveats of flow cytometry methods. To quantify abundance (cells mL^{-1}), the volume of each sample measured during flow cytometry was calculated by dividing the number of beads counted by the number of internal beads (uL^{-1}) in the sample, and sample particle counts were divided by the calculated volume. To subtract background and noise, an aliquot of each sample was filtered through a 0.2 μm sterile syringe filter (VWR, Radnor, PA) and processed immediately following each sample.

4.3.4 Statistical Evaluation

Analyses were performed using PRIMER V6.1.15 and PERMANOVA V1.0.5 software (87,88). All data were evaluated by draftsman plots in order to select appropriate transformation procedures and eliminate collinear variables. Non-collinear variables included in the analysis had correlations $|r| \leq 0.90$, a more stringent threshold than $|r| \leq 0.95$ as suggested by (87) in order to further reduce potential model bias while maintaining high resolution of variability within individual parameters. Transformation selections were further validated by comparison to both un-transformed data and data exposed to other transformation processes (Figure 2.4). *In situ* multivariate biotic data were transformed by log (1+y) in order to down-weigh the effects of a single group on the ordination and increase the contribution of rare groups (88). All biological abundance data were analyzed using Bray-Curtis resemblance matrices as is recommended for data sets that include zeros that potentially have ecological meaning. *In situ* multivariate abiotic environmental data for SST (°C), SSH (cm), salinity, nutrients (μmol L^{-1}) and ratios were square-root transformed in order to decrease skewness and increase linearity (88). Transformed environmental data were then normalized to account for differences in units of measurement and analyzed using

Euclidean distance resemblance matrices. Significant variability in combined abiotic parameters from each station were evaluated by Type III PERMANOVA main tests with unrestricted permutations of data. Principal coordinates ordinations were used to visualize similarities and dissimilarities in environmental conditions among stations. The largest Eigenvalue among factors identified the abiotic parameter most significantly correlated to each principal component (87).

Hierarchical cluster (CLUSTER) and similarity profile (SIMPROF, 97% similarity 9999 permutations) analyses were performed to cluster stations that had similar microbial community abundance and composition. Significant differences in community structure were identified between the clusters by SIMPROF and verified by subsequent PERMANOVA pairwise tests (data not shown). Dendrograms were used to visualize statistical variability across stations. Non-parametric multi-dimensional scaling (nMDS) ordinations were used to visualize similarities and dissimilarities in microbial abundance and community composition among clustered stations. The nMDS two-dimensional representation is considered acceptable for visual interpretations when the stress is less than 0.1 (88).

In order to quantify the relationship between measured environmental parameters and microbial community variability, predictor variables were identified using distance-based linear modeling (DISTLM). Models were generated using all possible combinations of predictor variable inputs with the “BEST” selection technique in PERMANOVA and both the Akaike information criterion corrected (AICc) and Bayesian information criterion (BIC). The top 10 models selected by each criterion test were plotted and overlapping models with the lowest AICc and BIC were considered (87,88). The amount of variability in microbial community abundance and structure explained by environmental predictor variables identified by the model was quantified within DISTLM. Relationships between environmental predictor variables or nutrient availability and microbial communities were visualized using nMDS ordinations and Spearman derived correlated vectors and corresponding maps of specific predictor variable values.

4.4 Results

4.4.1 Study Area Environmental Conditions

Transect 1 at 27°N (stations 1-13) included areas of negative SSH consistent with cyclonic circulation and positive SSH consistent with anti-cyclonic circulation associated with the Loop Current (Figure 4.1). Transect 2 at 28°N (stations 14-26) also included an area of pronounced negative SSH consistent with a cyclonic feature (Figure

Table 4.1 Physical and chemical parameters in surface samples (top 1m) at stations across transect 1 and transect 2.

Station	Temperature °C	Salinity (ppt)	NO_3^- (µg L^{-1})	HPO_4^{2+} (µg L^{-1})	SiO_2 (µg L^{-1})	NH_4^+ (µg L^{-1})	NO_2^- (µg L^{-1})	Urea (µg L^{-1})	SSH (cm)	Si*	N:P
1	29.96	38.51	0.02	0.04	0.03	0.03	0.01	0.02	3.38	0.05	1.31
2	30.60	39.08	0.04	0.10	0.06	0.00	0.01	0.05	2.60	0.05	0.52
3	30.98	39.28	0.06	0.10	0.03	0.01	0.00	0.01	1.97	0.01	0.74
4	30.24	38.93	0.02	0.05	0.03	0.03	0.01	0.01	2.29	0.05	1.08
5	30.08	39.16	0.05	0.10	0.03	0.03	0.00	0.03	4.13	0.02	0.77
6	30.03	39.09	0.03	0.09	0.04	0.01	0.00	0.01	7.81	0.05	0.41
7	30.08	38.69	0.02	0.09	0.04	0.02	0.00	0.00	14.40	0.06	0.43
8	30.46	39.20	0.03	0.08	0.05	0.01	0.00	0.00	23.75	0.06	0.47
9	30.42	38.94	0.04	0.07	0.04	0.05	0.01	0.02	34.20	0.04	1.36
10	30.53	38.80	0.02	0.08	0.06	0.01	0.00	0.00	43.66	0.07	0.38
11	30.14	39.00	0.03	0.09	0.06	0.01	0.00	0.00	49.64	0.07	0.42
12	29.91	38.69	0.02	0.09	0.05	0.03	0.00	0.01	49.42	0.06	0.57
13	29.68	39.54	0.03	0.06	0.04	0.02	0.00	0.01	49.36	0.05	0.76
14	29.72	39.58	0.03	0.09	0.05	0.03	0.01	0.01	20.43	0.06	0.79
15	29.68	39.13	0.04	0.08	0.03	0.04	0.01	0.04	20.84	0.03	1.05
16	29.48	39.10	0.02	0.08	0.03	0.05	0.01	0.02	19.46	0.04	1.13
17	29.59	39.19	0.03	0.09	0.02	0.04	0.01	0.01	16.20	0.03	0.86
18	29.64	39.04	0.03	0.08	0.01	0.02	0.01	0.00	13.04	0.01	0.76
19	28.99	38.05	0.02	0.09	0.05	0.01	0.00	0.00	11.14	0.06	0.42
20	28.19	35.40	0.04	0.12	0.04	0.03	0.01	0.08	10.24	0.03	0.68
21	29.22	36.69	0.03	0.09	0.05	0.05	0.00	0.04	10.33	0.05	0.98
22	29.24	36.14	0.02	0.09	0.03	0.03	0.00	0.00	11.07	0.04	0.62
23	30.33	37.43	0.05	0.13	0.02	0.08	0.01	0.09	11.84	0.00	1.05
24	29.86	37.16	0.02	0.09	0.04	0.01	0.00	0.01	12.19	0.05	0.38
25	30.02	37.59	0.04	0.11	0.08	0.04	0.00	0.05	12.38	0.07	0.82
26	30.16	38.13	0.02	0.10	0.05	0.01	0.00	0.00	12.45	0.07	0.28

observed from stations 19-26 (Table 4.1); at the remaining surface stations and all stations at depth (~30 m) salinity was on average >39.

Table 4.2 Correlations among abiotic parameters at ~1m depth as identified by draftsman plots of pairwise combinations of each parameter (PRIMER). None of the abiotic parameters include in the analysis were collinear based on the $|r| \geq 0.90$ threshold.

	Temp.	Salinity	NO_3^-	HPO_4^{-2}	SiO_2	NH_4^+	NO_2^-	Urea	SSH	Si*	N:P
Temp.											
Salinity	0.60										
NO_3^-	0.14	-0.03									
HPO_4^{-2}	-0.12	-0.43	0.53								
SiO_2	0.09	-0.03	-0.17	0.05							
NH_4^+	-0.28	-0.26	0.29	0.11	-0.34						
NO_2^-	-0.34	-0.07	0.21	-0.11	-0.41	0.56					
Urea	-0.22	-0.41	0.65	0.36	-0.07	0.58	0.57				
SSH	-0.02	0.21	-0.24	-0.05	0.34	0.01	-0.29	-0.28			
Si*	-0.12	0.03	-0.70	-0.36	0.76	-0.42	-0.34	-0.43	0.36		
N:P	-0.03	0.08	0.37	-0.35	-0.36	0.72	0.73	0.59	-0.21	-0.40	

Table 4.3 Correlations among abiotic parameters at ~30m depth as identified by draftsman plots of pairwise combinations of each parameter (PRIMER). None of the abiotic parameters include in the analysis were collinear based on the $|r| \geq 0.90$ threshold.

	Salinity	NO_3^-	HPO_4^{-2}	SiO_2	NH_4^+	NO_2^-	Urea	SSH	Si*	DIN:P
Salinity										
NO_3^-	-0.33									
HPO_4^{-2}	-0.10	0.50								
SiO_2	-0.38	0.41	0.42							
NH_4^+	-0.25	0.64	0.18	-0.09						
NO_2^-	0.17	0.41	0.17	-0.35	0.71					
Urea	-0.21	0.77	0.49	0.14	0.70	0.64				
SSH	-0.43	-0.06	0.00	0.49	-0.19	-0.43	-0.30			
Si*	0.10	-0.58	-0.09	0.42	-0.74	-0.71	-0.65	0.43		
N:P	-0.13	0.45	-0.39	-0.31	0.78	0.59	0.48	-0.24	-0.69	

All measured abiotic factors were included in principal coordinates and DISTLM analyses because none had correlations $|r| \geq 0.90$ indicating lack of collinearity (Tables 4.2 and 4.3). Abiotic factors varied significantly at both surface (PERMANOVA P=0.0001) and depth (PERMANOVA P=0.0001) (Table 4.1). SSH, SST, Si* and Si were greater when DIN: P, NO_3^-, NO_2^-, NH_4^+, and Urea were lower in water samples measured across both transects (Figure 4.4). The concentrations of NO_3^-, NO_2^-, NH_4^+, and Urea at the surface were on average 1.2 times higher at stations with negative (-10 to -30 cm) SSH and on average 0.2°C lower SST (Figure 4.4A) consistent with typical cyclonic circulation features. Typically, SST was on average 0.4°C higher at stations with positive (~10 to 30 cm) SSH (Table 4.1). Si was also on average 1.3 times higher at stations with positive (~10 to 30 cm) SSH conditions (Table 4.1). At depth, temperature was not recorded (Table 4.4); however, concentrations of NO_3^-, NO_2^-, NH_4^+, and Urea were on average 1.2 times higher at stations with negative (~-10 to -30 cm) SSH consistent with surface evaluations (Figure 4.4B). Additionally, Si concentration was on average 1.4 times higher at stations with positive (~10 to 30 cm) SSH (Figure 4.4B).

4.4.2 Distribution of Microbial Abundance

Autotrophic cellular abundance (combined A1-A5 cells mL^{-1}) ranged from 9.1 $x10^4$ – 4.2 $x10^5$ cells mL^{-1} at the surface and 3.0 $x10^4$ – 3.2 $x10^5$ cells mL^{-1} at depth. No significant difference (SIMPROF, $p \geq 0.01$) in autotrophic abundance was detected horizontally (between the stations) at either the surface or at depth. Vertically, significantly higher concentrations of autotrophic cells were present in the surface waters than at depth (PERMANOVA, $p = 0.004$). Heterotrophic cellular abundance (combined LNAB and HNAB cells mL^{-1}) ranged from 1.7 $x10^5$ – 1.1 $x10^6$ cells mL^{-1} at the surface and 2.0 $x10^5$ – 1.5 $x10^6$ cells $mL^{-}1$ at depth. No significant difference (SIMPROF, $p \geq 0.01$) in heterotrophic abundance was observed horizontally (between the stations) at either the surface or at depth. There was no significant vertical variability in heterotrophic concentration (PERMANOVA, $p = 0.521$).

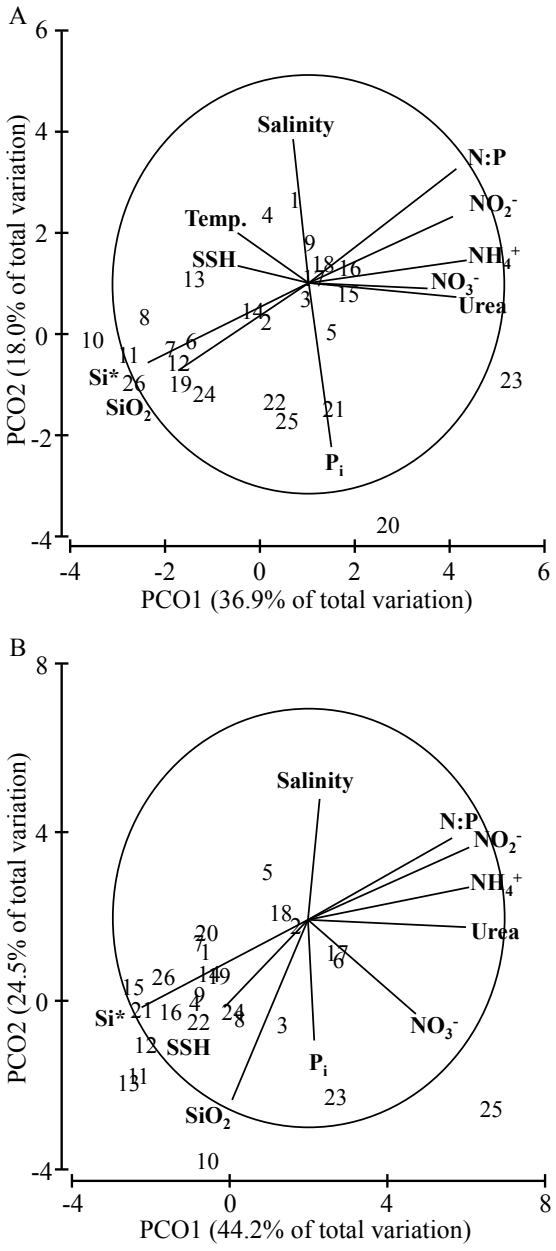

Figure 4.4 Principle coordinates ordinations visualizing the variability in measured abiotic conditions across 26 stations. Spearman correlations for each abiotic parameter to the overall variability in environmental conditions at all stations are identified. Line length within the frame of reference circle represents the relative strength of the correlation and direction corresponds to positive change. (A) 54.9% of the variability in abiotic conditions is represented in two dimensions for surface-water samples. Spearman correlation was strongest between PCO1 and Si* |r| =0.82 and PCO2 and salinity |r| =0.68. (B) 68.7% of the variability in abiotic conditions is represented in two dimensions for deep-water samples. Spearman correlation was strongest between PCO1 and Si* |r| =0.86 and PCO2 and salinity |r| =0.87.

Significant variability in abundance of any individual group was not detected horizontally across surface (SIMPROF, $p \geq 0.01$) or deep stations (SIMPROF, $p \geq 0.01$). Ranges in horizontal spatial distribution of individual groups are given for surface (Table 4.5) and depth (Table 4.6). Autotrophic group A1 ranged in abundance from 4.5 $x10^4$ – 2.0 $x10^5$ cells mL^{-1} at the surface and 5.3 $x10^4$ – 2.5 $x10^5$ cells mL^{-1} at depth. Autotrophic group A2 ranged in abundance from below detection limit (BDL) – 1.7 $x10^5$ cells mL^{-1} at the surface and was BDL throughout the sampling region at depth.

Table 4.4 Total abundance (cells mL^{-1}) of autotrophic (A1-A5) and heterotrophic (LNAB/HNAB) microbial groups for all stations sampled at the surface (~1m).

Station	Microbial Signature	LNAB	HNAB	A1	A2	A3	A4	A5
1	2	1.16x 10^5	2.42x 10^5	8.23x 10^4	BDL	3.43x 10^4	4.34x 10^3	1.89x 10^4
2	2	2.44x 10^5	2.61x 10^5	8.74x 10^4	BDL	2.79x 10^4	4.04x 10^3	2.05x 10^4
3	2	2.27x 10^5	1.70x 10^5	9.85x 10^4	BDL	5.39x 10^4	1.39x 10^3	2.26x 10^4
4	2	1.84x 10^5	1.53x 10^5	7.97x 10^4	BDL	3.23x 10^4	2.32x 10^3	1.70x 10^4
5	2	1.77x 10^5	2.59x 10^5	1.04x 10^5	BDL	6.63x 10^4	1.55x 10^4	2.65x 10^4
6	2	2.75x 10^5	2.23x 10^5	8.97x 10^4	BDL	4.35x 10^4	1.01x 10^4	2.35x 10^4
7	2	1.44x 10^5	2.64x 10^5	5.88x 10^4	BDL	4.80x 10^4	2.86x 10^3	1.80x 10^4
8	2	1.04x 10^5	2.69x 10^5	6.67x 10^4	BDL	2.33x 10^4	3.15x 10^3	2.48x 10^4
9	3	8.61x 10^4	2.64x 10^5	1.97x 10^5	BDL	1.96x 10^4	1.19x 10^3	1.15x 10^4
10	3	1.32x 10^5	1.23x 10^5	8.17x 10^4	BDL	2.75x 10^4	3.17x 10^2	7.76x 10^3
11	3	8.70x 10^4	1.70x 10^5	7.12x 10^4	BDL	2.40x 10^4	5.49x 10^2	7.01x 10^3
12	3	7.21x 10^4	1.79x 10^5	8.43x 10^4	BDL	1.31x 10^4	1.27x 10^3	7.12x 10^3
13	3	8.25x 10^4	1.86x 10^5	1.05x 10^5	BDL	7.03x 10^3	8.51x 10^2	7.84x 10^3
14	3	9.03x 10^4	2.16x 10^5	1.37x 10^5	BDL	1.80x 10^4	2.07x 10^3	7.40x 10^3
15	2	1.69x 10^5	2.24x 10^5	1.18x 10^5	BDL	3.11x 10^4	3.90x 10^3	2.28x 10^4
16	2	1.05x 10^5	2.59x 10^5	1.13x 10^5	BDL	2.16x 10^4	3.98x 10^3	1.60x 10^4
17	3	1.09x 10^5	1.88x 10^5	1.47x 10^5	BDL	1.27x 10^4	4.04x 10^3	1.03x 10^4
18	3	1.10x 10^5	1.87x 10^5	1.65x 10^5	BDL	2.82x 10^4	5.49x 10^3	9.91x 10^3
19	1	5.73x 10^5	2.69x 10^5	5.14x 10^4	1.55x 10^5	6.83x 10^3	3.57x 10^4	1.85x 10^4
20	1	5.90x 10^5	4.06x 10^5	7.58x 10^4	1.48x 104	5.07x 10^3	6.06x 10^4	1.77x 10^4
21	1	5.12x 10^4	1.84x 10^5	4.46x 10^4	8.65x 104	6.69x 10^3	2.71x 10^3	6.15x 10^3
22	1	1.03x 10^5	3.16x 10^5	1.15x 10^5	1.58x 10^5	8.27x 10^3	1.62x 10^4	1.25x 10^4
23	1	3.67x 10^5	3.75x 10^5	1.76x 10^5	1.68x 10^5	1.17x 10^4	2.62x 10^4	1.20x 10^4
24	1	1.60x 10^5	3.89x 10^5	1.09x 10^5	1.43x 10^5	5.15x 10^3	7.14x 10^3	8.79x 10^3
25	1	1.19x 10^5	3.16x 10^5	7.68x 10^4	1.67x 10^5	5.42x 10^3	1.81x 10^4	1.20x 10^4
26	1	1.16x 10^5	2.41x 10^5	1.18x 10^5	9.03x 10^4	4.96x 10^3	2.44x 10^3	5.03x 10^3

Table 4.5 Total abundance (cells mL^{-1}) of autotrophic (A1-A5) and heterotrophic (LNAB/HNAB) microbial groups for all stations sampled at the surface (~30m).

Station	Microbial Signature	LNAB	HNAB	A1	A2	A3	A4	A5
1	-	7.22×10^4	1.52×10^5	1.51×10^5	BDL	1.34×10^4	2.48×10^3	9.71×10^2
2	-	1.91×10^5	1.25×10^5	1.50×10^5	BDL	1.58×10^4	5.02×10^2	1.35×10^3
3	-	7.76×10^4	1.92×10^5	1.94×10^5	BDL	4.62×10^4	1.66×10^3	4.07×10^3
4	-	1.10×10^5	1.59×10^5	1.45×10^5	BDL	1.69×10^4	1.32×10^3	9.56×10^2
5	-	1.33×10^5	1.97×10^5	2.29×10^5	BDL	1.29×10^4	1.80×10^3	7.08×10^3
6	-	3.57×10^5	1.50×10^5	9.88×10^4	BDL	2.13×10^4	7.09×10^3	1.04×10^3
7	-	1.45×10^5	2.96×10^5	5.26×10^4	BDL	2.56×10^3	1.73×10^4	8.29×10^3
8	-	4.06×10^4	2.45×10^5	5.92×10^4	BDL	6.28×10^3	2.04×10^4	8.32×10^3
9	-	4.22×10^4	3.75×10^5	2.49×10^5	BDL	1.99×10^4	8.00×10^3	3.56×10^3
10	-	8.49×10^4	3.05×10^5	8.42×10^4	BDL	7.73×10^3	3.05×10^3	7.52×10^2
11	-	3.57×10^4	2.42×10^5	7.06×10^4	BDL	8.20×10^3	1.87×10^3	4.46×10^3
12	-	3.27×10^4	2.31×10^5	9.86×10^4	BDL	1.39×10^4	3.18×10^3	2.87×10^3
13	-	9.58×10^4	2.11×10^5	1.38×10^5	BDL	8.81×10^3	1.73×10^4	1.26×10^3
14	-	6.37×10^4	1.24×10^5	1.04×10^5	BDL	1.54×10^4	2.31×10^2	4.84×10^3
15	-	1.55×10^5	2.14×10^5	8.14×10^4	BDL	1.29×10^4	2.06×10^3	2.25×10^4
16	-	6.64×10^4	2.12×10^5	1.20×10^5	BDL	1.26×10^4	9.06×10^2	9.35×10^3
17	-	1.06×10^5	1.83×10^5	1.55×10^5	BDL	9.53×10^3	4.51×10^3	1.59×10^4
18	-	4.58×10^5	6.63×10^5	2.17×10^5	BDL	5.98×10^4	9.01×10^3	1.58×10^4
19	-	1.99×10^5	1.70×10^5	1.12×10^5	BDL	7.15×10^3	2.59×10^3	1.34×10^4
20	-	9.16×10^4	2.01×10^5	1.19×10^5	BDL	1.05×10^4	1.46×10^3	1.14×10^4
21	-	3.58×10^4	1.43×10^5	1.17×10^5	BDL	1.05×10^4	1.72×10^3	7.83×10^3
22	-	3.30×10^4	2.34×10^5	1.08×10^5	BDL	1.00×10^4	2.11×10^3	1.94×10^4
23	-	1.28×10^5	2.33×10^5	7.82×10^4	BDL	1.23×10^4	5.71×10^3	1.92×10^4
24	-	1.14×10^5	3.04×10^5	2.52×10^5	BDL	1.30×10^4	7.64×10^3	1.48×10^4
25	-	8.14×10^4	3.16×10^5	2.11×10^5	BDL	1.35×10^4	1.01×10^4	5.81×10^3
26	-	ND	ND	ND	ND	ND	ND	ND

Autotrophic group A3 ranged in abundance from $5.0 \times 10^3 – 6.6 \times 10^4$ cells mL^{-1} at the surface and $2.6 \times 10^3 – 6.0 \times 10^4$ cells mL^{-1} at depth. Autotrophic group A4 ranged in abundance from $3.2 \times 10^2 – 6.0 \times 10^4$ cells mL^{-1} at the surface and $2.3 \times 10^2 – 2.0 \times 10^4$ cells mL^{-1} at depth. Autotrophic group A5 ranged in abundance from $5.0 \times 10^3 – 2.7 \times 10^4$ cells mL^{-1} at the surface and $7.5 \times 10^2 – 2.3 \times 10^4$ cells mL^{-1} at depth. Heterotrophic group LNAB ranged in abundance from $5.1 \times 10^4 – 5.9 \times 10^5$ cells mL^{-1} at the surface and $3.3 \times 10^4 – 4.6 \times 10^5$ cells mL^{-1} at depth. Heterotrophic group HNAB ranged in abundance

from 1.2 x10^5 – 4.0 x10^5 cells mL^{-1} at the surface and 1.2 x10^5 – 6.6 x10^5 cells mL^{-1} at depth.

4.4.3 Distribution of Microbial Community Structure

Community structure is herein defined as the proportion of each microbial plankton group A1-A5, HNAB and LNAB compared to the total community at each station. Significant spatial variability (SIMPROF, $p<0.01$) of community structure was detected across transects in surface waters (Figure 4.5A). Three microbial signatures (i.e. three unique community structure profiles, in each of which relative abundance patterns were statistically homogeneous) were identified (Figure 4.5A) and their locations related to mesoscale circulation patterns are plotted in Figure 4.5B. A representative cytogram and relative proportion of each microbial group associated with the three microbial signature types are plotted in Figure 4.3B, D, and F. No significant spatial variability (SIMPROF, $p>0.01$) in microbial plankton community structure was detected across transects at depth.

Stations 19-26 along the 28°N transect 2 had a statistically similar microbial plankton community structure (SIMPROF, $p<0.01$) designated as microbial signature 1 (Figure 4.3A, 4.5A). These stations were characterized by the presence of autotrophic group A2, which was not observed beyond this region (Figure 4.5A). Concentrations of autotrophic group A3 (average 6.8 x10^3 ± 2.3 x10^3 cells mL^{-1}) were more than four times less concentrated when compared to stations with microbial signatures 2 and 3 (Table 4.5). Station 20, within this region, had the highest abundance (4.0 x10^5 cells mL^{-1}) of HNAB of all stations evaluated (Table 4.5). Stations 19 and 20 had the highest concentration of heterotrophic organisms (average 1.0 x10^6 ± 1.2 x10^5 cells mL^{-1}) observed in the study, greater than two times the average abundance observed at other stations.

Stations 1-8 along 27°N and 15-16 along 28°N had a statistically similar microbial plankton community structure (SIMPROF, $p<0.01$) designated as microbial signature 2 (Figure 4.3B, 4.5A). These stations were characterized by two times higher

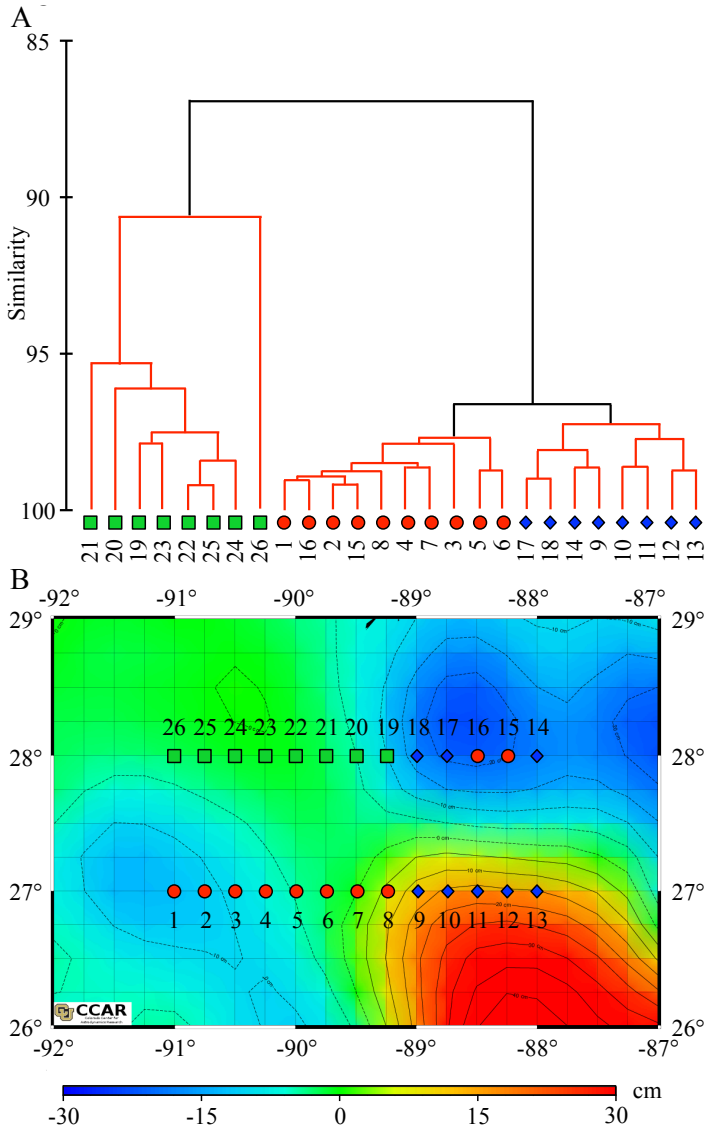

Figure 4.5 Variability in microbial community signature. (A) Dendrogram of group average cluster analysis based on community structure. Black lines indicate internal multivariate structure in the data at 97% similarity threshold ($p \leq 0.01$). Red dashed lines indicate a non-significant test result; samples below this point are homogeneous in community structure. Three significantly different microbial signatures (unique community structure based on relative abundance) were identified and are visualized by symbols with unique colors and shapes that are maintained throughout remaining figures. Microbial signature one is represented by green squares, red circles represent microbial signature two and blue diamonds represents microbial signature three. (B) Map of sea surface height anomaly (cm) within the sampling region; contours of similar SSH delineated by black dashed lines. Symbols represent the 3 significant signatures identified by CLUSTER and SIMPROF analyses. Cyclonic features are represented by cooler colors indicating negative SSH while the anti-cyclonic loop current is represented by warmer colors indicating positive SSH.

concentrations of autotrophic groups A3, A4 and A5 (average 2.1 x 10^4 ± 1.6 x10^4 cells mL^{-1}) when compared to stations with microbial signature 3 (Table 4.5). Similarly, these stations had 1.2 times higher concentrations of HNAB (average 2.3 x10^5 ± 4.1 x10^4 cells mL^{-1}) when compared to stations with microbial signature 3 (Table 4.5). Stations 9-13 along 27°N and 14, 17-18 along 28°N had a statistically similar microbial plankton community structure (SIMPROF, $p<0.01$) designated as microbial signature 3 (Figure 4.3C, 4.5A) and characterized by the lowest concentrations of autotrophic group A4 (average 1.9 x10^3 ± 1.8 x10^3 cells mL^{-1}), six times lower than other microbial signatures (Table 4.5). Additionally, there was considerably lower abundance of groups A3, A5 and HNAB compared to stations with microbial signature 2 (Table 4.5).

4.4.4 Statistical Correlation of Abiotic and Microbial Data

Salinity was the most influential parameter in DISTLM explaining 54.7% of the variability in microbial plankton community structure (Figure 4.6A), and also the primary driver of the separation of microbial signature 1 from 2 and 3. Because stations with microbial signature 1 are located in a region of pronounced lower salinity, these stations were removed and DISTLM re-run in order to identify other abiotic parameters separating microbial signatures 2 and 3. A combination of SSH and SST was identified as the overall BEST solution in DISTLM explaining 56.0% of the variability in microbial plankton community structure at stations with signatures 2 and 3 (Figure 4.6B). Remaining abiotic variables tested individually explained <0.5% of the variation in microbial plankton community structure for both models.

4.5 Discussion

Connectivity between variability in physicochemical conditions of the study region and statistically unique microbial signatures (based on total and relative microbial group abundance measured using flow cytometry) was observed once multivariate statistical analyses were applied. While we do not know the specific constituents of these

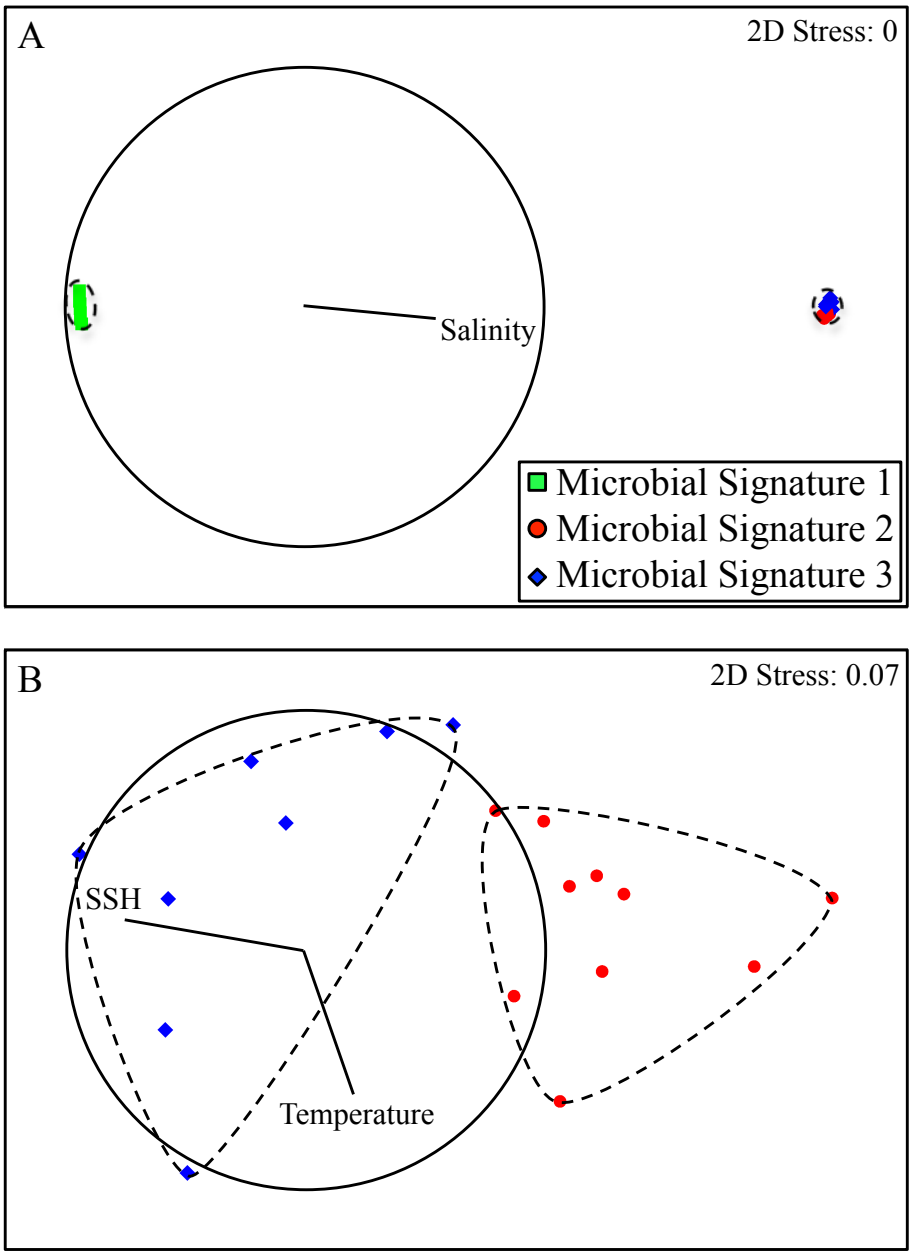

Figure 4.6 nMDS of variability in community structure between stations. The base variables identified by DISTLM are correlated to the ordination using Spearman statistics where line length within the frame of reference circle represents the relative strength of the correlation and direction corresponds to a positive relationship. (A) Separation of microbial signature 1 from 2 and 3. Dashed lines indicate 90% similarity of community structure. Forward R2, AICc, and BIC values for salinity were 0.0001, 80.43, and 82.24 respectively. (B) Separation of microbial signature 2 from 3. Dashed lines indicate 97% similarity of community structure. Forward R2 values for SST and SSH parameters were 0.0002 and 0.1331 respectively. The AICc, and BIC values for the combination of SST and SSH were 18.15, and 19.11 respectively.

microbial communities (genomic analyses were not possible), based on previous flow cytometric and NGOM studies (60,61), the dominant microbial plankton present were likely *Prochlorococcus*, *Synechococcus* groups lacking or containing different concentrations of phycourobilins, pico-eukaryotic algae and two groups of heterotrophs (high and low nucleic acid). Importantly, the unique microbial signatures observed were associated with apparently different water masses in the study site, each experiencing a unique set of coastal and/or mesoscale influences in the NGOM.

4.5.1 Microbial Plankton in a Region of Freshwater Entrainment

NGOM coastal ocean waters are subjected to large freshwater discharges from the Mississippi River and Atchafalaya River that can extend to our study region, beyond the continental shelf and into the loop current (123,131–133). It has previously been observed that low-salinity coastal water entrainments affect phytoplankton community structure in the NGOM (124,134,135). Additionally, the relative abundance of different nucleic acid containing heterotrophic microbial plankton was different between the Mississippi River plume and stations in the oligotrophic southeast GOM (60). In this study, stations with microbial signature 1 are geographically adjacent to one another and are primarily located outside of the influence of mesoscale circulation. Physicochemically, stations with this signature are characterized by having the lowest observed salinity of those sampled. Although there was a lack of significant statistical variability in microbial abundance or community structure at 30 m depth, DISTLM also predicted that salinity was the major driver of microbial variability below the surface (data not shown), further supporting entrainment of low-salinity coastal waters in the study region. Importantly, the lower salinity observed was still >32 indicating that this region remained within an oceanic water mass throughout the time of this study. Stations with microbial signature 1 also had the highest concentrations of inorganic nutrients, which is not surprising for coastal water entrainment. The major shift in community structure observed was the presence of autotrophic group A2 exclusively at these stations (Figure 4.3A, B). This could be a result of specific halo-tolerance or nutrient

requirement that is met by the conditions present in the low salinity, high nutrient waters. Alternatively, competitive or predatory interactions could also be affecting abundance (54) and structure of microbial plankton. Importantly, the presence of this group indicates that entrainments can potentially supply resident coastal microbes to open ocean environments.

4.5.2 Potential Relationships between Mesoscale Circulation and Microbial Plankton

A significant relationship between microbial plankton community structure and a combination of SSH and SST was also detected (Figure 4.6B). These characteristics are frequently utilized to identify regions of mesoscale circulation (136–138). SSH on its own, should not have a major affect on the microbial plankton community, as it is purely a physical measure of surface water. However, it has been documented that several physicochemical changes associated with SSH could impact microbial communities. For example, water temperature shifts associated with mesoscale circulation are extremely important to microbial organisms because physiologically, temperature can alter the kinetics of microbial metabolism and therefore the ability to compete and survive (54). Models predict that in the open ocean temperature can limit productivity of heterotrophic microorganisms while nutrients are typically more limiting to autotrophic microorganisms (139). The observed relationship between microbial plankton community structure and SST in this study indicates that thermal related limitations might exist for this size fraction of plankton. However, it is also possible that a different, unmeasured parameter is collinear with SSH and/or SST and is responsible for the observed relationship.

4.5.3 Nutrient Availability Structuring Microbial Communities

Classically, it has been predicted that limiting nutrients will be made available to the euphotic zone by doming pycnoclines in cyclonic circulation supporting higher abundance and productivity of autotrophic and heterotrophic plankton (31,140,141). At two stations, 13 and 16, corresponding mesocosm experiments were conducted and

results verified that significant shifts in microbial plankton community structure occurred within 24 hours of enrichment with nitrate supporting that nitrogen limitation of microbial plankton potentially exists in this region (data not shown, $p \leq 0.01$ at both stations, Monte Carlo PERMANOVA, partial type III pairwise test). However, in this study, DISTLM did not identify any of several growth limiting inorganic nutrients tested as having a significant relationship with microbial plankton community structure. There are several potential explanations. First, it is possible that mesoscale circulation did not facilitate significant nutrient enrichment. This is supported by a lack of significant collinearity between nutrients and SSH or SST. Previous research has observed that cyclonic eddies formed along the Leeuwin Current can be capped by warm Indian Ocean waters limiting upwelling from reaching the shallow euphotic zone (142). A similar circumstance may potentially be occurring in the NGOM as less dense coastal waters could cap upwelling in cyclonic features. Additionally, the intensity of pycnocline doming in mesoscale circulation features varies throughout their life cycle (31) and has been observed to shift regularly in GOM eddies (143).

Second, it is important to note, that several abiotic and biotic factors can influence microbial community abundance, structure and function (54) most notably grazing which was not examined in the current study. Therefore, the specific factors identified herein are likely not the only influences contributing to overall microbial abundance. It is possible that the size fraction of plankton targeted in this study are not being directly influenced by nutrient availability but are indirectly influenced by it. For example, if larger phytoplankton in this region are limited by nitrogen, which becomes available in the euphotic zone where mesoscale circulation is occurring, they might increase in abundance and compete with microbial plankton (54,144).

Third, it is possible that the variability in nutrient concentrations was too small to be considered significant by the DISTLM method when related to physiologically based groupings of microbial plankton, which is a potential limitation of flow cytometry derived community structure. To address these possibilities and increase the resolution of specific mesoscale impacts, nMDS ordinations of stations within each microbial

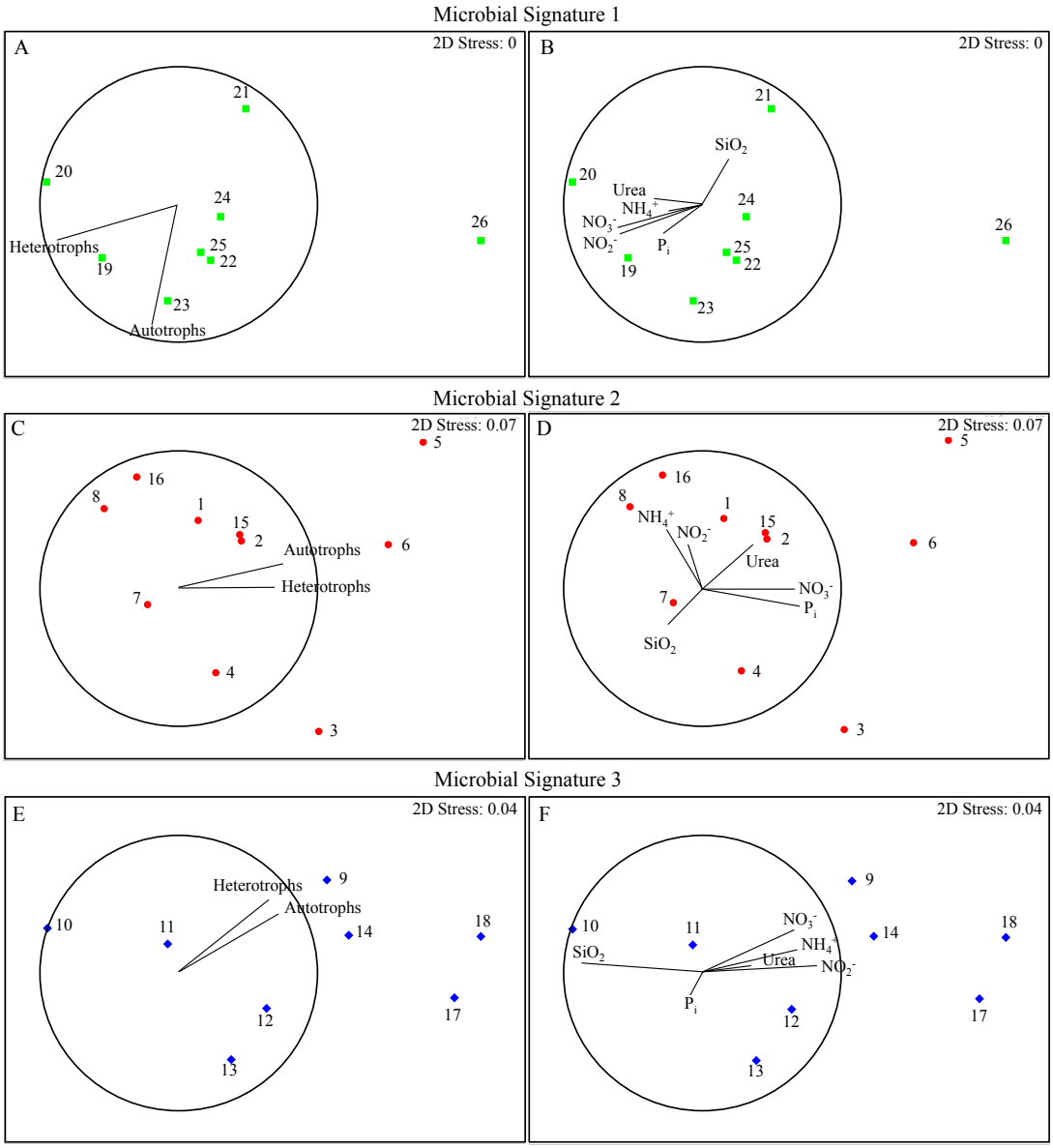

Figure 4.7 Nutrient availability correlated to microbial abundance NGOM. nMDS ordinations of variability in community structure between stations within each of the three significantly different microbial signatures. Spearman correlations between total autotrophic and heterotorphic pico- and nano-plankton abundance (A, C, E) and between measured nutrient concentrations (B, D, F) for those stations are plotted as vectors where line length within the frame of reference circle represents the relative strength of the correlation and direction corresponds to a positive relationship. (A, B) Variability of community structure and abundance at stations with microbial signature 1. (C, D) Variability of community structure and abundance at stations with microbial signature 2. (E, F) Variability of community structure and abundanceat stations with microbial signature 3.

signature group were correlated to nutrient availability and total microbial autotrophic and heterotrophic abundance rather than community structure using Spearman statistics (Figure 4.7). Important trends were observed based on Spearman vectors, suggesting that the strict DISTLM/community structure analysis of overall nutrient: microbial relationships may be limited in capturing all relevant connections and highlights the importance of considering several statistical approaches to validate findings when conducting flow-cytometric analyses.

4.5.4 Nutrient Availability Influencing Microbial Abundance

Potential relationships between microbial abundance and nutrient availability, specifically DIN, were detected across microbial signatures (Figure 4.7). Stations 21, 4 and 7, and 10-13 had the lowest microbial plankton abundance among stations within their respective microbial signatures (Figure 4.7A, C, E). Lower concentrations of DIN and sometimes P_i were measured at these stations (Figure 4.7B, D, F). Within groups of stations with the same microbial signature, stations with limited DIN and P_i were typically located either in regions outside of mesoscale circulation or in regions of positive SSH likely associated with anti-cyclonic features (Figure 4.5B). These findings support previous analyses suggesting that in oligotrophic waters off of the Louisiana/Texas shelf N and/or P_i are the principle limiting nutrients to primary producers (123,135,145). Interestingly, the proportion of LNAB:HNAB was the highest at stations 10-13 (microbial signature 3) within the study region. This potentially indicates that the heterotrophic bacterial community within the anti-cyclonic Loop Current is not only low in abundance but also less active (59). This could be an adaptation of the community to reduced availability of nutrients or limited organic carbon produced by larger autotrophs in this low-nitrogen region.

A negative relationship was observed between Si and DIN (Figure 4.7B, D, F). This observation implies that Si could be a limiting factor at stations where N and P_i are available consistent with reports of Si limitation of autotrophs in this region (146). The lower concentration of Si corresponding to increased concentrations of DIN supports the

premise that silicate-consuming organisms may be present at these stations. Previous research has shown that mesoscale circulation can induce blooms of diatoms (144,147) and a succession from microbial plankton to larger diatoms in central, high nutrient regions of cyclonic circulation is predicted (147). However, in the NGOM, the abundance of microbial plankton increased in regions of N availability and Si limitation indicating that they are not competing with larger organisms for limiting resources. One potential explanation is the recent finding that *Synechococcus* spp. contains high levels of silica under certain conditions (27). Although the reasons and mechanisms for uptake are not yet described, it is possible that the observed decreased Si concentration is the result of picocyanobacterial uptake of Si when nitrogen is available. Increased microbial plankton abundance associated with decreased Si but increased NO_3^- supports the theory proposed by (28) that unless Si* is optimal for diatom growth, microbial plankton will dominate the response to mesoscale circulation rather than diatoms. Alternatively, it is possible that there was a less severe succession in the circulation features in the NGOM driven by different responses of resident populations. Overall, these observations suggest that shifts in nutrient limitation across mesoscale features have important implications for plankton community ecology.

4.5.5 Microbial Abundance in Mesoscale Frontal Convergence Zones

Frontal convergence zones have previously been identified as 'hot spots' for increased microbial abundance and productivity associated with the shallowing of nutriclines (140,147). In this study, several examples of increased abundance were observed at stations where increased upwelling in frontal zones is predicted. Each of these examples was correlated to higher concentrations of NO_3^-, NO_2^- and NH_4^+, indicating that microbial plankton are dominantly nitrogen limited. An example is station 9, located along the western frontal zone of the anti-cyclonic Loop Current, which has highest abundance of microbial plankton among stations with microbial signature 3 (Figure 4.7E). Previous studies have shown that upwelling occurs at the margin of anti-cyclonic features (115,136) and in anti-cyclonic eddies in the GOM

(143). Because concentrations of NO_3^-, NH_4^+ and NO_2^- were higher at this station (Figure 4.7F), it is possible that upwelling caused a shift in nutrient concentrations that consequently increased microbial plankton abundance at this location. In addition, stations 14, 17, and 18 were located in a northern cyclonic mescoscale feature where typical cyclonic upwelling is supporting the higher concentrations of inorganic nitrogen observed and the corresponding higher microbial plankton abundance (Figure 4.7F).

4.5.6 Combined Physicochemical Influences on Microbial Plankton

A unique set of conditions was observed in the northern cyclonic feature (Figure 4.5B) because parts of the frontal convergence zone of this feature were also located within a low salinity region (Table 4.1). It has been proposed that lower salinity coastal water entrained into mescoscale circulation could supply different plankton species to these features (125). Two stations, 19 and 20, were located in the region where both mesoscale features and coastal influences were observed. These stations have the second and third highest total microbial plankton cellular abundance observed across the study region. Resident coastal microbial plankton entrained into mesoscale upwelling zones potentially respond more quickly to mesoscale nutrient pulses than organisms acclimated to oligotrophic conditions, resulting in the observed higher abundance. At these stations heterotrophs represented ~10% more of the total population observed elsewhere. Additionally, these stations have the highest concentrations of HNAB, which are generally associated with higher metabolic activity (54,59). Importantly, competition for dissolved organic matter can occur between autotrophic and heterotrophic prokaryotes in the microbial plankton size fractions (54). The observed heterotrophic increase potentially indicates that this region of combined nutrient enrichment from mesoscale circulation and coastal influences could shift microbial processes to net heterotrophy.

4.5.7 Potential Implications of Significant Spatial Variability in Microbial Plankton

The ecological implications of mesoscale driven shifts in microbial plankton abundance are particularly relevant to higher tropic consumers. Successful recruitment

of fish larvae to adult populations is imperative in maintaining sustainable fisheries (148,149). Several studies have proposed the match/mismatch hypothesis linking availability of plankton prey sources to eventual successful recruitment (148). Frontal convergence zones along the northern margin of the anti-cyclonic Loop Current in the GOM represent important early life habitat of several pelagic fish species including billfishes, tunas and swordfish (150–152) indicating that this region is an important spawning or nursery area (131). The increased abundance of microbial plankton observed in this study at stations proximal to the frontal zone of the Loop Current suggest that mesoscale induced increases in microbial plankton potentially contribute to bottom-up processes along the margin of this feature. Additionally, spatial dynamics of the Loop Current vary temporally resulting in changes in larval distributions (152) which could be linked to availability of prey. Therefore, generating a baseline understanding of microbial plankton responses to circulation is necessary to better understand trophic relationships and other potential impacts of changing microbial abundance in the Northern Gulf of Mexico.

CHAPTER V
CONCLUSIONS AND FUTURE DIRECTIONS

5.1 Chapter Synopses

5.1.1 Connections between Heterotrophic Microbes and Inorganic Nutrient Availability

Beyond the traditional concept of total community nutrient limitation, this study targeted the shift in physiological community structure of estuarine heterotrophs based on nucleic acid content characteristics. This trait-based approach connects variability in environmental conditions to potentially ecologically relevant differences in heterotrophic physiology. Heterotrophic microbes in the Trinity River Basin of Galveston Bay appear to undergo episodic nitrogen limitation. The most severe occurrence of nitrogen limitation was in August based on depleted *in situ* DIN concentrations. This occurred when temperature and dissolved organic carbon concentration were at the maximum values observed throughout this study, corresponding to previous research that has suggested that temperature and organic carbon availability predominantly control estuarine heterotrophic growth rates (15,55). Therefore, it is likely that heterotrophic limitation by inorganic nitrogen only occurs in the Trinity River Basin when high temperature stimulates increased cellular metabolic activity and carbon is saturated beyond heterotrophic requirements. The data herein suggest that a combination of these factors may ultimately co-limit heterotrophs.

In situ variability in heterotrophic groups during a month with strong nitrogen limitation (August) compared to a month with strong nitrogen saturation (November) suggest that heterotrophic microbes with lower nucleic acid content are able to out-compete heterotrophs with relatively higher nucleic acid content under high temperature, low nitrogen conditions, shifting to the opposite scenario under high nitrogen low temperature conditions. Significant responses to nutrient enrichment of relatively higher nucleic acid content groups suggest that these organisms are ultimately better competitors under nutrient replete conditions. Therefore it is likely that heterotrophic

groups with different physiological characteristics have different strategies to utilize potentially limiting nutrients in the Trinity River Basin.

5.1.2 Estuarine Heterotrophic and Autotrophic Nutrient Limitation

Microbial plankton can be categorized based on differences in traits related to energy acquisition pathways, in this study either autotrophy or heterotrophy. Variability in abundance of organisms with these traits can also be used to track potentially significant transitions in relation to environmental conditions. Spatiotemporal shifts in the relative abundance of autotrophic and heterotrophic microbial groups were significantly related to temperature, DIN, P_i and TOC. In general there were opposing gradients of DIN and P_i availability between two stations. Heterotrophic abundance and contribution to the entire microbial community was increased at a station in the Trinity River Basin during warm months, with higher TOC concentrations but decreased DIN, suggesting episodic nitrogen limitation at this station similar to results observed in Chapter II. It is predicted that a step-wise spatiotemporal co-limitation of microbial plankton in Galveston Bay exists such that temperature ultimately limits both autotrophic and heterotrophic fractions followed by P_i at station GB2 where nutrient pulses stimulated by freshwater inflows are infrequent. If P_i is available, as occurs in the Trinity River Basin (station GB1) then DIN becomes the limiting factor.

Under strictly environmental nutrient stress, autotrophic microbial plankton are better competitors for a combination of inorganic nitrogen and phosphorous because the overall response to nutrient enrichment was predominantly an increase in heterotrophic abundance. This could be an indication that because heterotrophic microbes cannot produce their own carbon they have to devote more resources toward obtaining energy and less toward nutrient requirements than autotrophic microbial plankton. This is consistent with the concept that heterotrophs will ultimately be carbon limited (13). However, the autotrophic fraction of microbial plankton contributed to significant nutrient enrichment responses in months where total Chlorophyll *a* concentration is high suggesting that when smaller autotrophs are competing with larger phytoplankton they

can become nutrient limited as well. This situation can potentially drive competition between autotrophic and heterotrophic fractions of the microbial plankton for limiting nutrients.

5.1.3 Scale of Nutrient Availability: Could Mesoscale Processes Influence Microbial Groups?

Using relative nucleic acid and photo-pigment characteristics, physiological groupings can be resolved within the heterotrophic and autotrophic fractions respectively. In the northern Gulf of Mexico (NGOM) two heterotrophic and five autotrophic groups were observed across transects that intersected a coastal freshwater entrainment, cyclonic circulation and the anti-cyclonic loop current, three major oceanographic mesoscale features. A significant shift in the relative contribution of these groups to microbial plankton abundance (microbial signature) was related to salinity, associated with the coastal freshwater entrainment. Among stations outside the freshwater entrainment, a shift in microbial signature was related to SSH and temperature indicating that mesoscale circulation features were playing a role in structuring marine microbial plankton communities.

Although significant relationships with inorganic nutrients typically associated with nutrient limitation were not observed at the scale of initial analysis, resolving variation in total abundance within microbial signatures associated with specific mesoscale features indicated potential relationships. Total abundance of heterotrophs and autotrophs was correlated to increased availability of dissolved nitrogen and phosphorous at stations characterized by all three microbial signatures. These relationships indicate that regions within the oceanographic features may have varying nutrient availability that corresponds to changes in total abundance. For example, in frontal convergence zones within the anti-cyclonic loop current and cyclonic eddy high nutrient concentrations corresponded to increased microbial abundance. In a region where freshwater entrainment merged with a frontal convergence zone particularly high relative abundances of heterotrophs were observed. Specifically, high concentrations of

HNAB indicate that this region of combined nutrient enrichment from mesoscale circulation and coastal influences, could shift microbial processes to heterotrophy. Overall, physically driven nutrient shifts in the NGOM likely influence the microbial plankton community structure, which is reflected in changing physiological characteristics.

5.1.4 Relevance in the Context of Previous Research

Marine microbial ecology is a broad and diverse field that over the past fifty years has developed into a major research focus, specifically among ocean scientists (153). The connection between microbes and marine biogeochemical cycles has garnered special interest given that these relationships have global consequences (1,23). Some examples of how the work conducted herein contributes to the current understanding of marine microbial ecology can be presented in the context of seminal findings regarding nutrient/microbial relationships. Limitation of heterotrophic bacterial abundance by inorganic nutrients has been observed despite the theoretical consensus that availability of carbon resources ultimately limits these communities (7,100,154). In freshwater and estuarine systems the subsidy of allochthonous carbon to autochthonous resources has been proposed to saturate heterotrophic requirements resulting in microbial nutrient limitation (15,102,108). Additionally, in several open-ocean systems including in the Northern Atlantic, Pacific and Arctic Oceans, inorganic nitrogen and/or phosphorous limitation of heterotrophic growth rates and production has been shown (7,14,154) suggesting that this phenomenon may occur globally. This study supports these findings, by showing that naturally occurring pulses of nutrients correlate to increased heterotrophic abundance across two different marine systems in the Gulf of Mexico, where these relationships have not previously been quantified. This study further advances that understanding by showing that nutrient limitation of heterotrophs occurs beyond total abundance or growth rate and is actually acting differently on certain fractions of the community. Molecular analyses have confirmed shifts in microbial community structure associated with nutrient enrichment (155,156), and changes in size

have been observed (94), altered nucleic acid content has not been specifically targeted. This study provides empirical support to previously suggested hypotheses that fractions of heterotrophic marine microbes may have different ecological strategies toward nutrient utilization that are reflected in their genome length (nucleic acid content) (66,91). Because heterotrophic groups are limited by inorganic nutrients, competition between bacteria and other organisms is expected but not fully resolved (14,100,157). The results herein support that competition for limiting nutrients in estuaries occurs between the heterotrophic and autotrophic fractions of the microbial community and the consequences of these interactions should be investigated further and across many systems. Finally, this study promotes that trait-based ecological approaches are appropriate and informative when examining microbial communities and should continue to be utilized to validate and formulate microbial ecological theories (45).

5.2 Broader Impact

Marine microbial plankton are known to contribute to several important ecosystem functions. Two specific cases will be highlighted to represent potential broader impacts of this research. Estuaries are considered some of the most economically and ecologically important systems in the world (158,159). Nutrient flux and processing in marine estuaries is a component within these dynamic systems that remains an important topic of interest because anthropogenic eutrophication of estuaries has altered the health of these systems and is predicted to continue to change with increasing human impacts (158,160,161). Pelagic microbes have been linked with estuarine biogeochemical cycling (162,163). In Galveston Bay, Texas however, very little research has been done examining potential relationships between nutrients and microbial plankton. Resolving connections between inorganic nutrients and microbial communities in estuaries could be invaluable toward generating a predictive framework in order to remove microbes from the “black-box” often utilized in estuarine modeling (55), which will better enable policymakers to create productive management strategies, especially given continued expectations for anthropogenic change. These contributions

will help to maintain a healthy and safe environment for millions of humans consuming resources from and inhabiting areas within Galveston Bay.

Another important impact of nutrient availability for microbial plankton is when considering energy transfer to higher trophic orders. Preferential consumption of autotrophic or heterotrophic plankton as prey has been observed within the microbial size fraction (164). Therefore nutrient stimulated variability in microbial groups could have impacts on the food web in both estuarine and oligotrophic environments (34,104,148). For example, the frontal convergence zones along the northern margin of the anti-cyclonic Loop Current represent important early life habitat of several pelagic fish species (150,151). Results correlating shifts in microbial abundance with increased nutrient availability associated with frontal convergence features suggest that it is possible that microbial subsidies of energy could contribute to prey items there. Ultimately this could influence the successful recruitment of fish larvae to adult populations, which is imperative in maintaining sustainable fisheries (148).

5.3 Future Considerations

Evidence supports strong connections between inorganic nutrients and shifts in physiological characteristics of microbial communities emphasizing the possibility that the type of approach taken herein could be used to pursue several interesting research directives. Utilizing the trait-based categorization of microbes has great potential to resolve ecologically relevant variability in order to better apply accepted ecological theories or develop new ones for marine microbes. Importantly, flow cytometry can quantify multiple expressed traits simultaneously, which greatly improves the capacity to detect potential for trait interactions, including trade-offs that could have ecological significance. In particular, combining flow-cytometric sorting of physiological groups with taxonomic probing, stable isotope incorporation, and hybridization with functional probes could begin to bridge the widely recognized gap between microbial form and function (49,165,166). One important question that remains unresolved by this study is whether the observed shifts in physiological community structure are related to the rapid

evolution of individual characteristics within the same taxonomic community or if succession occurs where genetically distinct groups with different physiological characteristics are favored by changing conditions and out-compete initial groups. Future experimentation examining shifts in average group characteristics (56) or combining molecular and flow-cytometric methodologies (166) could begin to evaluate these types of questions.

REFERENCES

1. Church MJ. The trophic tapestry of the sea. Proc Natl Acad Sci. 2009;106(37):15519–20.

2. Whitman WB, Coleman DC, Wiebe WJ. Prokaryotes: the unseen majority. Proc Natl Acad Sci. 1998;95(12):6578–83.

3. Grob C, Hartmann M, Zubkov MV, Scanlan DJ. Invariable biomass-specific primary production of taxonomically discrete picoeukaryote groups across the Atlantic Ocean: Invariable primary production of picoeukaryotes. Environ Microbiol. 2011 Dec;13(12):3266–74.

4. Li WKW, Subba Rao DV, Harrison WG, Smith JC, Cullen JJ, Irwin B, et al. Autotrophic picoplankton in the tropical ocean. Science. 1983 Jan 21;219(4582):292–5.

5. Field CB, Behrenfeld MJ, Randerson JT, Falkowski P. Primary production of the biosphere: Integrating terrestrial and oceanic components. Science. 1998 Jul 10;281(5374):237–40.

6. Jiao N, Herndl GJ, Hansell DA, Benner R, Kattner G, Wilhelm SW, et al. Microbial production of recalcitrant dissolved organic matter: Long-Term Carbon Storage in the Global Ocean. Nat Rev Microbiol. 2010 Aug;8:593–9.

7. Rivkin RB, Anderson MR. Inorganic nutrient limitation of oceanic bacterioplankton. Limnol Oceanogr. 1997;42(4):730–40.

8. Howarth RW, Marino R. Nitrogen as the limiting nutrient for eutrophication in coastal marine ecosystems: evolving views over three decades. Limnol Oceanogr. 2006;51(1part2):364–76.

9. Falkowski PG, Raven JA. Aquatic photosynthesis. Second. New Jersey, USA: Princeton University Press; 2007.

10. Liebig JF von, Playfair L. Organic chemistry in its applications to agriculture and physiology. London: Printed for Taylor and Watson; 1843. 418 p.

11. Blackman FF. Optima and limiting factors. Ann Bot. 1905;19(73-76):281–96.

12. Sterner RW, Elser JJ. The biology of elements from molecules to the biosphere. Ecological Stoichiometry. New Jersey, USA: Princeton University Press; 2002.

13. Bratbak G, Thingstad TF. Phytoplankton-bacteria interactions: an apparent paradox? Analysis of a model system with both competition and commensalism. Mar Ecol Prog Ser Oldendorf. 1985;25(1):23–30.

14. Thingstad TF, Bellerby RGJ, Bratbak G, Børsheim KY, Egge JK, Heldal M, et al. Counterintuitive carbon-to-nutrient coupling in an Arctic pelagic ecosystem. Nature. 2008 Sep 18;455(7211):387–90.

15. Hitchcock JN, Mitrovic SM. Different resource limitation by carbon, nitrogen and phosphorus between base flow and high flow conditions for estuarine bacteria and phytoplankton. Estuar Coast Shelf Sci. 2013 Dec;135:106–15.

16. Azam F, Fenchel T, Field JG, Gray JS, Meyer-Reil LA, Thingstad F. The ecological role of water-column microbes in the sea. Mar Ecol Prog Ser Oldendorf. 1983;10(3):257–63.

17. Joint I, Henriksen P, Fonnes GA, Bourne D, Thingstad TF, Riemann B, et al. Competition for inorganic nutrients between phytoplankton and bacterioplankton in nutrient manipulated mesocosms. Aquat Microb Ecol. 2002;29(2):145–59.

18. Martinez-Garcia M, Swan BK, Poulton NJ, Gomez ML, Masland D, Sieracki ME, et al. High-throughput single-cell sequencing identifies photoheterotrophs and chemoautotrophs in freshwater bacterioplankton. ISME J. 2012;6(1):113–23.

19. Harpole WS, Ngai JT, Cleland EE, Seabloom EW, Borer ET, Bracken MES, et al. Nutrient co-limitation of primary producer communities: Community co-limitation. Ecol Lett. 2011 Sep;14(9):852–62.

20. Redfield AC. The biological control of chemical factors in the environment. Am Sci. 1958;230A – 221.

21. Tyrell T. The relative influences of nitrogen and phosphorous on oceanic primary productivity. Nature. 1999 Aug 5;400(6744):525–31.

22. Karl DM. Nutrient dynamics in the deep blue sea. TRENDS Microbiol. 2002;10(9):410–8.

23. Moore CM, Mills MM, Arrigo KR, Berman-Frank I, Bopp L, Boyd PW, et al. Processes and patterns of oceanic nutrient limitation. Nat Geosci. 2013 Mar 31;6(9):701–10.

24. Howarth RW, Marino R, Lane J, Cole JJ. Nitrogen fixation in fresh-water, estuarine, and marine ecosystems. 1. Rates and importance. Limnol Oceanogr. 1988;33(4 part 2):669–87.

25. Dugdale RC, Wilkerson FP, Minas HJ. The Role of a silicate pump in driving new production. Deep-Sea Res I. 1995;42(5):697–719.

26. Irwin AJ. Scaling-up from nutrient physiology to the size-structure of phytoplankton communities. J Plankton Res. 2006 Jan 10;28(5):459–71.

27. Baines SB, Twining BS, Brzezinski MA, Krause JW, Vogt S, Assael D, et al. Significant silicon accumulation by marine picocyanobacteria. Nat Geosci. 2012 Nov 18;5(12):886–91.

28. Bibby TS, Moore CM. Silicate:nitrate ratios of upwelled waters control the phytoplankton community sustained by mesoscale eddies in sub-tropical North Atlantic and Pacific. Biogeosciences. 2011 Mar 14;8(3):657–66.

29. Finkel ZV. Does phytoplankton cell size matter? The evolution of modern marine food webs. Boston, Elsevier; 2007

30. Finkel ZV, Beardall J, Flynn KJ, Quigg A, Rees TAV, Raven JA. Phytoplankton in a changing world: cell size and elemental stoichiometry. J Plankton Res. 2010 Jan 1;32(1):119–37.

31. McGillicuddy DJ, Robinson AR, Siegel DA, Jannasch HW, Johnson R, Dickey TD, et al. Influence of mesoscale eddies on new production in the Sargasso Sea. Nature. 1998;394(6690):263–6.

32. Corno G, Karl D, Church M, Letelier R, Lukas R, Bidigare R, et al. Impact of climate forcing on ecosystem processes in the North Pacific subtropical gyre. J Geophys Res-Oceans. 2007 Apr 26;112(C4).

33. Lomas MW, Steinberg DK, Dickey T, Carlson CA, Nelson NB, Condon RH, et al. Increased ocean carbon export in the Sargasso Sea linked to climate variability is countered by its enhanced mesopelagic attenuation. Biogeosciences. 2010;7(1):57–70.

34. Davidson K, Gilpin LC, Hart MC, Fouilland E, Mitchell E, Á lvarez Calleja I, et al. The influence of the balance of inorganic and organic nitrogen on the trophic dynamics of microbial food webs. Limnol Oceanogr. 2007;52(5):2147–63.

35. Kremer C, Shepard AK, Fong A, Kellerman A, Tuscano B, Tolar B, et al. Realizing the potential of trait-based aquatic ecology: New tools and collaborative approaches. Prep.

36. Mcgill B, Enquist B, Weiher E, Westoby M. Rebuilding community ecology from functional traits. Trends Ecol Evol. 2006 Apr;21(4):178–85.

37. Violle C, Navas M-L, Vile D, Kazakou E, Fortunel C, Hummel I, et al. Let the concept of trait be functional! Oikos. 2007 May;116:882–92.

38. Rappé MS, Giovannoni SJ. The uncultured microbial majority. Annu Rev Microbiol. 2003 Oct;57(1):369–94.

39. Pernthaler J, Amann R. Fate of Heterotrophic microbes in pelagic habitats: Focus on populations. Microbiol Mol Biol Rev. 2005 Sep 1;69(3):440–61.

40. Stackebrandt E, Goebel BM. A place for DNA-DNA reassociation and 16S rRNA sequence analysis in the present species definition in bacteriology. Int J Syst Bacteriol. 1994 Oct;44(4):846–9.

41. Brown MV, Ostrowski M, Grzymski JJ, Lauro FM. A trait based perspective on the biogeography of common and abundant marine bacterioplankton clades. Mar Genomics. 2014 Jun;15:17–28.

42. Gifford SM, Sharma S, Booth M, Moran MA. Expression patterns reveal niche diversification in a marine microbial assemblage. ISME J. 2012;7(2):281–98.

43. Lauro FM, McDougald D, Thomas T, Williams TJ, Egan S, Rice S, et al. The genomic basis of trophic strategy in marine bacteria. Proc Natl Acad Sci. 2009;106(37):15527–33.

44. Grossart H-P. Ecological consequences of bacterioplankton lifestyles: changes in concepts are needed: Ecological consequences of bacterioplankton lifestyles. Environ Microbiol Rep. 2010 Dec;2(6):706–14.

45. Krause S, Le Roux X, Niklaus PA, Van Bodegom PM, Lennon JT, Bertilsson S, et al. Trait-based approaches for understanding microbial biodiversity and ecosystem functioning. Front Microbiol [Internet]. 2014 May 27 [cited 2015 Apr 14];5. Available from: http://journal.frontiersin.org/article/10.3389/fmicb.2014.00251/abstract

46. Prosser JI, Bohannan BJ, Curtis TP, Ellis RJ, Firestone MK, Freckleton RP, et al. The role of ecological theory in microbial ecology. Nat Rev Microbiol. 2007;5(5):384–92.

47. Fontana S, Jokela J, Pomati F. Opportunities and challenges in deriving phytoplankton diversity measures from individual trait-based data obtained by scanning flow-cytometry. Front Microbiol [Internet]. 2014 Jul 1 [cited 2015 Apr 14];5. Available from: http://journal.frontiersin.org/article/10.3389/fmicb.2014.00324/abstract

48. Litchman E, Klausmeier CA. Trait-based community ecology of phytoplankton. Annu Rev Ecol Evol Syst. 2008 Dec;39(1):615–39.

49. Wang Y, Hammes F, De Roy K, Verstraete W, Boon N. Past, present and future applications of flow cytometry in aquatic microbiology. Trends Biotechnol. 2010 Aug;28(8):416–24.

50. Raes J, Letunic I, Yamada T, Jensen LJ, Bork P. Toward molecular trait-based ecology through integration of biogeochemical, geographical and metagenomic data. Mol Syst Biol. 2014 Apr 16;7(1):473–473.

51. Campbell L. Flow cytometric analysis of autotrophic picoplankton. Methods Microbiol. 2001;30:317–43.

52. Hammes F, Egli T. Cytometric methods for measuring bacteria in water: advantages, pitfalls and applications. Anal Bioanal Chem. 2010 Jun;397(3):1083–95.

53. Del Giorgio PA, Gasol JM. Physiological structure and single-cell activity in marine bacterioplankton. Microbial Ecology of the Oceans. Second. Hoboken, New Jersey, USA: John Wiley & Sons, Inc.; 2008. p. 243–85.

54. Kirchman DL. Introduction and Overview. Microbial ecology of the oceans. Second. Hoboken, New Jersey, USA: John Wiley & Sons, Inc.; 2008. p. 1–26.

55. Moràn XAG, Ducklow HW, Erickson M. Single-cell physiological structure and growth rates of heterotrophic bacteria in a temperate estuary (Waquoit Bay, Massachusetts). Limnol Oceanogr. 2011 Jan;56(1):37–48.

56. Bouvier T, del Giorgio PA, Gasol JM. A comparative study of the cytometric characteristics of High and Low nucleic-acid bacterioplankton cells from different aquatic ecosystems. Environ Microbiol. 2007 Aug;9(8):2050–66.

57. Robertson BR, Button DK. Characterizing aquatic cacteria according to population, cell size, and apparent DNA content by flow cytometry. Cytometry. 1989;10:70–6.

58. Li WKW, Jellet JF, Dickie PM. DNA distributions in planktonic bacteria stained with TOTO or TO-PRO. Limnol Oceanogr. 1995 Dec;40(8):1485–95.

59. Lebaron P, Servais P, Agogue H, Courties C, Joux F. Does the high nucleic acid content of individual bacterial cells allow us to discriminate between active cells and inactive cells in aquatic systems? Appl Environ Microbiol. 2001 Apr 1;67(4):1775–82.

60. Jochem FJ, Lavrentyev PJ, First MR. Growth and grazing rates of bacteria groups with different apparent DNA content in the Gulf of Mexico. Mar Biol. 2004 Nov;145(6):1213–25.

61. Liu H, Dagg M, Campbell L, Urban-Rich J. Picophytoplankton and bacterioplankton in the Mississippi River plume and its adjacent waters. Estuaries. 2004;27(1):147–56.

62. Gasol JM, del Giorgio PA. Using flow cytometry for counting natural planktonic bacteria and understanding the structure of planktonic bacterial communities. Sci Mar. 2000;64(2):197–224.

63. MorÃ¡n XAG, Calvo-DÃ-az A. Single-cell vs. bulk activity properties of coastal bacterioplankton over an annual cycle in a temperate ecosystem: Single-cell activity of coastal bacterioplankton. FEMS Microbiol Ecol. 2009 Jan;67(1):43–56.

64. Franco-Vidal L, Morán XAG. Relationships between coastal bacterioplankton growth rates and biomass production: Comparison of leucine and thymidine uptake with single-cell physiological characteristics. Microb Ecol. 2011 Feb;61(2):328–41.

65. Pedros-Alio C. Dipping into the Rare Biosphere. Science. 2007 Jan 12;315(5809):192–3.

66. Vila-Costa M, Rinta-Kanto JM, Sun S, Sharma S, Poretsky R, Moran MA. Transcriptomic analysis of a marine bacterial community enriched with dimethylsulfoniopropionate. ISME J. 2010;4(11):1410–20.

67. Zubkov MV, Fuchs BM, Burkill PH, Amann R. Comparison of cellular and biomass specific activities of dominant bacterioplankton groups in stratified waters of the Celtic Sea. Appl Environ Microbiol. 2001 Nov 1;67(11):5210–8.

68. Schattenhofer M, Wulf J, Kostadinov I, Glöckner FO, Zubkov MV, Fuchs BM. Phylogenetic characterisation of picoplanktonic populations with high and low nucleic acid content in the North Atlantic Ocean. Syst Appl Microbiol. 2011 Sep;34(6):470–5.

69. Philippot L, Andersson SG, Battin TJ, Prosser JI, Schimel JP, Whitman WB, et al. The ecological coherence of high bacterial taxonomic ranks. Nat Rev Microbiol. 2010;8(7):523–9.

70. Pinhassi J, Gómez-Consarnau L, Alonso-Sáez L, Sala MM, Vidal M, Pedrós-Alió C, et al. Seasonal changes in bacterioplankton nutrient limitation and their effects on bacterial community composition in the NW Mediterranean Sea. Aquat Microb Ecol. 2006;45(3):241–52.

71. Zimmerman AE, Allison SD, Martiny AC. Phylogenetic constraints on elemental stoichiometry and resource allocation in heterotrophic marine bacteria:

Stoichiometry and resource allocation in marine bacteria. Environ Microbiol. 2014 May;16(5):1398–410.

72. Santschi PH. Seasonality in nutrient concentrations in Galveston Bay. Mar Environ Res. 1995;40(4):337–62.

73. Castro MS, Driscoll CT, Jordan TE, Reay WG, Boynton WR. Sources of nitrogen to estuaries in the United States. Estuaries. 2003;26(3):803–14.

74. Örnólfsdóttir EB, Lumsden SE, Pinckney JL. Nutrient pulsing as a regulator of phytoplankton abundance and community composition in Galveston Bay, Texas. J Exp Mar Biol Ecol. 2004 Jun;303(2):197–220.

75. Roelke D, Li H, Hayden N, Miller C, Davis S, Quigg A, et al. Co-occurring and opposing freshwater inflow effects on phytoplankton biomass, productivity and community composition of Galveston Bay, USA. Mar Ecol Prog Ser. 2013 Mar 12;477:61–76.

76. Dellapenna TM, Allison MA, Gill GA, Lehman RD, Warnken KW. The impact of shrimp trawling and associated sediment resuspension in mud dominated, shallow estuaries. Estuar Coast Shelf Sci. 2006 Sep;69(3-4):519–30.

77. Dupuis KW, Anis A. Observations and modeling of wind waves in a shallow estuary: Galveston Bay, Texas. J Waterw Port Coast Ocean Eng. 2013 Jul;139(4):314–25.

78. Clement CS, Bricker B, Pirhalla DE. State of the Coast Report: Eutrophic conditions in estuarine waters [Internet]. Silver Spring, MD: National Oceanic and Atmospheric Administration; 2001 p. on – line. Available from: http://state-of-coast.noaa.gov/bulletins/html/eut_18/eut.html

79. Quigg A, Broach L, Denton W, Miranda R. Water quality in the Dickinson Bayou watershed (Texas, Gulf of Mexico) and health issues. Mar Pollut Bull. 2009 Jun;58(6):896–904.

80. Thronson A, Quigg A. Fifty-five years of fish kills in coastal Texas. Estuaries Coasts. 2008 Sep;31(4):802–13.

81. Madden CJ, Day JW. An instrument system for high-speed mapping of chlorophyll-a and physicochemical variables in surface waters. Estuaries. 1992 Sep;15(3):421–7.

82. Guo L, Hung C-C, Santschi PH, Walsh ID. 234 Th scavenging and its relationship to acid polysaccharide abundance in the Gulf of Mexico. Mar Chem. 2002;78(2):103–19.

83. Xu C, Santschi PH, Hung C-C, Zhang S, Schwehr KA, Roberts KA, et al. Controls of 234Th removal from the oligotrophic ocean by polyuronic acids and modification by microbial activity. Mar Chem. 2011 Jan;123(1-4):111–26.

84. Fisher TR, Gustafson AB, Sellner K, Lacouture R, Haas LW, Wetzel RL, et al. Spatial and temporal variation of resource limitation in Chesapeake Bay. Mar Biol. 1999;133(4):763–78.

85. Kamiya E, Izumiyama S, Nishimura M, Mitchell JG, Kogure K. Effects of fixation and storage on flow cytometric analysis of marine bacteria. J Oceanogr. 2007;63(1):101–12.

86. Marie D, Partensky F, Jacquet S, Vaulot D. Enumeration and cell cycle analysis of natural populations of marine picoplankton by flow cytometry using the nucleic acid stain SYBR Green I. Appl Environ Microbiol. 1997;63(1):186–93.

87. Anderson MJ, Gorley RN, Clarke KR. PERMANOVA+ for PRIMER: Guide to software and statistical methods. First. Plymouth, United Kingdom: PRIMER-E Ltd.; 2008.

88. Clarke KR, Warwick RM. Change in marine communities: An approach to statistical analysis and interpretation. Second. Plymouth, United Kingdom: PRIMER-E Ltd.; 2001.

89. Clarke KR, Gorley RN. PRIMER v6: User Manual/Tutorial. First. Plymouth, United Kingdom: PRIMER-E Ltd.; 2006.

90. Huete-Stauffer T, Morán X. Dynamics of heterotrophic bacteria in temperate coastal waters: similar net growth but different controls in low and high nucleic acid cells. Aquat Microb Ecol. 2012 Nov 2;67(3):211–23.

91. Giovannoni SJ, Thrash JC, Temperton B. Implications of streamlining theory for microbial ecology. ISME J. 2014;8(8):1553–65.

92. Gieskes WW, Kraay GW, Baars MA. Current 14C Methods for measuring primary production: Gross underestimates in oceanic waters. Neth J Sea Res. 1979;13(1):58–78.

93. Calvo-Diaz A, Diaz-Perez L, Suarez LA, Moran XAG, Teira E, Maranon E. Decrease in the autotrophic-to-heterotrophic biomass ratio of picoplankton in oligotrophic marine waters due to bottle enclosure. Appl Environ Microbiol. 2011 Aug 15;77(16):5739–46.

94. Lebaron P, Servais P, Troussellier M, Courties C, Muyzer G, Bernard L, et al. Microbial community dynamics in Mediterranean nutrient-enriched seawater

mesocosms: changes in abundances, activity and composition. FEMS Microbiol Ecol. 2001;34:255–66.

95. Del Giorgio PA, Gasol JM, Vaque D, Mura P, Agusti S, Duarte CM. Bacterioplankton community structure: Protists control net production and the proportion of active bacteria in a coastal marine community. Limnol Oceanogr. 1996 Sep;41(6):1169–79.

96. Lester LJ, Gonzalez L. The State of the Bay: A characterization of the Galveston Bay ecosystem. [Internet]. Webster, Texas, USA: Galveston Bay Estuary Program; 2002. Available from: http://gbic.tamug.edu/sobdoc/sob2/sob2page.html

97. Buzan D, Lee W, Culbertson J, Kuhn N, Robinson L. Positive relationship between freshwater inflow and oyster abundance in Galveston Bay, Texas. Estuaries Coasts. 2009 Jan;32(1):206–12.

98. Quigg A, Finkel ZV, Irwin AJ, Rosenthal Y, Ho T-Y, Reinfelder JR, et al. The evolutionary inheritance of elemental stoichiometry in marine phytoplankton. Nature. 2003;425(6955):291–4.

99. Quigg A, Irwin AJ, Finkel ZV. Evolutionary inheritance of elemental stoichiometry in phytoplankton. Proc R Soc B Biol Sci. 2011 Feb 22;278(1705):526–34.

100. Church MJ. Resource control of bacterial dynamics in the sea. Microbial ecology of the oceans. Second. Hoboken, New Jersey, USA: John Wiley & Sons, Inc.; 2008. p. 335–71.

101. Kirchman DL, Wheeler PA. Uptake of ammonium and nitrate by heterotrophic bacteria and phytoplankton in the sub-Arctic Pacific. Deep Sea Res Part Oceanogr Res Pap. 1998;45(2):347–65.

102. Almeida MA, Cunha MA, Alcântara F. Relationship of bacterioplankton production with primary production and respiration in a shallow estuarine system (Ria de Aveiro, NW Portugal). Microbiol Res. 2005 Jul;160(3):315–28.

103. Munk WH, Riley GA. Absorption of nutrients by aquatic plants. J Mar Res. 1952;11(2):215–40.

104. Sherr EB, Sherr BF. Significance of predation by protists in aquatic microbial food webs. Antonie Van Leeuwenhoek. 2002;81:293–308.

105. Agawin NS, Duarte CM, Agusti S. Nutrient and temperature control of the contribution of picoplankton to phytoplankton biomass and production. Limnol Oceanogr. 2000;45(3):591–600.

106. Shiah F-K, Ducklow HW. Temperature and substrate regulation of bacterial abundance, production and specific growth rate in Chesapeake Bay, USA. Mar Ecol Prog Ser. 1994;103:297–308.

107. Moran XAG, Calvo-Díaz A, Ducklow HW. Total and phytoplankton mediated bottom-up control of bacterioplankton change with temperature in NE Atlantic shelf waters. Aquat Microb Ecol. 2010;58:229–39.

108. Hoch MP, Kirchman DL. Seasonal and inter-annual variability in bacterial production and biomass in a temperate estuary. Mar Ecol Prog Ser Oldendorf. 1993;98(3):283–95.

109. Arar EJ, Collins GB. Method 445.0. *In Vitro* determination of chlorophyll a and pheophytin a in marine and freshwater algae by fluorescence. Methods for the determination of chemical substances in marine and estuarine environmental matrices. Second. Cincinnati Ohio, USA: National Exposure Research Laboratory; 1997.

110. Dang H, Jiao N. Perspectives on the microbial carbon pump with special reference to microbial respiration and ecosystem efficiency in large estuarine systems. Biogeosciences. 2014 Jul 24;11(14):3887–98.

111. Massana R. Eukaryotic Picoplankton in surface oceans. Annu Rev Microbiol. 2011 Oct 13;65(1):91–110.

112. Benitez-Nelson CR, McGillicuddy DJ. Mesoscale physical–biological–biogeochemical linkages in the open ocean: An introduction to the results of the E-Flux and EDDIES programs. Deep Sea Res Part II Top Stud Oceanogr. 2008 May;55(10-13):1133–8.

113. Benitez-Nelson CR, Bidigare RR, Dickey TD, Landry MR, Leonard CL, Brown SL, et al. Mesoscale eddies drive increased silica export in the subtropical Pacific Ocean. Science. 2007 May 18;316(5827):1017–21.

114. Mourino-Carballido B, McGillicuddy DJ. Mesoscale variability in the metabolic balance of the Sargasso Sea. Limnol Oceanogr. 2006;51(6):2675–89.

115. Sweeney EN, McGillicuddy DJ, Buesseler KO. Biogeochemical impacts due to mesoscale eddy activity in the Sargasso Sea as measured at the Bermuda Atlantic Time-series Study (BATS). Deep Sea Res Part II Top Stud Oceanogr. 2003 Nov;50(22-26):3017–39.

116. Chérubin LM, Morel Y, Chassignet EP. Loop current ring shedding: The formation of cyclones and the effect of topography. J Phys Oceanogr. 2006;36(4):569–91.

117. Hurlburt HE, Thompson JD. A numerical study of Loop Current intrusion and eddy shedding. J Phys Oceanogr. 1980;10:1611–51.

118. Ichiye T. Circulation and water-mass distribution in the Gulf of Mexico. Geofis Int. 1962;2:47–76.

119. Walker N, Leben R, Anderson S, Haag A, Pilley C. High Frequency Satellite Surveillance of Gulf of Mexico Loop Current Frontal Eddy Cyclones. OCEANS 2009, MTS/IEEE Biloxi-Marine technology for our future: Global and local challenges [Internet]. IEEE; 2009 [cited 2015 Apr 14]. p. 1–9. Available from: http://ieeexplore.ieee.org/xpls/abs_all.jsp?arnumber=5422154

120. Biggs DC, Mullerkarger FE. Ship and satellite-observations of chlorophyll stocks in interacting cyclone-anticyclone eddy pairs in the Western Gulf of Mexico. Geophys Res-Oceans. 1994;99(C4):7371–84.

121. Sahl LE, Wiesenburg DA, Merrell WJ. Interactions of mesoscale features with Texas shelf and slope waters. Cont Shelf Res. 1997;17(2):117–36.

122. Brooks DA, Legeckis RV. A ship and satellite view of hydrographic features in the western Gulf of Mexico. J Geophys Res-Oceans. 1982;87(6):4195–206.

123. Lohrenz SE, Dagg MJ, Whitledge TE. Enhanced primary production at the plume oceanic interface of the Mississippi River. Cont Shelf Res. 1990;10(7):639–64.

124. Dorado S, Rooker J, Wissel B, Quigg A. Isotope baseline shifts in pelagic food webs of the Gulf of Mexico. Mar Ecol Prog Ser. 2012 Sep 19;464:37–49.

125. Ressler PH, Jochens AE. Hydrographic and acoustic evidence for enhanced plankton stocks in a small cyclone in the northeastern Gulf of Mexico. Cont Shelf Res. 2003;23(1):41–61.

126. Evans C, Thomson PG, Davidson AT, Bowie AR, van den Enden R, Witte H, et al. Potential climate change impacts on microbial distribution and carbon cycling in the Australian Southern Ocean. Deep Sea Res Part II Top Stud Oceanogr. 2011 Nov;58(21-22):2150–61.

127. Koch C, Harnisch F, SchrÃ¶der U, MÃ¼ller S. Cytometric fingerprints: evaluation of new tools for analyzing microbial community dynamics. Front Microbiol [Internet]. 2014 Jun 4 [cited 2015 Apr 14];5. Available from: http://journal.frontiersin.org/article/10.3389/fmicb.2014.00273/abstract

128. Dohan K, Maximenko N. Monitoring ocean currents with satellite sensors. Oceanography. 2010 Dec 1;23(4):94–103.

129. Collier JL, Campbell L. Flow cytometry in molecular aquatic ecology. Hydrobiologia. 1999;401:33–53.

130. Marie D, Simon N, Vaulot D. Phytoplankton cell counting by flow cytometry. Algal Cult Tech. 2005;3:253.

131. Leben RR, Biggs DC, Zimmerman RA, Gasca R, Suarez-Morales E, Castellanos I. Note on plankton and cold-core rings in the Gulf of Mexico. Fish Bull. 1997;95:2.

132. Dai A, Qian T, Trenberth KE, Milliman JD. Changes in continental freshwater discharge from 1948 to 2004. J Clim. 2009 May;22(10):2773–92.

133. Shiller AM. Comparison of nutrient and trace element distributions in the delta and shelf outflow regions of the Mississippi and Atchafalaya Rivers. Estuaries. 1993 Sep;16(3):541.

134. Qian Y, Jochens AE, Kennicutt Ii MC, Biggs DC. Spatial and temporal variability of phytoplankton biomass and community structure over the continental margin of the northeast Gulf of Mexico based on pigment analysis. Cont Shelf Res. 2003;23(1):1–17.

135. Zhao Y, Quigg A. Nutrient limitation in Northern Gulf of Mexico (NGOM): Phytoplankton communities and photosynthesis respond to nutrient pulse. Campbell DA, editor. PLoS ONE. 2014 Feb 14;9(2):e88732.

136. Calil PHR, Richards KJ, Jia Y, Bidigare RR. Eddy activity in the lee of the Hawaiian Islands. Deep Sea Res Part II Top Stud Oceanogr. 2008 May;55(10-13):1179–94.

137. Dickey TD, Nencioli F, Kuwahara VS, Leonard C, Black W, Rii YM, et al. Physical and bio-optical observations of oceanic cyclones west of the island of Hawai'i. Deep Sea Res Part II Top Stud Oceanogr. 2008 May;55(10-13):1195–217.

138. Nencioli F, Kuwahara VS, Dickey TD, Rii YM, Bidigare RR. Physical dynamics and biological implications of a mesoscale eddy in the lee of Hawai'i: Cyclone Opal observations during E-Flux III. Deep Sea Res Part II Top Stud Oceanogr. 2008 May;55(10-13):1252–74.

139. Laws EA, Falkowski P, Smith WO, Ducklow HW, McCarthy JJ. Temperature effects on export production in the open ocean. Glob Biogeochem Cycles. 2000;14(4):1231–46.

140. Ewart CS, Meyers MK, Wallner ER, McGillicuddy DJ, Carlson CA. Microbial dynamics in cyclonic and anticyclonic mode-water eddies in the northwestern Sargasso Sea. Deep Sea Res Part II Top Stud Oceanogr. 2008 May;55(10-13):1334–47.

141. Falkowski PG, Ziemann D, Kolber Z, Bienfang PK. Role of eddy pumping in enhancing primary production in the Ocean. Nature. 1991;352(6330):55–8.

142. Waite AM, Thompson PA, Pesant S, Feng M, Beckley LE, Domingues CM, et al. The Leeuwin Current and its eddies: An introductory overview. Deep Sea Res Part II Top Stud Oceanogr. 2007 Apr;54(8-10):789–96.

143. Rivas D, Badan A, Sheinbaum J, Ochoa J, Candela J. Vertical velocity and vertical heat flux observed within Loop Current eddies in the central Gulf of Mexico. J Phys Oceanogr. 2008 Nov;38(11):2461–81.

144. Brown SL, Landry MR, Selph KE, Jin Yang E, Rii YM, Bidigare RR. Diatoms in the desert: Plankton community response to a mesoscale eddy in the subtropical North Pacific. Deep Sea Res Part II Top Stud Oceanogr. 2008 May;55(10-13):1321–33.

145. Quigg A, Sylvan JB, Gustafson AB, Fisher TR, Oliver RL, Tozzi S, et al. Going West: Nutrient limitation of primary production in the northern Gulf of Mexico and the importance of the Atchafalaya River. Aquat Geochem. 2011 Sep;17(4-5):519–44.

146. Dortch Q, Whitledge TE. Does nitrogen or silicon limit phytoplankton production in the Mississippi River Plume and nearby regions. Cont Shelf Res. 1992;42(5):1293–309.

147. Morán XAG, Taupier-Letage I, Vázquez-Domínguez E, Ruiz S, Arin L, Raimbault P, et al. Physical-biological coupling in the Algerian Basin (SW Mediterranean): influence of mesoscale instabilities on the biomass and production of phytoplankton and bacterioplankton. Deep Sea Res Part Oceanogr Res Pap. 2001;48(2):405–37.

148. Beaugrand G. Monitoring pelagic ecosystems using plankton indicators. ICES J Mar Sci. 2005 May;62(3):333–8.

149. Cowen RK. Scaling of connectivity in marine populations. Science. 2006 Jan 27;311(5760):522–7.

150. Lamkin J. The Loop Current and the abundance of larval Cubiceps pauciradiatus (Pisces: Nomeidae) in the Gulf of Mexico: Evidence for physical and biological interaction. Fish Bull. 1997;95(2):250–66.

151. Rooker JR, Kitchens LL, Dance MA, Wells RJD, Falterman B, Cornic M. Spatial, temporal, and habitat-related variation in abundance of pelagic fishes in the Gulf of Mexico: Potential implications of the Deepwater Horizon oil spill. Tsikliras AC, editor. PLoS ONE. 2013 Oct 10;8(10):e76080.

152. Rooker JR, Secor DH, De Metrio G, Schloesser R, Block BA, Neilson JD. Natal homing and connectivity in Atlantic Bluefin Tuna populations. Science. 2008 Oct 31;322(5902):742–4.

153. Caron DA. Marine microbial ecology in a molecular world: what does the future hold? Sci Mar. 2005;69(S1):97–110.

154. Karl DM. Microbially mediated transformations of Phosphorus in the sea: New views of an old cycle. Annu Rev Mar Sci. 2014 Jan 3;6(1):279–337.

155. Schäfer H, Bernard L, Courties C, Lebaron P, Servais P, Pukall R, et al. Microbial community dynamics in Mediterranean nutrient-enriched seawater mesocosms: changes in the genetic diversity of bacterial populations. FEMS Microbiol Ecol. 2001;34(3):243–53.

156. Carlson CA, Giovannoni SJ, Hansell DA, Goldberg SJ, Parsons R, Otero MP, et al. Effect of nutrient amendments on bacterioplankton production, community structure, and DOC utilization in the northwestern Sargasso Sea. Aquat Microb Ecol. 2002;30(1):19–36.

157. Fuhrman JA, Hagstrom A. Bacterial and archaeal community structure and its patterns. Microbial Ecology of the Oceans. Second. Hoboken, New Jersey, USA: John Wiley & Sons, Inc.; 2008. p. 45–90.

158. Costanza R, Andrade F, Antunes P, Van Den Belt M, Boersma D, Boesch DF, et al. Principles for sustainable governance of the oceans. Science. 1998;281(5374):198–9.

159. Crooks S, Turner RK. Integrated coastal management: Sustaining estuarine natural resources. Adv Biol Res. 1999;29:241–79.

160. Nixon SW. Coastal marine eutrophication: A definition, social causes, and future concerns. Ophelia. 1995 Feb;41:199–219.

161. Paerl HW, Gardner WS, McCarthy MJ, Peierls BL, Wilhelm SW. Algal blooms: Noteworthy nitrogen. Sci N Y NY. 2014;346(6206):175–175.

162. Statham PJ. Nutrients in estuaries — An overview and the potential impacts of climate change. Sci Total Environ. 2012 Sep;434:213–27.

163. Lunau M, Voss M, Erickson M, Dziallas C, Casciotti K, Ducklow H. Excess nitrate loads to coastal waters reduces nitrate removal efficiency: mechanism and implications for coastal eutrophication: Excess nitrate reduces nitrate removal efficiency. Environ Microbiol. 2013 May;15(5):1492–504.

164. Tarbe A-L, Unrein F, Stenuite S, Pirlot S, Sarmento H, Sinyinza D, et al. Protist herbivory: A key pathway in the pelagic food web of Lake Tanganyika. Microb Ecol. 2011 Aug;62(2):314–23.

165. Lomas MW, Bronk DA, van den Engh G. Use of flow cytometry to measure biogeochemical rates and processes in the ocean. Annu Rev Mar Sci. 2011 Jan 15;3(1):537–66.

166. McInnes AS, Shepard AK, Raes EJ, Waite AM, Quigg A. Simultaneous quantification of active carbon- and nitrogen-fixing communities and estimation of fixation rates using fluorescence *In Situ* hybridization and flow cytometry. Appl Environ Microbiol. 2014 Nov 1;80(21):6750–9.